University of Alberta

Library Release form

Name of Author: GE LI

Title of Thesis:

ANTI-AMYLOID PROTEIN MONOCLONAL ANTIBODIES FOR DIAGNOSTICS
AND THERAPUTICS OF ALZHEIMER'S DISEASE

Degree: Master of Science

Year this Degree Granted: 2002

University of Alberta

ANTI-AMYLOID PROTEIN MONOCLONAL ANTIBODIES FOR DIAGNOSTICS
AND THERAPUTICS OF ALZHEIMER'S DISEASE

By

GE LI   ©

A thesis submitted to the Faculty of Graduate Studies and Research in partial fulfillment
of the requirements for the degree of Master of Science.

In
Pharmaceutical Sciences

Faculty of Pharmacy and Pharmaceutical Science

Edmonton, Alberta

Spring 2002

University of Alberta

Faculty of Graduate Studies and Research

The undersigned certify that they have read, and recommend to the Faculty of Graduate Studies and Research for acceptance, a thesis entitled anti-amyloid protein monoclonal antibodies for diagnostics and therapeutics of Alzheimer's disease submitted by Ge Li in partial fulfillment of the requirements for the degree of Master of Science in Pharmaceutical Science.

DEDICATION

To the most important people in my life: my husband, Qing Zhang, and my daughter, Larissa. Only with their love, sacrifice and patience, was I able to complete my Master's Program.

To my mother, Guizhi Yao, my aunt, Guiqing Yao and my uncle Dr. J. Wu who continue provide encouragement to me.

ABSTRACT

Alzheimer's disease (AD) is the most common cause of dementia in the world. There are three pathological changes of AD including extensive neuronal loss, the presence of numerous neurofibrillary tangles and amyloid plaques. The amyloid plaques contain amyloid fibrils derived from β-amyloid (Aβ). The advent of molecular genetics has firmly established the central role of amyloid in the pathogenesis of AD and strongly supports the amyloid cascade hypothesis. The aim of this project is to develop and characterize specific antibodies against Aβ or its precursor protein (APP). Such antibodies will be invaluable tool for the basic research on amyloid in research lab and may also later be developed as diagnostic or therapeutic agents. Monoclonal antibodies were produced by hybridoma fusion technology. We obtained a series of monoclonal antibodies against Aβ_{1-40} peptide as well as the C terminal region of the longer and more amyloidogenic Aβ_{1-42} peptide. Also two rabbit polyclonal antibodies were obtained. The first polyclonal antibody is directed against the Aβ_{1-42}. The second polyclonal antibody is directed against the β-secretase site of the APP protein.

Preliminary studies were initiated to develop a specific ELISA capable to detect Aβ_{1-42}. Finally we also evaluated the potentials of Aβ antibodies as agents capable to inhibit Aβ aggregation and agents capable to promote Aβ clearance. Such studies were performed by Atomic Force Microscopy and Confocal Microscopy. We demonstrated that anti-Aβ antibodies can inhibit protofibril formation and promote Aβ phagocytosis by macrophages.

`

ACKNOWLEDGMENTS

TABLE OF CONTENTS

LIST OF TABLES

LIST OF FIGURES

LIST OF ABBREVIATIONS

aa	Amino acid
Ab	Antibody
Aβ	Beta amyloid peptide
AD	Alzheimer's disease
ADDLs	Aβ-derived diffusible ligands
AFM	Atomic force microscopy
AP	Ammonium persulphate
APP	Amyloid precursor protein
BACE	Beta-site APP-cleaving enzyme
BBB	Blood-brain barrier
BSA	Bovine serum albumine
CM	Culture medium
CNS	Central nervous system
CTF	C-terminal fragment
DMSO	Dimethyl sulphoxide
EDTA	Ethylenediaminetetraacetic acid tetrasodium: hydrate ($C_{10}H_{12}N_2O_8Na_4$)
ELISA	Enzyme linked immunosorbent assay
ER	Endoplasmic reticulum
ERT	Estrogen replacement therapy
FITC	Fluorescein isothiocyanate
HAT	Hypoxanthine, aminopterin, thymidine
HT	Hypoxanthine, thymidine

GM-CSF	Granulocyte Macrophage Colony Stimulating Factor
IgG	Immunoglobulin G
IgM	Immunoglobulin M
i.p.	Intraperitoneal
i.v.	Intravenous
KLH	Keyhole limpet hemocyanin
KPI	Kunitz-type serine protease inhibitor
M	Molar
mAb	Monoclonal antibody
MAO-B	Monoamine oxidase-B
MBP	Mannan binding protein
2ME	2-mercaptoethanol
mM	Millimoles per litre
mg	Milligram
MM	Materials and Methods
ng	Nanogram
nm	Nanometer
NSAID	Non-steroid anti-inflammatory drugs
PAGE	Polyacrylamide gel electrophoresis
PBS	Phosphate buffered saline
PBST	Phosphate buffered saline Tween
PD APP	Amyloid precursor protein driven by a platelet-derived growth factor promoter
PEG	Polyethylene glycol

PF	Protofibrils
PS1	Presenilin 1
PS2	Presenilin 2
ROS	Reactive oxygen species
sAPP	Secreted APP
sAPPα	Secreted α fragment of APP
sAPPβ	Secreted β fragment of APP
SDS	Sodium dodecyl sulphate
s.c.	Subcutaneous
SM	Standard media
TEMED	N,N,N',N'-tetramethylene-ethylenediamine
TM	Transmembrane

CHAPTER 1 INTRODUCTION

1.1 The Significance of Alzheimer's Disease

Alzheimer's disease (AD) is the most common form of dementia. In the United States, it affects approximately 4 million people (Diaz Brinton and Yamazaki, 1998), a figure that will triple over next 50 years (US Government Report). Approximately 60% of people suffering from AD are age 65 and older (Ritchie, 1995), and nearly 30% of them are age 85 and older (Bachman *et al.*, 1993). In Canada, 8% of all Canadians aged 65 and older are affected by AD. It is predicted that the number of Canadians with this dementia will rise to 592,000 by the year 2021 (Canadian Study of Health and Aging, 1994). Currently an estimated 12 million people are suffering from the disease worldwide. As the population grows and people live longer, those numbers will explode—more than threefold by the year 2050, an estimate by *TIME Magazine* (2000).

AD has a significant impact on the old age group. It can strike adults at any age, but occurs most commonly in people over 65. There are two forms of AD: Familial Autosomal Dominant (FAD), which can strike adults at any age, and the more common Sporadic, which usually occurs after the age of 65. Up to one in ten people over the age of 80 are likely to suffer from AD, for which there is no effective cure.

AD not only affects patients but also millions of relatives and other persons involved in their care. It has been estimated that both direct costs (actual dollar expenditures) and

indirect costs (resource loss not involving dollar expenditures) is up to $90 billion annually in the US (Ernst *et al.*, 1994). The annual societal cost of care per patient increases significantly with severity of AD. In Canada, It was estimated that the annual cost per patient is to be $9,451 for mild disease, $16,054 for mild to moderate disease, $25,724 for moderate disease, and $36,794 for severe disease. Institutionalization was the largest component of cost, accounting for as much as 84% of the cost for people with severe disease (Hux *et al.*, 1998).

1.2 Objective of Thesis and Research

1.2.1. Investigate Aβ Aggregation in vitro by Atomic Force Microscopy (AFM)

In order to study the formation and the components of amyloid plaques, many previous investigations focused on *in vivo* and *in vitro* studies of brain tissue obtained from AD patients at autopsy. The advantage of these studies is that it can distinguish different components in amyloid plaques. However, the limitation is that it cannot reconstruct the formation of the amyloid plaques.

With the emergence of new techniques such as AFM, researchers have new tools to study the aggregation of Aβ. In this project, the author intends to study the time, temperature and concentration effects on Aβ aggregation using the tapping mode of AFM, and examine whether there is any link between *in vivo* and *in vitro* studies on Aβ aggregation. The research will provide information to improve the diagnosis and treatment of AD.

1.2.2. Develop and Evaluate Antibodies Against Different Regions of Amyloid Precursor Protein (APP)

Several antibodies will be developed in this project. They are BL01.94 monoclonal antibody against $A\beta_{1-40}$, BL03.21 monoclonal antibody against $A\beta_{1-42}$, polyclonal antibodies against $APP\beta$, and polyclonal antibodies against $A\beta_{1-42}$. Through AFM and MTT Assay, this project will study the capacity of these antibodies to inhibit $A\beta$ aggregation and neurotoxicity. Confocal microscopy technology will be the main tool to study the interaction of $A\beta$ peptide with macrophages and the ability of anti-$A\beta$ antibodies to promote the capture of $A\beta$ by macrophages. Finally, BL03.21 will be evaluated for the development of an immunoassay specific for $A\beta_{1-42}$. The experimental results will serve as a guide for the evaluation of the potential utility of the produced antibodies for the diagnosis and treatment of AD.

1.3 Project Planning

1.3.1. Investigate the Aβ Aggregation in Vitro by AFM

In the project, the author intends to study $A\beta$ Aggregation under three different concentrations of $A\beta$ in PBS (50µM, 115µM & 250µM). Each concentration of $A\beta$ solution will be incubated at 4°C, room temperature, or 37°C, respectively and for time intervals varying from 10 minutes to 1 week.

1.3.2. Develop and Evaluate Antibodies Against Different Regions of APP

1.3.2.1 Develop Antibodies Against Different Regions of APP

The Hybridoma fusion technique will be used to produce monoclonal antibodies such as BL01.94 & BL03.21. Polyclonal antibodies will be raised in rabbits.

1.3.2.2 Study the Inhibition of Aβ Aggregation by BL01.94 & BL03.21 mAbs with AFM

Compare the aggregation process of the pure Aβ samples to those of the mixtures of Aβ with BL01.94, BL03.21, or control antibodies. The samples will be aged at 37°C for 1 week. Each sample will be viewed and imaged by AFM at the University of Houston.

1.3.2.3. Studying the Inhibition of Aβ Neurotocixity by BL01.94 & BL03.21 mAbs on the SK-N-SH Cell Line

Prepare the samples as indicated in Chapter 3 and verify the Aβ neurotoxicity of the samples on SK-N-SH cell line. The samples will be aged at 37°C for 1 week, then added to the wells containing SK-N-SH cells. Neurotoxicity of Aβ alone and Aβ mixed with chosen antibodies will be studied by MTT assay.

1.3.2.4. Studying the Interaction of Aβ Peptide with Macrophages

The author intends to study the interaction of Aβ peptide with macrophages through confocal microscopy. Different samples of pure Aβ, mixtures of Aβ with BL01.94 mAb, or non-specific antibody will be incubated with macrophages overnight at 37°C. View the slides by using Confocal Microscopy.

1.4 Brief Introduction of the Chapters

Chapter 2 provides a literature review of current research on diagnosis and therapies in Alzheimer's disease. Chapter 3 describes the materials and experimental methods for this project. Chapter 4 illustrates the results of the experiments and discusses the findings of the project. Chapter 5 presents the key findings and concludes the project. Finally, Chapter 6 recommends future work to further improve the research on AD.

CHAPTER 2 LITERATURE REVIEW

2.1 What Is Alzheimer's Disease?

At the turn of the twentieth century, the German psychiatrist and neurologist, Alois Alzheimer, first described a middle-aged patient suffering from a progressive deterioration of language, memory, and behavior. After the patient's death, Alzheimer applied a new staining technique to the patient's autopsied brain tissue and showed neuropathologic features for the disease: neurofibrillary tangles and amyloid plaques in the neocortex and other brain regions.

During the early stages of AD, people suffer from memory impairment such as: forgetting phone numbers, seldom-used names, details of recent events or conversation and infrequently used words, or words with multiple or subtle meaning. But often those symptoms are unnoticed by others. As the disease progresses, people with AD may experience some difficulties to speak, calculate, or understand abstract concepts. In the moderate-to-severe stages of AD, patients' memory seriously deteriorates; gradually they will lose their daily living activities. They begin to show changes of behavior, including suspiciousness, delusion, hyperactivity, restlessness and wandering and hallucinations. In the most advanced stages of the disease, patients with AD will be totally dependent on their caregivers. The time between initial sign of symptoms and death is highly variable among different individuals.

Alzheimer's disease is characterized clinically by progressive memory loss and the decline of other mental functions. However, a definite diagnosis of AD (McKhann G. *et al.*, 1984) can only be determined by histopathologic examination of brain tissue after the patient's death. AD brains show extensive cortical atrophy as a result of massive neuronal degeneration. The two neuropathological hallmarks of AD are the accumulation in specific brain regions of extracellular amyloid plaques largely composed of deposits of amyloid β peptide, and neurofibrillary tangles composed of intracellular filamentous aggregates of hyperphosphorylated tau protein (Figure 2-1).

Normal	Alzheimer's
Normal Neurons in the Brain	Abnormal Neurons in the Brain of Alzheimer's Disease Patients
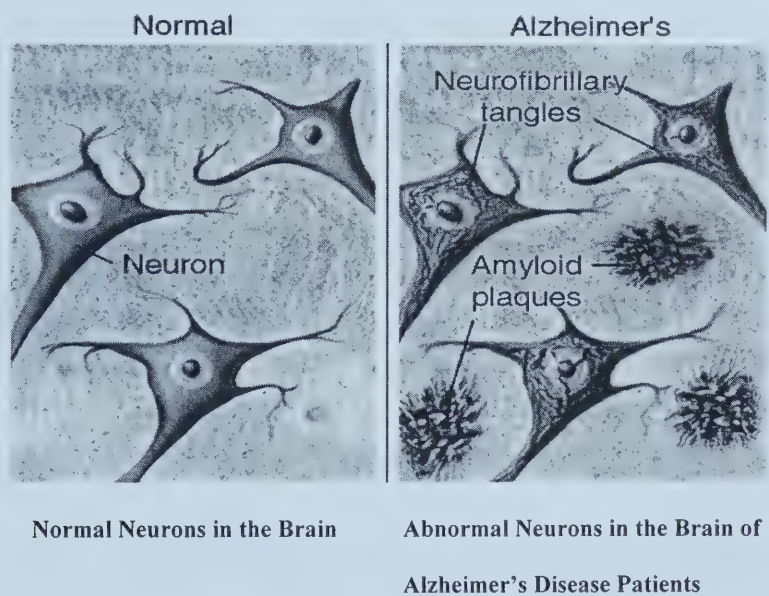
Figure 2-1 Comparison of Normal Neurons to Abnormal Neurons of AD Patients

Extensive research has been conducted to determine whether the tangles or plaques are causative or merely markers of the disease. Numerous genetic, biochemical and animal studies have bolstered the view that the accumulation and deposition of Aβ in the brain

7

over decades leads to neuronal dysfunction and eventually clinical manifestation of the disease (the amyloid hypothesis).

2.2 The Amyloid Cascade Hypothesis

AD is a clinicopathological syndrome in which different gene defects can lead – directly or indirectly – to altered Amyloid Precursor Protein (APP) expression or proteolytic processing or to changes in Aβ stability or aggregation. These result in a chronic imbalance between Aβ production and clearance. Gradual accumulation of aggregated Aβ initiates a complex, multistep cascade that includes inflammatory changes, neuritic/synaptic change, tangles and transmitter loss (the amyloid cascade hypothesis, Figure 2-2).
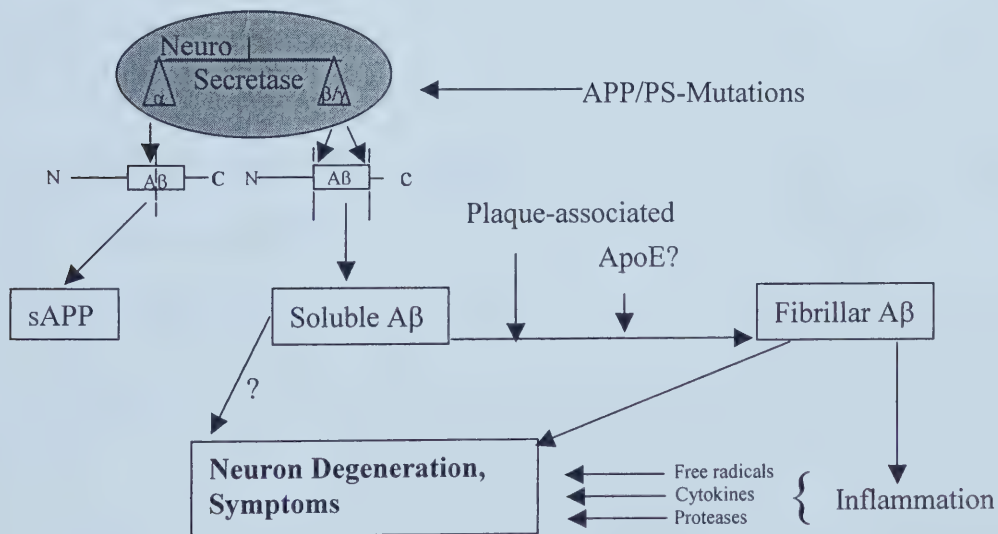
Figure 2-2 The Amyloid Cascade Hypothesis[*]
[*]Modified from Fassbender et al, 2001

Since the basic pathology of AD is common to both familial and sporadic forms of the disease, knowledge of the genetics of AD might give many insights into the molecular events in the pathogenesis of AD. The amyloid cascade hypothesis is strongly supported by the genetic observation that mutations, which lead to an abnormal APP processing, increased Aβ production and/or AB aggregation, cause severe early onset forms of AD. This is a straightforward argument for the significance of Aβ in the progression of AD, and indicates a final common pathological pathway (Haass, 1997; Hardy, 1997). Besides this genetic evidence, the amyloid cascade hypothesis is also supported by other critical evidence that Aβ can directly act as a neurotoxin under certain conditions (Yankner *et al.*, 1990a).

Although many AD researchers regard the amyloid cascade hypothesis as correct, and many data are mounting in support of this pathogenic concept, there are some drawbacks of this concept. With respect to the *in vivo* pathology, the number of NFT's and the extent of loss of cortical neurons show a much higher correlation with the severity of dementia than the occurrence of Aβ deposits, if one applies the amyloid cascade hypothesis to the disease pathology (Terry *et al.*, 1991). There is an alternative view that more soluble Aβ may be of greater importance than the insoluble Aβ that comprises the plaques (Vickers *et al.*, 2000).

2.3 The Amyloid β Peptide

2.3.1. The Mechanism of Aβ Production

The Aβ sequence and its position within APP are shown in (Figure 2-3). The carboxy-terminus of Aβ contains many hydrophobic residues, and comprises the outer part of the trans-membrane domain of APP. Although the metabolism of APP and the production of Aβ are rather complex, different APP processing pathways have been suggested, including secretory cleavage of APP at the cell surface as well as internalization and lysosomal degradation (Golde *et al.*, 1992). There are two secretory pathways (the non-amyloidogenic pathway and in the amyloidogenic pathway).

2.3.1.1 Non-amyloidogenic Pathway

The non-amyloidogenic secretory pathway includes cleavage of APP by an α-secretase between amino acids 16 and 17 of Aβ sequence (Figure 2-4), which generates sAPPα and C-terminal fragment. Although APP is a trans-membrane protein, most of it is actually subjected to the α-secretase cleavage before reaching the cell surface (Citron *et al.*, 1995) and most of the APP reaching the cell surface has been cleaved within the Aβ sequence. Thus, sAPPα is released from the membrane and can be subsequently secreted from cells. The soluble sAPPα can be detected in the culture medium (CM) of transfected cells, plasma and cerebrospinal fluid (CSF). Experimental evidence suggests that sAPPα may have a neuroprotective effect and may enhance learning and cognition (Meziane *et al.*,

1998); thus, augmenting α-secretase processing of APP to release sAPPα, might be beneficial in treating AD.
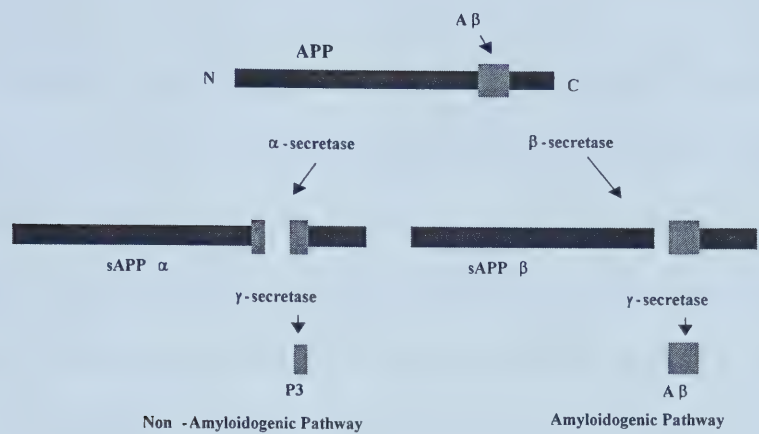
Figure 2-3 Processing of the Amyloid Precursor Protein by α-, β-, γ-secretase
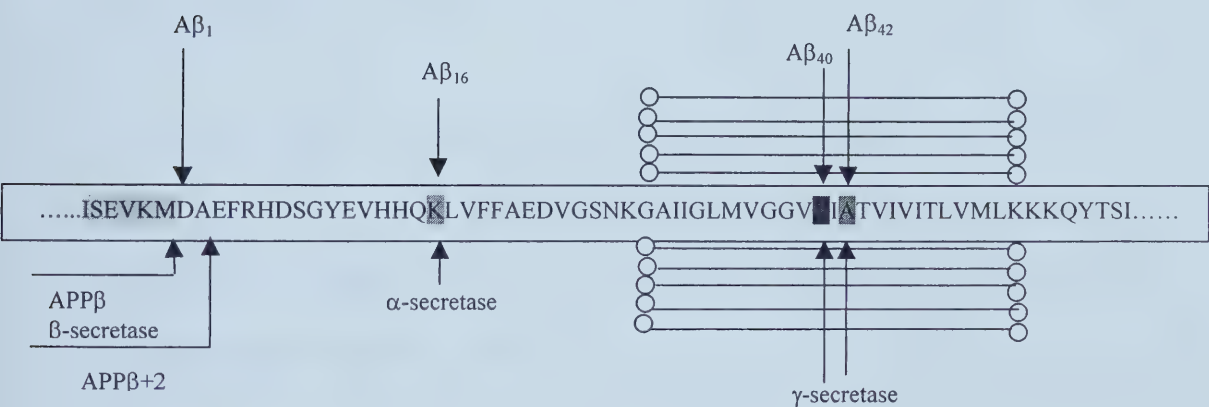
Figure 2-4 The Aβ Region of Amyloid Precursor Protein

While cleavage by α-secretase requires APP to be membrane bound, such cleavage occurs in the secretory membrane. That is, cleavage at the α-secretase site does not require re-internalization of the cell surface APP (Koo and Squazzo, 1994). The membrane-anchored C-terminal fragment of APP remains in the cell (Figure 2-3) and is then cleaved by γ-

secretase to the P3 protein and the C-terminus is degraded in the endosomal-lysosomal compartment after internalization to the cytoplasm (Selkoe, 1998).

The α-secretase is thought to reside at the plasma membrane in micro-domains called caveola or in the trans-Golgi network (Clippingdale *et al.*, 2001). The α-secretase(s) need to be identified, although more than one enzyme may well be involved, as the preferential cleavage site varies in different cell types (Zhong *et al.*, 1994). It can be concluded that the "normal" cellular metabolism of APP precludes the formation of Aβ. Thus, cleavage by α-secretase precludes production of Aβ (Esch *et al.*, 1990; Sisodia *et al.*, 1990;).

2.3.1.2. Amyloidogenic Pathway

It was formerly thought that Aβ formation was the result of aberrant APP processing (Sisodia *et al.*, 1990), but Aβ generation and its extracellular release are features of normal cellular metabolism of APP. This has been confirmed by many investigators and is widely accepted (Shoji *et al.*, 1992).

Aβ is generated from APP by two sequential proteolytic cleavages. First, β-secretase activity releases the N terminus of Aβ, generating a membrane-anchored C-terminal APP fragment. Second, γ-secretase activity cleaves this fragment to release the Aβ C-terminus (Estus *et al.*, 1992; Paganetti *et al.*, 1996).

The amyloidogenic pathway is initiated by β-secretase cleavage of APP. APP is cleaved by β-secretase just before the Aβ region to create its N-terminus and sAPPβ. A truncated form of sAPPβ ends precisely at Met-596 (for the 695 isoform of APP) (Figure 2-4), a marker of endoproteolytic cleavage to release the N-terminus of Aβ. β-secretase was recently identified as a protein with homology to the pepsin family of aspartyl proteases (Vassar *et al.*, 1999). β-Secretase mRNA is highly expressed in the brain and is also found in a variety of human tissues (Lin *et al.*, 2000), consistent with the finding that Aβ is normally produced by many cell types (Shoji *et al.*, 1992). The β-secretase protein is present primarily in the Golgi apparatus and in endosomes, although the enzyme can be detected at the plasma membrane as well. The gene for β-secretase (also referred to as beta-site APP-cleaving enzyme, or *BACE*) is located on chromosome 11, but no AD-causing mutation in this gene has been identified so far (Saunders *et al.*, 1999). β-secretase appears to be an optimal therapeutic target for the prevention and treatment of AD: The protease catalyzes the initial step in Aβ production. Still, significant hurdles remain before the development of useful therapies. For agents to work effectively *in vivo*, the compounds must not only cross the blood-brain barrier, but they must also be taken up by cells. As they must work inside the cell, these agents should be highly selective: interference with other intracellular proteases and critical signaling pathways must be minimized. Another concern is that β-secretase may process substrates in addition to APP.

Subsequent to the action of β-secretase, the cleavage by a γ-secretase at position 40, or less commonly at position 42 or 43 (Figure 2-4), of the Aβ sequence leads to the release of Aβ from APP. Thus the Aβ peptide is heterogeneous at C-termini such as $A\beta_{40}$, $A\beta_{42}$

13

and $A\beta_{43}$. However, in cultured neural cells, $A\beta_{1-40}$ consists of 90-95% of the total secreted $A\beta$. (Asami-Odaka *et al.*, 1995). In contrast, intracellular $A\beta$ produced in the neural cells contains relatively more $A\beta_{1-42}$ (up to 25%) (Tienari *et al.*, 1997). The $A\beta_{1-42}$ peptide, with its two additional hydrophobic residues (isoleucine and alanine), aggregates into amyloid fibrils far more rapidly than does the $A\beta_{1-40}$ (Selkoe, 1998).

Much evidence supports the concept that $A\beta_{1-42}$ is generated in the ER/intermediate Golgi compartment in neurons, whereas $A\beta_{1-40}$ is generated in the trans-Golgi compartment (Cook *et al.*, 1997). There is also some evidence that different γ-secretases may act at these two locations. Although the mechanism arising in C-terminal heterogeneity of $A\beta$ has not been determined, there are several hypotheses. One is that different forms of γ-secretase may exist in different preferred cleavage sites. Another is that C-terminal cleavage by γ-secretase may occur in several intracellular compartments. A combination of both hypotheses is also possible, such that a mixture of different γ-secretases exists in different compartments, thereby resulting in differing $A\beta_{40}/A\beta_{42}$ ratios (Mills and Reiner, 1998).

The formation of $A\beta$ might differ in neural and non-neural cells. $A\beta$ can be rapidly secreted by both cell types after generation (Shoji *et al.*, 1992), and the secreted $A\beta$ seems to be derived mainly from cleavage of endocytosed, full-length, cell-surface APP (Haass *et al.*, 1992; Koo and Squazzo 1994). However, neuronal cell lines generate larger amounts of $A\beta$ than other cell types (Seubert *et al.*, 1993), and most is derived from APP at an earlier stage, before the APP has reached the cell surface (Tienari *et al.*, 1997).

Indeed, Aβ can be detected intracellularly in neural cells, but not other cell types (Fuller *et al.*, 1995; Wertkin *et al.*, 1993). Despite intense efforts, the identity of γ-secretase still remains to some extent a mystery. This is in large part due to its unusual properties, the most peculiar being its ability to cut in the middle of the trans-membrane region of its substrate. How hydrolysis takes place in what is otherwise a water-excluded environment is unclear. It is believed that γ-secretase acts by forming a channel in the membrane to provide the space required accommodating and cleaving the alpha-helical trans-membrane substrate.

During the search for genes on chromosomes 14 and 1 responsible for most cases of familial AD, it was thought that the encoded proteins would reveal at least one, if not both, of the proteases involved in Aβ production. When the search identified the presenilins-1 and -2 (PS1 and PS2) (Rogaev, *et al.*, 1995), it was far from clear what the normal function of these multipass membrane proteins might be and how mutant forms might lead to AD. Remarkably, the presenilins are the sites of dozens of AD-causing mis-sense mutations (Hardy, 1997): More than 70 such mutations have now been identified, with all but six occurring in PS1 (www.alzforum.org/members/resources/pres_mutations/index.html). Intriguingly, these AD-causing mutations result in specific increases in $A\beta_{42}$ production in transfected cells, in transgenic mice, and in plasma and brain from human carriers (Tomita, *et al.*, 1997). Thus, these mutant presenilins somehow modulate γ-secretase activity to enhance production of $A\beta_{42}$. However, it seems clear that presenilins do not work alone, that they are part of a larger γ-secretase complex.

2.3.2. The Mechanism of Aβ Aggregation

In vitro studies of Aβ assembly have revealed three main types of oligomers: 1) Aβ-(1-40) oligomers ranging from dimer through hexamer (Garzon-Rodriguez *et al.*, 1997); 2) Aβ-derived diffusible ligands (ADDLs), oligomers of $Aβ_{1-42}$ ranging in molecular mass between 17,000 and 42,000 Da (corresponding to tetramers through decamers) (Lambert *et al.*, 1998); and 3) protofibrils (PF), narrow, flexible, fibril intermediates formed by Aβ peptides (Walsh *et al.*, 1997).

Jarrett *et al.* (1993) and Lomakin *et al.* (1997) suggested that Aβ polymerization is considered to be a two-stage process. This process is initiated by the association of Aβ monomers into small, nucleating "seeds" and is accompanied by conformational change: random coil to an amyloidogenic β-sheet. Subsequent to nucleation, the Aβ seeds assemble in a chain-like manner to yield intermediate protofibrils. (Sunde *et al.*, 1997; Blake and Serpell, 1996). Finally, protofibrils are converted into fibrils. A number of recent studies have shown that the presence of preformed oligomers or polymers of Aβ in solution increases the polymerization rate dramatically, because these multimers of Aβ can act as templates for the polymerization. Tjernberg *et al.* (1999) also suggested that polymerization starts with the formation of dimers, which in turn form tetramers or oligomers. Walsh *et al.* (1999) studied the assembly, structure, and biological activity of protofibrils: They found that protofibrils:

1) are in equilibrium with monomeric or dimeric Aβ;

2) have a secondary structure characteristic of amyloid fibrils;

3) appear as beaded chains;

4) give rise to mature, amyloid-like fibrils; and

5) affect the normal metabolism of cultured neurons.

The conversion of protofibrils into fibrils *in vivo* can be affected by factors such as the amyloid-binding Apolipoprotein E (Schmechel *et al.*, 1993), the amount of $A\beta_{1-42}$ (Jarrett *et al.*, 1993), and the other chaperone elements that may control $A\beta$ self-association. ApoE, a well-established risk factor for AD (Strittmatter, 2000) has also been suggested to promote $A\beta$ formation. (Wisniewski *et al.*, 1994; Soto *et al.*, 1995). In the case of ApoE, there are conflicting data suggesting that ApoE can enhance, as well as inhibit, amyloidogenesis (Wood, Chan and Wetzel, 1996; Evans *et al.*, 1995). It has also been suggested that the charged molecules, such as gangliosides (Choo-Smith *et al.*, 1997) and metal ions, including Zn^{2+} and Cu^{2+} (Clippingdale, 2001), may enhance formation of amyloid *in vitro* and *in vivo*. $A\beta$ can be secreted by normal cellular pathways, and soluble $A\beta$ can be detected in blood and cerebrospinal fluid. However, the level is usually in the low nano- to picomolar range. At these concentrations the peptide polymerizes at a very slow rate (Jarret and Lansbury, 1993).

2.3.3. The Mechanism of Aβ Clearance and Degradation

The neuron is able to control and balance two opposing events: one involving the mechanisms of protein and membrane synthesis, and the other involving the processes that degrade or digest proteins. Unlike other types of cells in the body, nerve cells do not replicate after birth. Instead, they constantly degrade or digest old proteins and synthesize new proteins. The system of protein synthesis and degradation in nerve cells is well regulated and any disruption could have catastrophic functional consequences. For example, protein production increases abnormally with a normal degradation system, excess proteins could form aggregates. If proteins are not properly digested or broken down, they could accumulate, forming harmful aggregates. Aβ peptide is normally produced by neurons. Either increased production or decreased degradation of Aβ could lead to the aggregation of Aβ. $Aβ_{1-42}$, in particular, is highly insoluble and resistant to degradation, thus readily accumulating within the nervous system.

Under normal conditions, soluble Aβs are bound to various Aβ binding proteins and are quickly cleared from cerebrospinal fluid into the bloodstream (Ghersi-Egea et al., 1996), most likely via receptor transport mechanisms across the blood–brain barrier (Poduslo et al., 1999). The removal and degradation of Aβs from the brain could also be affected by certain Aβ binding proteins (Biere et al., 1996; Ghiso et al., 1993) as well as by the production and activation of Aβ-degrading proteases (Kurochkin and Goto, 1994).

Two enzymes have been identified, neprilysin (Iwata *et al.*, 2000) and insulin degrading enzyme (Vekrellis *et al.*, 2000), as potential candidate for AB degradation (Selkoe, 2001).

2.3.4. Neurotoxicity of Aβ Peptide

Whereas the physiological role of Aβ in the brain and particularly in the pathogenesis of AD remains to be elucidated, numerous studies have been done on the fundamental cellular action of Aβ, and its fragments, and their effects on neuron-neuron or neuron-glia signaling. *In vitro* pharmacological data on the dose- (Mattson *et al.*, 1992) and conformation-dependent (Pike *et al.*, 1993) neurotoxic potentials of Aβ have been collected. Yankner *et al.*, (1990) reported that Aβ acts as neurotoxin above a threshold concentration. Interestingly, some investigators found that picomolar concentrations of Aβ may enhance neurite outgrowth or nerve cell survival *in vitro* (Whiston *et al.*, 1989). Moreover, Aβ may play a role as a potent cholinergic neuromodulator (Auld *et al.*, 1998). Abundant evidence supports the concept that Aβ is toxic to neurons, Both fibrillar and soluble, oligomeric forms of Aβ have potent neurotoxic activities. The major mechanisms proposed for Aβ-induced cytotoxicity involve the loss of Ca^{2+} homeostasis and the generation of reactive oxygen species (ROS). For both mechanisms it has been suggested that the insertion of Aβ within the membrane bilayer is at the origin of the observed neurotoxicity.

In vitro studies demonstrate that Aβ can directly intercalate within the lipid bilayer and form ion channels (Lin *et al.*, 2001). Continued accumulation of Aβ channels over an

19

extended period would allow considerably higher Ca^{2+} uptake, disruption of calcium homeostasis and activation of signal transduction pathways leading to cellular degeneration.

Evidence for increased oxidative stress (ROS, lipid peroxidation, protein modification and oxidation of mitochondrial DNA) has been presented in the Alzheimer's disease (AD) brain. The Aβ has been identified as a possible source of oxidative stress in the AD brain because it can acquire a free radical state contributing to its toxic effects. The demonstration of ROS production by Aβ and direct evidence of oxidative damage in neurons by Aβ supported the hypothesis of "Aβ-induced free radical-mediated neurotoxicity" (Varadarajan *et al.*, 2000).

2.4 Diagnosis

No definitive tests for the diagnosis are available, and AD is a diagnosis of inclusion based on patient history, physical examination, neuropsychological testing, and laboratory studies.

Researchers are examining the types and the sequence of cognitive changes in AD in order to develop appropriate tests for early diagnosis, and to test the effectiveness of new treatments and therapies. Researchers are also working towards developing more sensitive and specific testing procedures for earlier diagnosis. Obtaining an accurate and early diagnosis for AD is critically important for treatment. Non-pharmacological as well as pharmacological therapies can be initiated once a diagnosis is obtained.

Researchers have been looking for biochemical markers to identify AD for many years. Several biomarkers are now being used to identify patients with AD. For early-onset AD, sequencing presenilin 1 was found to be a good indicator in laboratory tests. Therefore, in early-onset familial AD, it is appropriate to search for mutations in the presenilin 1, presenilin 2 and amyloid precursor protein genes (Figure 2-3). For late-onset and sporadic AD, the Apolipoprotein E e4 allele has a positive predictive value of 94-98%. It has been suggested that detecting an ApoE e4 allele can add confidence to the clinical diagnosis. However, it is clear that ApoE e4 allele is a risk factor for AD and not a diagnostic marker as many individuals who inherit ApoE e4 allele do not develop the disease.

The recent progress to identify bio-markers of AD has been focusing on substances in the cerebrospinal fluid (CSF) and several studies support the use of $A\beta_{1-42}$ and tau protein as useful bio-markers.

Motter *at al* (1995) measured both total $A\beta$ levels, which include the predominantly present species $A\beta_{1-40}$, and the amyloidogenic fragment $A\beta_{1-42}$ which makes up 5% of total soluble $A\beta$. Total $A\beta$ levels did not differ from AD patients and age-related healthy controls or diseased controls. However, the levels of $A\beta_{1-42}$ were significantly lower in AD patients *vs.* either control group. These initial findings were then extended as well as confirmed by other independent groups. Other studies on $A\beta_{1-42}$ in CSF show that $A\beta_{1-42}$ is reduced in the CSF in the 375 patients studied in comparison to 206 age-matched controls and patients with other disorders including vascular, frontotemporal, and Parkinson's dementia. Levels of $A\beta_{1-42}$ are not correlated with age or age of onset of

disease. Thus lower levels of $A\beta_{1-42}$ are not part of the normal aging process and may be a direct measurement of a pathological change. Similarly there is no correlation of $A\beta_{1-42}$ with gender, or cognitive test scores. Therefore the $A\beta_{1-42}$ peptide is of importance to the disease pathology and the measurement of CSF $A\beta_{1-42}$ is causally related to the disease process.

Cerebrospinal fluid levels of tau protein were shown to be significantly increased in patients with Alzheimer's disease, Although sensitivity is high, poor specificity limits the diagnostic value of this marker.

Combining both markers ($A\beta_{1-42}$ and tau protein) could improve specificity at least allowing differentiation between Alzheimer's disease, normal aging and depressive pseudodementia (Engelborghs and De Deyn 2001).

CT and MRI can be used to facilitate the diagnosis and monitoring of AD, and novel imaging techniques such as the visualization of the accumulation of $A\beta$ *in vivo* are being developed. Since amyloid deposition begins 10-20 years before the appearance of clinical dementia, this new technique may have a great potential for the clinical detection of AD pathology (Bacskai *et al.*, 2001).

2.5 Therapeutic Approaches

Many factors that may contribute to the cause and progression of AD are investigated at present, such as how genetic risk factors interact with each other and how they interact with biochemical factors and unmodified risk factors in the environment (Figure 2-5). By obtaining a better understanding of the disease processes of AD, hopefully effective drug and related therapies could be developed to stop the disease or delay its symptoms.

2.5.1. Risk Factors

There are multiple factors that contribute to the neuropathology of AD (Figure 2-5). Genetic factors, including APP, the presenilin gene products, and the ApoE genotype, affect the relative risk of AD. The search for effective drugs to block these factors is just beginning. A number of biochemical factors, such as inflammation, oxidative stress, nerve growth factor deficits, and estrogen deficiencies, are likely contribute to the progression of AD. Several trials of drugs may delay disease progression by modifying these factors.

Other risk factors include advanced age, smaller head size, and possibly, a lower level of education. It is difficult or impossible to modify those risk factors. However, available treatments for AD diminish only some symptoms and cannot stop the progress of it. To date, more and more interests have focused on the anti-amyloid therapy. Currently available therapies and strategies under development are discussed below.

2.5.2. Cholinergic Agents

Due to a prominent central cholinergic system deficiency in AD, investigators have focused on cholinergic strategies. The most common treatment of AD has been cholinesterase inhibition. Initial studies of physostigmine showed measurable but modest improvements in memory (Davis and Mohs, 1982). Its short duration (1-2 hours) is a major disadvantage. Two other cholinesterase inhibitors, tacrine (Qizilbash, 2000) and donepezil (Doody, 1999), are currently available for the treatment of AD, and several other compounds, such as Rivastigmine (Jann, 2000), Metrifonate (Ringman, 1999) and Propentofylline (Rother, 1998) are currently under phase III study for treating cognitive symptoms of AD. HupA is a potent, reversible and selective inhibitor of acetylcholinesterase (Bai, 2000) and represents a therapeutic agent for AD.

2.5.3. Anti-inflammatory Therapies

There are several inflammatory processes that may contribute to the neural destruction in AD. One is the acute-phase response made by the acute-phase proteins, such as α1-antichymotrypsin and α2-macroglobulin, Increased amounts of which are present in the brains of AD patients. They are also found as components of amyloid plaques, and may play a role in the formation of amyloid fibrils (Bauer *et al.*, 1991; Eikelenboom *et al.*, 1992). The complement cascade is activated in AD, and products of this pathway can be found surrounding the amyloid plaques. In addition, activated microglia are also present

around plaques (McGeer and McGeer, 1992). Therefore, non-steroid anti-inflammatory drugs (NSAIDs) may have a protective effect against AD.

Genetic Factors • APP mutation • Presenilin 1&2 • ApoE E4	
Biochemical Factors • Inflammation • Free Radicals • Nerve Growth Factor Deficit • Estrogen Deficit	Neuropathology • β-Amyloid Deposits • Neurofibrillary Tangles • Neuronal Loss • Synaptic Loss
Unmodifiable Risk Factors • Age • Head Size • Educational Level • Gender	Neuropathological Outflow • Cholinergic Deficit • Noradrenergic Deficit • Serotonergic Deficit

Figure 2-5 Risk Factors for Alzheimer's Disease and Their Relationship to Its Pathogenesis (Farlow MR, 1998)

Considerable epidemiological evidence shows an inverse correlation between sustained NSAID use and the risk of developing AD. However, although a small clinical trial of indomethacin for the treatment of AD provided supporting data for these epidemiological studies, a larger trial on COX-2 inhibitor Celecoxib failed, and a small trial on diclofenac was inconclusive (Bradbury, 2001).

The conflictive results over the possible neuroprotective effect of NSAIDs may be at least partly explained by the recent discovery that the timing and the duration of the use of the

25

NSAIDs appear to be critical to their apparent neuroprotective effect (in't veld et al., 2001). They found that the risk of developing Alzheimer's decreased with increasing NSAID intake. Compared to non-users, those who took NSAIDs for up to two years had a 0.83 relative risk of developing AD. For those who took the drugs even longer, the relative risk dropped markedly, to 0.2.

In addition, although *NSAIDs* are generally thought to work in Alzheimer's disease by reducing brain inflammatory responses, Weggen and colleagues recently suggest a different *mechanism of action*. They found that high doses of some, but not all, *NSAIDs* preferentially reduce the concentration of the highly amyloidogenic $A\beta_{1-42}$ peptide *in vitro*. Additionally, short-term ibuprofen treatment of transgenic mice expressing mutant APP, reduces concentrations of $A\beta_{1-42}$ in the brain. The authors suggest that some *NSAIDs* may be inducing a subtle change in the activity of γ-secretase, the enzyme responsible for $A\beta_{1-42}$ production.

2.5.4. Estrogen

Several epidemiological studies indicate that estrogen substitution in postmenopausal women decreases the risk for AD (Paganini-Hill and Henderson 1996). Estrogens may improve memory and aspects of other cognitive performance through a variety of mechanisms, including cholinergic neuroprotective and neurotrophic effects.

Whereas many small interventional studies have suggested a beneficial effect of estrogen substitution (Henderson, 1997), two very recent double-blind and placebo-controlled studies revealed that estrogen therapy in older female AD patients over 4 months did not significantly alter the disease course (Henderson *et al.*, 2000, Mulnard, 2000). This does not preclude the possibility that long-term estrogen substitution in younger postmenopausal women who are still healthy could be valuable in primary prevention of the disease.

Further studies are needed to definitively show the benefits of long-term estrogen use in the prevention of AD (Sramek and Cutler, 1999; Monk, 2000).).

2.5.5. Antioxidants and Monoamine Oxidase Inhibitors

Free radicals are byproducts of oxidative metabolism. They could easily damage cell membranes and tissue, and contribute to neuronal degeneration and death (Smith *et al.*, 1996). Drugs or vitamins (such as vitamin E) protect against oxidative damage and may reduce neuronal damage or slow the progression of AD (Vatassery, 1998). Based on the oxidative stress hypothesis of AD, numerous approaches for an effective antioxidant neuroprotector have been developed, such as monoamine oxidase-B (MAO-B) inhibitor (Selegiline), which could be effective in treating AD (Thomas, 2000).

2.5.6. Nerve Growth Factor

Koliatsos *et al.*, (1991) showed that nerve growth factor (NGF) could prevent the degeneration of basal forebrain cholinergic neurons in experimental models of AD. But NGF does not cross the blood-brain barrier (BBB) and must be administrated intraventricularly or must be carried to the cell by implanted viral vectors. Rosenberg *et al.* (1988) suggested that using viral vectors to transport NGF into the basal forebrain from a surgical implantation site may be a possible way to treat AD. Stimulating NGF receptors or stimulating other cells in the CNS to produce NGF is also a possible approach. Both Idebenone and AIT-082 have been reported to stimulate production of NGF in the brain. Both are currently in clinical trials (Farlow and Evans, 1998).

2.5.7. Anti-amyloid Therapies

According to the amyloid hypothesis, a number of therapeutic strategies for AD are theoretically possible. For example, since the production of Aβ requires cleavage of APP at two distinct locations, termed the β-secretase and γ-secretase sites, production of the peptide can theoretically be reduced by inhibition of either of these cleavage events. Once the peptide is formed, it may follow various fates. Aβ may simply be cleared from the brain by bulk flow or undergo further proteolysis and rendered benign. Alternatively, the peptide may self-aggregate, form fibrils, and develop new plaques or associate with existing plaques. In the latter case, there is likely an equilibrium between free and bound peptide. This amyloidogenic scenario suggests several additional therapeutic targets for AD. Inhibitors that block self-aggregation of Aβ or the elongation of Aβ fibrils might reduce plaque burden. Alternatively, agents that block the neurotoxicity associated Aβ

may also be of benefit to patients. It is also possible to produce agents that stimulate the active clearance of the peptide or plaques from the brain.

2.5.7.1. Inhibition of Aβ Production

2.5.7.1.1 Inhibition of β or γ-secretases

The modulation of APP processing is an attractive therapeutic approach for AD. The primary enzymes targets are the β- and γ-secretases which are directly responsible for the production of Aβ peptide.

A number of pharmaceutical companies have programs aimed at the development of small molecule inhibitors of each of the responsible enzyme activities (Wolfe, 2001). An interesting finding comes also from the recent work of Weggen et al who demonstrate that some NSAIDs can reduce the production of $A\beta_{1-42}$ and suggest that these drugs modulate γ-secretase activity.

5.7.1.1.2 Cholesterol lowering drugs

Epidemiological, and laboratory studies suggest that cholesterol may play a role in the pathogenesis of AD (Simons *et al.*, 2001). It is likely that cholesterol influences Aβ metabolism in several ways, including Aβ production and perhaps altering Aβ deposition and clearance. Cholesterol-lowering drugs thereby provide another therapeutic approach

to reduce Aβ levels and amyloid deposition. Preliminary pilot studies on the therapeutic effects of statins in AD patients are in progress.

2.5.7.2. Promotion of AB Clearance - Amyloid Vaccine

Immunization against Aβ has been suggested as a possible preventive or therapeutic treatment for AD. The approaches involve either injection of various forms of Aβ (active immunization) to stimulate an endogenous immune response or injection of anti-Aβ antibodies (passive immunization).

Two years ago, data from transgenic amyloid-producing mice (PDAPP mice) indicated that immunization against AB_{1-42} (prepared under amyloid fibril-promoting conditions) can reduce deposits of fibrillar amyloid and maintain healthy neurite morphology (Schenk et al., 1999). While convenient, active immunization with Aβ peptide raises safety concerns. Recent work has indicated that Aβ exists in equilibrium with peripheral Aβ. Hence Aβ might also enter the brain and exacerbate plaque formation, especially in elderly people who frequently do not mount a strong antibody response. This problem could be resolved with passive vaccination using anti-Aβ antibodies, which were shown also to reduce the amyloid burden in transgenic mice (Bard et al., 2000; DeMattos, 2001). A different vaccination strategy was also used by Frenkel et al, using as antigen filamentous phages displaying the Aβ EFRH-epitope on the phage surface The authors show that high titer Aβ antibodies can be obtained in guinea pigs and mice, (Frenkel et al., 2000). This is another alternative approach could be used in human.

Of particular interest is the recent finding that vaccination ameliorates behavioral deterioration in mice (Helmuth 2000; Janus *et al.*, 2000; Morgan *et al.*, 2000) and even can clear existing plaques (Bacskai *et al.*, 2001). However, in some transgenic mice that carried presenilin 1, as well as APP transgenes, cognitive protection due to vaccination was obtained despite no significant decrease in amyloid burden (Morgan *et al.*, 2000). The authors hypothesized that vaccination might target soluble, non-fibrillar toxins derived from Aβ. This explanation for memory protection is consistent with the finding that ADDLs are potent inhibitors of long-term potentiation (Lambert *et al.,* 1998; Klein *et al.*, 2001). Aβ immunization is currently being tested in a phase II clinical trial (ELAN pharmaceuticals) towards the goal of treatment and possibly prevention of AD.

The profound reduction of pathology by Aβ immunization in mice raises a number of issues regarding its mechanism of action. Immunohistochemical analyses of brain tissues from mice immunized with $A\beta_{1-42}$ showed that microglia were often seen in the vicinity of the remaining amyloid plaques. Confocal analysis showed that these microglia frequently contained intracellular Aβ, suggesting that the cells actively phagocytosed Aβ (Schenk *et al.*, 1999). A possible trigger mechanism for this process is the decoration of many Aβ plaques with IgG molecules. A small quantity of IgG is free to pass into the brains of healthy mice and humans, and this may be sufficient to allow enough anti-Aβ antibodies to accumulate on plaques and trigger Fc-mediated phagocytosis by microglia or monocytes. Microglia also express $C1qR_P$, a receptor for complement protein C1q, which, *in vitro,* enhances phagocytosis of immune complexes formed with IgG levels below those

required for optimal FcR-mediated phagocytosis. C1qR$_P$-mediated events may promote efficient ingestion of Aβ at low Aβ titers (Webster *et al.*, 2001).

Bard *et al.*, administered anti-Aβ antibodies (i.p.) in the PDAPP mice, and showed that the antibodies cross the blood-brain barrier (BBB), enter the central nervous system (CNS), bind to amyloid plaques, activate microglial cells, and induce the clearance of preexisting amyloid. Based on the foregoing, there is little doubt that, once anti-Aβ antibodies gain entry into the brain and bind to amyloid, microglia would clear them. The passage of Aβ-antibodies across the BBB was however not observed in a recent work performed by DeMattos et al. in 2001. In this case the monoclonal antibodies (m266) were administered intravenously into transgenic mice (PDAPP). A dramatic 1,000-fold increase in plasma Aβ level within hours after injection of the mAb was observed. The plasma levels of Aβ in the untreated animals were very low and Aβ is produced only in the brains of these mice. Therefore the authors proposed that m266 in the plasma acts as a "peripheral Aβ sink" to facilitate the efflux of Aβ from brain to plasma in the PDAPP mice. Long-term peripheral administration of m266 to PDAPP mice markedly reduces a burden .

Aβ immune therapy appears to be much more efficacious in younger transgenic mice without amyloid deposition than older mice that contain extensive brain amyloid plaques (Schenk *et al.*, 1999; Bard *et al.*, 2000; Janus *et al.*, 2000; Morgan *et al.*, 2000; Das *et al.*, 2001). This observation is more consistent with the peripheral Aβ sink hypothesis, because in the absence of Aβ deposits, the sequestration of soluble Aβ by anti-Aβ antibodies in the plasma of young PDAPP mice effectively reduces soluble brain Aβ

levels such that there would be insufficient Aβ left in the brain of these mice to aggregate into insoluble deposits. On the other hand, the reduced effectiveness of Aβ immunotherapy in older mice could be explained by the inability of aggregated insoluble Aβ to convert into freely diffusible soluble Aβ. In this scenario, although circulating anti-Aβ antibodies can still sequester newly synthesized soluble Aβ and limit further amyloid deposition, the highly insoluble amyloid plaques could only be eliminated slowly by a normal turnover process.

Single chain anti-Aβ antibodies obtained by phage display may also have potential as therapeutic agents for AD. Such antibodies dissolve fibrils *in vitro* and prevent toxicity in PC12 cells (Frenkel *et al.*, 2000a,b). Using two-photon microscopy to image plaque dynamics in the brains of living mice, Bacskai et al reported at the neuroscience conference (2001) that a variety of antibodies, including single chain antibodies, when applied directly through a hole drilled into the skulls of mice, can clear up plaques within 3 days.

One concern about the clinical use of a vaccination strategy for Aβ is based on the fact that the majority of individuals at risk of with AD are elderly, and it remains to be determined whether in the case of active immunization, an appropriate adjuvant can be found which will initiate a sufficiently robust immune response to be effective in human being.

Antibodies against an autoantigen may also be toxic. Aβ and its precursor protein are physiological and widely expressed components of many tissues, and Aβ immunization may either interfere with the normal functions of these proteins or alternatively initiate autoimmune disease. A recent study by Hyman *et al.* shows that low titers antibodies that recognize Aβ are fairly common in the elderly population with no clear toxicity associated with the presence of such antibodies. Furthermore, no unexpected adverse effects have been seen in animal studies with the Aβ therapy. Anti-Aβ antibodies have also been found in the CSF of AD patients and age-matched controls (Du *et al.*, 2001). Although Hyman et al report that the low plasma levels of anti-Aβ antibodies did not confer protection against developing dementia, the CSF anti-Aβ antibodies titers were significantly lower in patients with AD compared with healthy control subjects (Du *et al.*, 2001) and the authors suggest that the CSF anti-Aβ antibody titers may be helpful in better understanding the effect of future immunologic therapies for AD.

2.5.7.3. Inhibition of Aβ Assembly

Soluble Aβ can be transported rapidly from cerebral spinal fluid (CSF) to plasma. Agents that block self-aggregation of Aβ and its deposition into insoluble aggregates may, by altering the dynamic equilibrium of Aβ between brain, CSF, and plasma, favor the efflux of brain Aβ to the CSF and into the circulation. In addition to their ability to promote Aβ clearance, inhibitors of Aβ assembly may prevent the formation of neurotoxic Aβ species such as ADDLs or protofibrils and therefore have a neuroprotective activity.

Preparing mAbs against aggregating epitopes may provide a tool for preventing Aβ aggregation. Researchers showed that appropriate mAbs interact at protein-folding initiation sites, leading to an inhibition of Aβ aggregation. Solomon and his colleagues found that site-directed Abs (monoclonal or single chain antibodies) towards the N-terminal region of AB interfere with the aggregation of Aβ and trigger reversal to its nontoxic, normal components. In addition these antibodies bind to Aβ fibrils and are capable to enable their resolubilization (Frenkel *et al.*, 2000; Frenkel *et al.*, 1999; Frenkel *et al.*, 1998). Other approaches include the use of soluble Aβ derivatives and small compounds that bind to and inhibit Aβ fibrillization (Soto *et al.*, 1998; Leveugle *et al.*, 1998; Kisilevsky, 1997).

2.5.8. Combination Therapies

In AD, cholinergic deficit is a major neuropathologic deficit among deficits in other neurotransmitters. Furthermore, several factors, such as inflammation, oxidative stress, and neurotoxins, appear to influence the neurodegenerative process. Combination drug therapy is based on these multiple aspects of AD. In theory, agents that act on complementary targets may produce additive or synergistic effects when administered in combination.

Although this approach is more promising, not all drug combinations will provide greater benefits than those achieved with each drug alone. For example, the selegiline-vitamin E regimen was only as effective as either drug alone and no additive or synergistic effects

were observed. Also the efficacy, as well as the safety, of each potential drug combination must be evaluated through randomized, controlled clinical trials.

CHAPTER 3 MATERIALS AND METHODS

3.1 Materials

Peptides: $A\beta_{1-40}$ peptide, $A\beta_{25-35}$ peptide and $A\beta_{1-16}$ peptide were obtained from Sigma. $A\beta_{1-40}$, $A\beta_{1-42}$, Biotinylated $A\beta_{1-40}$ was obtained from Oncogene Research Products (Boston, MA, USA). APPβ-KLH and Biotin-APPβ was obtained from American Peptide Company (Sunnyvale, California, USA).

Antibodies: Goat anti-mouse polyvalent Ig (whole molecule) was obtained from Sigma. Goat anti-mouse Ig (H+L)-HRP, clonotyping system-HRP were obtained from Southern Biotechnology Associates Inc. (Birmingham, AL, USA). Rabbit anti-human $A\beta_{1-40/42}$ and mouse anti-human $A\beta_{1-16}$ were obtained from Chemicon international Inc. (Temecula CA).

Other Reagents: RPMI-1640 medium, fetal bovine serum (FBS), L-glutamine, streptomycin, penicillin, HAT Supplement, OPI media supplement were obtained from Life Technologies GIBCO BRL (Burlington, ON, Canada). Complete Freund's adjuvant (CFA), Incomplete Freund's adjuvant (IFA), trypan blue solution, thimerosal, pristane (2,6,10,14-tetramethyldecanoic acid), Keyhole Limpet Hemocyanin (KLH), glutaraldehyde, SDS, EDTA, Glycine, TRIZMA Base (Tris [hydroxymethyl] aminomethane), streptavidin-phycoerythrin, and PEG solution were obtained from Sigma. Granulocyte Macrophage Colony Stimulating Factor (GM-CSF) was from Pepro Tech

Inc. (Rocky Hill, NJ, USA). The Mannan Binding Protein column was obtained from PIERCE (Rockford, IL, USA). Filters 0.22μm and 0.45μm were obtained from Millipore (Bedford, MA, USA). Dialysis membrane (MW cutoff, 12,000-14,000 Dalton) was obtained from Fisher Scientific (Nepean, ON, Canada). Mini-PROTEAN II 2-D cell, 40% Acrylamide/Bis solution, the SDS-PAGE molecular weight standard markers, TEMED (N,N,N'N'-Tetra methylethylenediamine) were obtained from BIO-RAD (Hercules, CA, USA). Calcium chloride and Sodium chloride were obtained from BDH Inc. (Toronto, ON, Canada). Adjuvant QUIL A was obtained from Calbiochem (SD, USA). The ultrafiltration cell-8200 model, YM 30,000 membranes were obtained from Amicon Canada Ltd. (Oakville, ON, Canada). ABTS H_2O_2 solution and ABTS peroxidase substrate were obtained from Kirkegaard & Peery Laboratories Inc. (Gaithersburg, MD, USA). All other reagents were of analytical grade or equivalent purity.

Animals and cells: Balb/c mice (5 and 6 weeks age), DBA 2J mice and New Zealand rabbits were obtained from Health Sciences Laboratory Animal Services (University of Alberta, Edmonton, AB, Canada). Sp2/0 (murine myeloma cells), SK-N-SH (human neuroblastoma cells), and Mouse dendritic cells and macrophages were obtained from The American Type Culture Collection (Rockville, MD, CRL-11904/CRL-2278).

3.2 Generation of Monoclonal Antibodies

3.2.1. Immunization

3.2.1.1. Conjugation of Peptides to Carrier Proteins

3.2.1.1.1 KLH-conjugation

There is a correlation between the size of a macromolecule and its immunogenicity. The best immunogens tend to have a molecular mass approaching 100,000 Da. Generally substances with a molecular mass less than 5000-10,000 Da are poor immunogens. Since the peptides that we used for immunization are of very low molecular weight (about 4 kDa), strong responses may be elicited by coupling them to an immunogenic carrier molecule (KLH).

1.5 mg of KLH and 300 μg of peptide were mixed at a protein-to-peptide ratio of 1/250~300. The amount of KLH was first dissolved in PBS. Due to the poor solubility of KLH, the KLH solution was placed on ELISA plate rocker at 4°C overnight. Next day, the KLH solution was centrifuged at 2700 rpm for 10 min in order to get rid of undissolved KLH. Then, the peptide was added to a KLH solution in PBS. At the same time, 2.5% glutaraldehyde solution was prepared in water. The glutaraldehyde solution was added dropwize to the stirring mixture of Aβ and KLH at a glutaraldehyde-to-peptide ratio of 3:1. The mixture was mixed well and incubated at room temperature for 1 hour.

Then excess glycine was added to the mixture in order to neutralize the excess glutaraldehyde and stop the reaction.

3.2.1.1.2 BSA-conjugation

The procedure of conjugation of peptide to BSA is completed as follows. 5 mg of peptide was added to 13 mL of a 1mg/mL BSA solution in PBS. The peptide-to-protein ratio was maintained at 40:1. The mixture was stirred at medium speed. Then, 0.6 mL of 0.5% freshly prepared glutaraldehyde solution was added dropwize into the stirring mixture. The well-mixed solution was incubated at room temperature for 2 hours. Extra glycine was added to the mixture to neutralize the excess glutaraldehyde and stop the reaction. The final concentration of peptide was 0.361 mg/mL.

3.2.1.2 Immunization Schedules

The immunization schedules are given in Table 3-1, 3-2, 3-3 & 3-4. At regular intervals, serum was collected by tail bleeding to measure the immune response against the injected antigen. Three days after the final booster injection, the spleens were collected under sterile conditions and immediately used for fusion.

3.2.1.3 Measurement of the Immune Response in the Serum of Immunized Mice

3.2.1.3.1 Assays for $A\beta_{1-40}$ Antibodies

The detection of antibodies specific for $A\beta_{1-40}$ in the serum of immunized mice was performed by ELISA assay as described in Section 3.4.3.

3.2.1.3.2 Assays for $A\beta_{37-42}$ Antibodies

The detection of antibodies specific for $A\beta_{37-42}$ in the serum of immunized mice was performed by ELISA assays as described in Section 3.4.5. & 3.4.6.

Table 3-1 Immunization Schedule for Balb/c Mouse #1 for Fusion BL01

Date	Immunization	Serum collection	Dose per injection		Route
			Immunogen	**Adjuvant**	
Day 0		×			
Day 3	Primary Immunization		($A\beta_{1-40}$ –KLH) 50µg/150µL	CFA (150µL)	IP
Day 17	Booster 1		($A\beta_{1-40}$ –KLH) 50µg/150µL	ICFA (150µL)	IP
Day 24	Booster 2		($A\beta_{1-40}$ –KLH) 50µg/150µL	Quil-A(10ug/150µL)	SC
Day 28		×			
Day 31	Booster 3		($A\beta_{1-40}$ –KLH) 50µg/150µL	ICFA(150µL)	IP
Day 35		×			
Day 38	Booster 4		($A\beta_{1-40}$ –KLH) 50µg/150µL	ICFA (150µL)	IP

Table 3-2 Immunization Schedule for Balb/c Mouse #2 for Fusion BL01[*]

Date	Immunization	Serum Collection	Dose of injection Immunogen	Adjuvant	Route
Day 0		×			
Day 3	Primary Immunization		$A\beta_{1-40}$ (50μg/150μL)	CFA (150μL)	IP
Day 17	Booster 1		$A\beta_{1-40}$ (50μg/150μL)	ICFA (150μL)	IP
Day 24	Booster 2		$A\beta_{1-40}$ (50μg/150μL)	Quil-A (10μg/150μL)	SC
Day 28		×			
Day 31	Booster 3		$A\beta_{1-40}$ (50μg/150μL)	ICFA (150μL)	IP
Day 35		×			
Day 38	Booster 4		$A\beta_{1-40}$ (50μg/150μL)	ICFA (150μL)	IP
Day 42	Booster 5		$A\beta_{1-40}$ (50μg/150μL)		IV
Day 47	Booster 6		$A\beta_{1-40}$ ~42μg by IP & ~8μg by IV		IV & IP
Day 49	Fusion	×			

*$A\beta_{1-40}$ was a self-aggregated peptide.

Table 3-3 Immunization Schedule for Balb/c Mouse #1 for Fusion BL03

Date	Immunization	Serum collection	Dose per injection Imunogen	Adjuvant	Route
Day 0		×			
Day 3	Primary Immunization		$(A\beta_{37-42}$-KLH) 50μg/150μL	CFA (150μL)	IP
Day 10	Booster 1		$(A\beta_{37-42}$-KLH) 50μg/150μL	ICFA (150μL)	IP
Day 17	Booster 2		$(A\beta_{37-42}$-KLH) 50μg/150μL	Quil-A(10μg/150μL)	SC
Day 21		×			
Day 24	Booster 3		$(A\beta_{37-42}$-KLH) 50μg/150μL	ICFA (150μL)	IP
Day 28		×			
Day 31	Booster 4		$(A\beta_{37-42}$-KLH) 50μg/150μL		Intrasplenic injection
Day 33	Fusion	×			

Table 3-4 Immunization Schedule for Balb/c Mouse #2 for Fusion BL03

Date	Immunization	Serum collection	Dose per injection Imunogen	Adjuvant	Route
Day 0		×			
Day 3	Primary Immunization		($A\beta_{37-42}$-KLH) 50μg/150μL	CFA (150μL)	IP
Day 10	Booster 1		($A\beta_{37-42}$-KLH) 50μg/150μL	ICFA (150μL)	IP
Day 17	Booster 2		($A\beta_{37-42}$-KLH) 50μg/150μL	Quil-A(10μg/150μL)	SC
Day 21		×			
Day 24	Booster 3		($A\beta_{37-42}$-KLH) 50μg/150μL	ICFA (150μL)	IP
Day 28		×			

3.2.2 Fusion

3.2.2.1 Preparation of SP2/0 Myelomas and Spleen Cells

SP2/0 myelomas were prepared five days before fusion and cultured in RPMI-20 (RPMI-1640 supplemented with 2mM L-glutamine, 50U/mL penicillin and 50U/mL streptomycin, 20% v/v FBS). One day before fusion, SP2/0 myelomas were split into fresh RPMI-20. The mouse was sacrificed by cervical dislocation and the spleen was harvested aseptically. Then the spleen was transferred into a sterile 100-mm-diameter Petri dish filled with 10 mL sterile RPMI and cleaned by removing the surface fat. The cell strainer was put into another Petri dish filled with 10mL RPMI. The spleen was transferred into the cell strainer and minced with a syringe plunger. The spleen cell suspension was transferred to a sterile centrifuge tube, centrifuged 8 min at 1100 rpm, and the supernatant was discarded. The pellet was resuspended in 5mL ACK lysing buffer for

5 min in order to lyse red blood cells. After 5 min, 5 mL sterile RPMI was added and the suspension was centrifuged as before. The pellet was resuspended in 10mL sterile RPMI and centrifuged twice as before. While spleen cells are being washed, the SP2/0 myeloma cells were harvested separately by transferring the cells to 50-mL conical centrifuge tubes and centrifuged 8 min at 1100 rpm, room temperature, and supernatant was discaded. Then myeloma cells were resuspended in sterile RPMI and washed three times as mentioned above. The number of cells and viability of each cell suspension were assessed by theTrypan blue exclusion method using a hemacytometer.

3.2.2.2. Cell Fusion

SP2/0 myeloma and spleen cells were mixed at a 1:1 or 1:3 ratio in a 50-mL conical centrifuge tube. The tube containing cell mixture was filled with RPMI and centrifuged 8 min at 1100 rpm, room temperature. Supernatant was discarded from the mixed-cell pellet. Using a 2-mL pipet, 2 mL 50% PEG was added to the mixed-cell pellet dropwize over 1 min, the cells were stirred with the pipet tip after each drop. Then 1 mL RPMI-20 was added to the cell mixture dropwize over 1 min, stirred after each drop. This was repeated once with an additional 1 mL of RPMI-20. Another 6 mL RPMI-20 was added with a 10-mL pipet. A small aliquot of cell suspension was removed for counting. The cell suspension was centrifuged 8 min at 1100 rpm, room temperature and the supernatant was discarded. The cell pellet was discharged forcefully with 10mL RPMI-20 by using a 10-mL pipet. Additional RPMI-20 was added in order to reach a cell concentration of 10^6

cells /mL. The cell suspension was added to 96 well flat bottom plates (100μL/well) and the plates were incubated in a humidified 37°C, 5% CO_2 incubator.

3.2.2.3. Monitoring and Feeding Hybridoma Cells

After one day of incubation, wells were checked with an inverted microscope. 100μL of 2× HAT was added to each well. The plates were put in humidified 37°C, 5% CO_2 incubator. The plates were examined on a regular basis for arising clones. Two weeks later, the hybridomas were ready for screening.

3.2.3 Screening Assays

3.2.3.1 Screening Assays for $A\beta_{1-40}$ Antibodies

The presence of the anti-$A\beta_{1-40}$ antibodies in the cell supernatant of arising clones was detected by two different ELISA assays as described in Section 3.4.2, 3.2.3. & 3.4.5.

3.2.3.2 Screening Assays for $A\beta_{37-42}$ Antibodies

The presence of the anti-$A\beta_{37-42}$ antibodies in the cell supernatant of arising clones was detected by ELISA assays as described in Section 3.4.5. & 3.4.6.

3.2.4 Cloning of Selected Clones by Limiting Dilution

The desired hybridoma cells were resuspended in SM and a small aliquot (20 µL) of cells was counted by using a hemacytometer and the viability of the cells assessed by the Trypan blue exclusion method. A cell suspension of 10-50 viable cells/mL was prepared. 96-well plates were seeded with cell suspensions at 100 µL/well and incubated 7 to 10 days in a humidified 37°C, 5% CO_2 incubator. Polyclonal growth was evidenced by more than one cluster of cells per well, those wells were not selected. The clone was expanded and frozen.

3.2.5 Determination of Antibody Class

Knowledge of antibody class and subclass is helpful in determining the strategy of purification. The antibody class was determined by ELISA with clonotyping system-HRP kits.

3.2.6 Antibody Production and Purification

3.2.6.1. Ascites Production

Adult mice (six weeks old) were primed by injecting 0.7mL of pristane (2,6,10,14-tetramethyldecanoic acid) into the peritoneum (*i.p.*). One week later the mice were injected *i.p.*, with $2\sim5 \times 10^6$ hybridoma cells resuspended in 1mL of PBS. Ascitic fluid

46

was tapped from mice 2 times. The collected fluid was centrifuged at 2700 rpm for 10 minutes and the supernatant was harvested and stored at 4°C until all collection was completed.

3.2.6.2. Purification of IgM mAb

3.2.6.2.1 Mannan Binding Protein Affinity Chromatography

The ascites containing the IgM was dialyzed against binding buffer (10mM Tris, 1.25M NaCl, 20mM $CaCl_2$ at a pH of 7.4) for 36 hours. The MBP (Mannan Binding Protein) column was prewashed with 2 column volumes (20mL) of elution buffer (10mM Tris, 1.25M NaCl, 2mM EDTA at pH of 7.4), and then equilibrated with 4 column volumes (40mL) of binding buffer. The ascites (0.5mL/5mL of gel) was applied to the column, allowed to completely enter the gel, and incubated at 4°C for 30 minutes. The column was washed with 9 column volumes of the binding buffer to remove the unbound proteins. The washing was monitored for the presence of proteins by measuring the absorbance at 280nm, using the binding buffer as a reference. Then the column was removed from the cold and incubated with the elution buffer at room temperature for 1 hour, after which the column was washed with the elution buffer, and 14 additional fractions were collected each with a volume of 3mL. The elution of IgM was monitored for the presence of proteins by spectrophotometer at 280nm using the elution buffer as a reference.

At the completion of the purification the column was washed with 2 column volumes of deionized water and then with 2 column volumes of 4°C binding buffer and stored at 4°C.

3.2.6.3 Euglobulin Precipitation Method

The Euglobulin precipitation method is a non-chromatographic method used for the purification of murine IgM mAbs, which takes advantage of their Euglobulin properties. This method was performed as described by (*Garcia-Gonzalez et al.*, 1988).

$CaCl_2$ was added the ascitic fluid (final concentration, 25mM) to generate fibrin formation. When the clot was formed, it was removed by paper filtration. Then the filtered ascitic fluid was dialyzed for 15 hours at 4°C against 100 volumes of demineralized water (pH 5.5). The ascitic fluid was centrifuged in a Beckman L8-55 ultracentrifuge at 22,000 × g for 30 minutes and the precipitate was recovered and suspended in 1M NaCl/0.1M Tris-HCl, pH 8. Dialysis and precipitation were repeated twice. The purified pellet with a high lipid content was mixed with 1.7M NaCl and centrifuged for 3 hours at 27,000 × g. Lipid supernatant was discarded, the clarified mAbs solution was dialyzed against 0.1M Tris HCl, 1M NaCl, pH 8, and centrifuged at 22,000 × g for 30 minutes. The purified pellet was suspended in PBS.

3.2.6.4. Purification of IgG1 mAb

3.2.6.4.1 Protein G Affinity Chromatography

The 5 mL GammaBind Plus Sepharose column was washed with 2 column volumes of elution buffer (0.1M glycine-HCl adjusted to pH 2.8). Then the column was equilibrated with several column volumes of binding buffer (0.1M sodium acetate, pH 5). The ascites sample containing (IgG1) antibodies was diluted 1:10 v/v with binding buffer and loaded on the column at a rate of 0.75 mL/minute. Then the column was washed with several column volumes of binding buffer, at a rate of 1.0 mL/minute. The collected fractions containing unbound proteins were checked by spectrophotometer at 280 nm, using the binding buffer as a reference. The column was washed with several column volumes of elution buffer. Because the acidic condition of elution buffer was not ideal for antibodies, 65μL of 1M Tris-HCl was added to the eluted fractions to neutralize the solution. Elution of bound proteins was monitored by spectrophotometer at 280 nm, using the elution buffer as a reference.

At the completion of the purification the column was washed with 2 column volumes of cleaning buffer (1M acetic acid, pH 2.5), followed by re-equilibration with 2-3 volumes of binding buffer. The column containing the gel was stored at 4°C.

3.3 Generation of Polyclonal Antibodies

3.3.1. Immunization

The immunization schedules are given in Table 3-5, 3-6. The NZW rabbits were immunized by the intramuscular and subcutaneous routes with antigen emulsified in Freund's adjuvant. The initial injection used CFA and booster injections used ICFA. The injection series consisted of injections (0.25mL/ site SC and 0.5mL/site IM) given every three weeks for approximately three months (see Table 3-5, Table 3-6).

3.3.2 Measurement of Immune Response in the Serum of Immunized Rabbits

3.3.2.1 Assay for Anti-Aβ_{37-42} Polyclonal Antibodies

The presence of the anti-Aβ_{37-42} polyclonal antibodies in rabbit serum was detected by ELISA assay as described in Section 3.4.5.

3.3.2.2 Assay for Anti-APPβ Polyclonal Antibodies

The presence of the anti-APPβ polyclonal antibodies in rabbit serum was detected by ELISA assays as described in Section 3.4.7. & 3.4.8.

3.3.3 Purification of Anti-Aβ37-42 Polyclonal Antibodies and Anti-APPβ Polyclonal Antibodies

Protein G affinity chromatography was described in Section 3.2.6.3.

Table 3-5 Immunization Schedule in Rabbits for the Production of Polyclonal

Antibodies against APPβ

Date	Immunization	Serum collection	Dose per injection		Route & Dose
Day 0		×	Imunogen	Adjuvant	
Day 3	Primary Immunization		(APPβ -KLH) 400µg/1mL	CFA (1mL)	7X Sc, 1X IM
Day 24	Booster 1		(APPβ -KLH) 400µg/1mL	ICFA (1mL)	7X Sc, 2X IM
Day 45	Booster 2		(APPβ -KLH) 400µg/1mL	ICFA (1mL)	5X Sc, 2X IM
Day 59		×			
Day 63		×			
Day 66	Booster 3		(APPβ -KLH) 400µg/1mL	ICFA (1mL)	6X Sc, 1X IM
Day 81		×			
Day 89	Booster 4		(APPβ -KLH) 400µg/1mL	ICFA (1mL)	6X Sc, 1X IM
Day102		×			
Day108		×			

Table 3-6 Immunization Schedule in Rabbits for the Production of Polyclonal

Antibodies against Aβ$_{37-42}$

Date	Immunization	Serum collection	Dose per injection Imunogen	Adjuvant	Route & Dose
Day 0		×			
Day 3	Primary Immunization		(Aβ$_{37-42}$-KLH) 400μg/1mL	CFA (1mL)	5X Sc, 1X IM
Day 25	Booster 1		(Aβ$_{37-42}$-KLH) 400μg/1mL	ICFA (1mL)	6X Sc, 1X IM
Day 46	Booster 2		(Aβ$_{37-42}$-KLH) 400μg/1mL	ICFA (1mL)	6X Sc, 1X IM
Day 60		×			
Day 66	Booster 3		(Aβ$_{37-42}$-KLH) 400μg/1mL	ICFA (1mL)	5X Sc, 2X IM
Day 74		×			
Day 90	Booster 4		(Aβ$_{37-42}$-KLH) 400μg/1mL	ICFA (1mL)	6X Sc, 1X IM
Day 90		×			
Day112	Booster 5		(Aβ$_{37-42}$-KLH) 400μg/1mL	ICFA (1mL)	4X Sc, 2X IM
Day112		×			
Day124		×			

3.4 ELISA

3.4.1 The General Protocol

Microtiter strips were coated with 5-10μL/mL antigen in 100μL of PBS and incubated

overnight at 4°C. The coating solution was discarded by suction and washed once with

PBST, 300μL/well. Then 150μL of blocking buffer (2% sucrose, 3% BSA in PBS) was

added to each well in order to block the non-specific binding sites on the wells. After one

hour of incubation at room temperature the plates were washed three times with PBST. 100μL/well of the samples to be tested was added. All wells were incubated for 1 hr at room temperature, followed by three washings with PBST. Then 100μL of corresponding HRP-labeled secondary antibody diluted in binding buffer or PBS was added to each well (see manufacturer's pamphlet for dilution), incubated for 1 hr, and followed by three washings with PBST. The activity of the tested sample was determined by adding 100μL of ABTS (Peroxidase solution B and ABTS peroxidase substrate, 1:1 v/v dilution) to each well. The optical density was measured at dual wavelength, 405nm and 492nm on a microplate reader.

3.4.2. ELISA on Immobilized $A\beta_{1-40}$

$A\beta_{1-40}$ was immobilized on an ELISA plate (0.5μg/mL) followed by incubation with the samples to be tested for the presence of anti-Aβ antibodies. Bound antibodies were detected with corresponding HRP-labeled secondary antibodies. Commercially available anti-Aβ antibodies were used as positive controls (see Figure 3-1).

3.4.3. ELISA with Biotinylated $A\beta_{1-40}$ Immobilized on Streptavidin Coated Plate

Biotinylated $A\beta_{1-40}$ (0.5μg/mL) was incubated on a streptavidin-coated plate (0.5μg/mL), followed by an incubation with the samples to be tested for the presence of anti-$A\beta_{1-40}$ antibodies. Bound antibodies were detected with corresponding HRP-labeled secondary

antibody. Commercially available anti-Aβ_{1-40} antibodies were used as positive controls (see Figure 3-2).

3.4.4. ELISA Using Anti-murine Ig as a Capture Antibody and Biotinylated Aβ_{1-40} as Detecting Agent

Samples to be tested for the presence of anti-Aβ_{1-40} antibodies were incubated on a goat anti-mouse polyvalent Ig coated plate (5μg/mL), followed by an incubation with biotinylated Aβ_{1-40} (0.5μg/mL). Bound Aβ peptide was detected with HRP-streptavidin. Commercially available anti-Aβantibodies were used as positive controls (Figure 3-3).

3.4.5. ELISA on Immobilized Aβ_{37-42}-BSA

The conjugate of Aβ_{37-42}-BSA was immobilized on the ELISA plate (5μg/mL), followed by an incubation with the samples to be tested for the presence of anti-Aβ_{37-42} antibodies. Bound antibodies were detected with corresponding HRP-labeled secondary antibodies (Figure 3-1).

3.4.6. Direct ELISA on Immobilized Aβ_{1-42}

Aβ_{1-42} (5μg/mL) was immobilized on the ELISA plate followed by incubation with the samples to be tested for the presence of anti-Aβ_{37-42} antibodies. Bound antibodies were detected with corresponding HRP-labeled secondary antibodies (see Figure 3-1).

3.4.7. ELISA on Immobilized Biotinylated APPβ-peptide

Biotinylated APPβ-peptide was immobilized on the ELISA plate (5µg/mL), followed by incubation with the samples to be tested for the presence of anti-APPβ antibodies. Bound antibodies were detected with corresponding HRP-labeled secondary antibodies (see Figure 3-1).

3.4.8. ELISA with Biotinylated APPβ immobilized on Streptavidin-Coated Plate

Biotinylated APPβ-peptide (1µg/mL) was incubated on the streptavidin-coated plate followed by incubation with the samples to be tested for the presence of anti-APPβ antibodies. Bound antibodies were detected with corresponding HRP-labeled secondary antibodies (see Figure 3-2)

3.4.9. Competitive ELISA for the Inhibition of BL01.94 mAb Binding to Aβ

3.4.9.1 Inhibition by Anti-Aβ Antibodies of Known Specificity

Biotin-Aβ$_{1-40}$ was immobilized on the streptavidin-coated plate (5µg/mL), followed by incubation with BL01.94 (at non-saturating concentration) alone or the mixture of BL01.94 (IgM) and murine anti-human Aβ (IgG1) of known specificity. Bound Ig antibodies were detected with corresponding HRP-labeled secondary antibodies (see Figure 3-4).

3.4.9.2 Inhibition with $A\beta_{1-16}$ Peptide

Biotin-$A\beta_{1-40}$ was immobilized on the streptavidin-coated plate (5µg/mL), followed by incubation with BL01.94 alone or a mixture of BL01.94 and $A\beta_{1-16}$ peptide (5 to 0.156 µg/mL). Murine anti-human $A\beta_{1-16}$ was used as positive control mAb. Bound antibodies were detected with corresponding HRP-labeled secondary antibodies (see Figure 3-4). In all experiments, anti-Aß antibodies were used at a non-saturating concentrations.

3.4.9.3. Inhibition with $A\beta_{25-35}$ Peptide

Biotin-$A\beta_{1-40}$ was immobilized on the streptavidin-coated plate (5µg/mL), followed by incubation with BL01.94 alone or a mixture of BL01.94 and $A\beta_{25-35}$ peptide (500 µg/mL). Bound antibodies were detected with corresponding HRP-labeled secondary antibodies (see Figure 3-4). In all experiments, anti-Aß antibodies are used at a non-saturating concentration.

3.4.10. ELISA for Detecting Antibody Titers on $A\beta_{1-40}$ and $A\beta_{1-42}$ Coated Plate

$A\beta_{1-40}$ (5µg/mL) was immobilized on the ELISA plate followed by incubation with anti-$A\beta_{37-42}$ mAb or rabbit anti-$A\beta_{37-42}$ antibodies in different dilutions. Bound antibodies were detected with corresponding HRP-labeled secondary antibodies (see Figure 3-1).

Aβ_{1-42} (5µg/mL) was immobilized on the ELISA plate followed by incubation with anti-Aβ_{37-42} mAb or rabbit anti-Aβ_{37-42} antibodies in different dilutions. Bound antibodies were detected with corresponding HRP-labeled secondary antibodies (see Figure 3-1).

3.4.11. ELISA for Detecting the Immune Response of Anti-Aβ_{37-42} mAb or Rabbit Anti-Aβ_{37-42} Antibodies towards Decreasing Concentration of Aβ_{1-40} and Aβ_{1-42}

Decreasing concentrations of Aβ_{1-40} were immobilized on the ELISA plate followed by incubation with anti-Aβ_{37-42} mAb (1:1000) or rabbit anti-Aβ_{37-42} antibodies (1:6000). Bound antibodies were detected with corresponding HRP-labeled secondary antibodies (see Figure 3-1).

Decreasing concentrations of Aβ_{1-42} were immobilized on the ELISA plate followed by incubation with anti-Aβ_{37-42} mAb (1:1000) or rabbit anti-Aβ_{37-42} antibodies (1:6000). Bound antibodies were detected with corresponding HRP-labeled secondary antibodies (see Figure 3-1).

Anti-mouse/rabbit Ig (H + L) - HRP

Murine / rabbit anti-peptide antibody

peptide

Figure 3-1 Direct ELISA

Anti-mouse/rabbit Ig (H + L) - HRP

Murine / rabbit anti-peptide antibody

Biotinylated peptide

Streptavidin

Figure 3-2 Solid Streptavidin-Based Sandwich ELISA Assay

Streptavidin-HRP

Biotinylated Aß peptide

Murine anti-Aß antibodies

Polyclonal goat anti-murine Ig
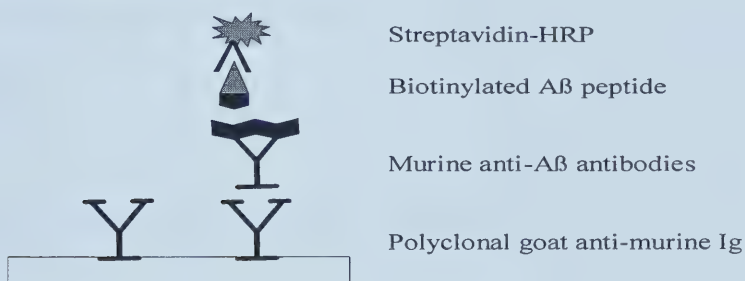
Figure 3-3 Solid Phase IgG-Based Sandwich ELISA Assay

Anti-mouse IgG1/IgM-HRP

Murine anti-Aβ_{1-40} BL01.94 [IgM]

Biotinylated Aβ_{1-40} peptide

Streptavidin

Inhibitor Antibody or Peptide
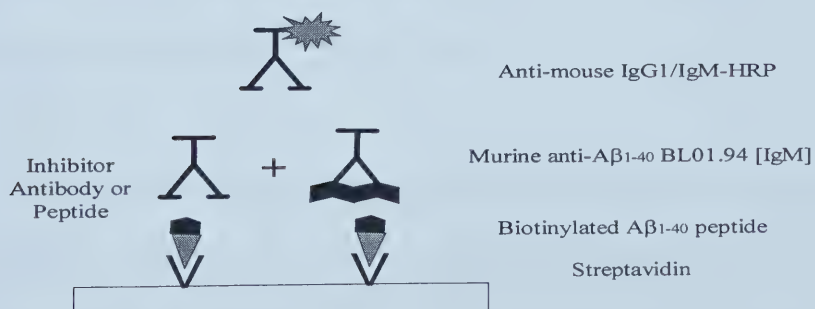
Figure 3-4 Sandwich Inhibition Assay

3.5 Specificity of the Antibodies (BL01.94 mAb, Rabbit Anti-APPβ Antibodies, BL03.21 mAb and Rabbit Anti-Aβ$_{37-42}$ Antibodies)

3.5.1. Characteristics of BL01.94

3.5.1.1 Binding Reactivity of BL01.94

Binding reactivity of BL01.94 towards the region of Aβ$_{1-16}$, the region of Aβ$_{25-35}$, and the C-terminal sequence of Aβ was determined by three competitive ELISA assays described in Section 3.4.9.

3.5.1.2. Binding Specificity of BL01.94 mAb to Neuroblastoma

SK-N-SH is a human neuroblastoma cell line, which secretes APP and Aβ. The SK-N-SH cell line was obtained from ATCC. SK-N-SH cells were adherent and maintained in standard medium (SM) (RPMI-1640 supplemented with 2mM L-glutamine, 50U/mL penicillin and 50U/mL streptomycin, 10% v/v FBS).

Cell ELISA for determining binding specificity of BL01.94 IgM mAb to neuroblastoma SK-N-SH cells were grown to a subconfluent state on 24 well plates. The BL01.94 IgM mAb and murine anti-human Aβ$_{1-16}$ IgG1 were incubated on the SK-N-SH cell-coated ELISA plate. Bound antibodies were detected with corresponding HRP-labeled secondary antibodies.

3.5.2. Characteristics of Anti-APPβ Antibodies

Binding specificity of rabbit anti-APPβ antibodies towards APP/APPβ was analyzed by using conditioned medium and cell lysate of SK-N-SH neuroblastoma cells with Western blot technology.

3.5.3 Characteristics of BL03.21

Antibody titers of BL03.21 mAb and rabbit anti-$A\beta_{37-42}$ antibodies on $A\beta_{1-40}$ and $A\beta_{1-42}$ coated plates were determined by ELISA assays described in Section 3.4.9.

Reactivity of BL03.21 mAb and rabbit anti-$A\beta_{37-42}$ antibodies towards decreasing concentrations of $A\beta_{1-40}$ and $A\beta_{1-42}$ were determined by ELISA assays described in Section 3.4.10.

3.6 Evaluation of the Potential Utility of the Antibodies for the Study of AD

3.6.1. Preliminary Study for the Development of a Sandwich ELISA Specific for $A\beta_{1-42}$

In order to develop a sandwich ELISA specific for $A\beta_{1-42}$, there were two sandwich ELISA designs which needed to be tested. First, capture antibody was anti-$A\beta_{37-42}$ BL03.21 mAb, detecting antibody was anti-$A\beta_{1-40}$ BL01.94 mAb. Second, purified rabbit anti-$A\beta_{37-42}$ antibodies were capture antibodies, anti-$A\beta_{1-40}$ mAb was detecting antibody.

Third, capture antibody was purified rabbit anti-Aβ_{37-42} antibodies and detecting antibody was anti-Aβ_{1-16} IgG1.

3.7 Evaluation of the Potential Utility of the Antibodies for AD Therapy

3.7.1. Investigating the Process of Aβ Aggregation by SDS-PAGE and AFM

3.7.1.1. Detection of Aβ Aggregation by SDS-PAGE (Tricine/Tris Containing 8M Urea)

A 15% polyacrylamide separating gel solution was prepared according to the protocol (Appendix II). The separating gel solution was pipetted into the assembled gel chamber. Water-saturated 2-butanol was overlaid on the top of separating gel solution until the gel was polymerized. Then 2-butanol was removed, and the gel was rinsed with deionized water. The water was also removed. The stacking gel solution was prepared. The stacking gel solution was poured on the top of the separating gel, the comb was inserted directly into the stacking gel until it polymerized. After complete polymerization, the gels were placed into the running chamber. The cathode buffer and anode buffers were added. The samples (125µM of Aβ_{1-40} in PBS at 4°C/37°C for I week) were diluted with 2× sample buffer and heated for 3-5min at 95°C. The samples, including the molecular weight markers, were loaded carefully in the sample pockets. The gel was run at 100V until the blue dye reached the end of the gel.

3.7.1.2. Investigating the Process of Aβ Aggregation by Atomic Force Microscopy

Atomic Force Microscopy (AFM) is part of a large family Scanning Probe Microscopy (SPM), which was invented in 1981 by Binning and Rohrer. AFM, developed in 1986, generates images based on the attraction and repulsion forces between the scanning tip and the samples on the slide. By scanning an AFM tip of a few nanometers in diameter over a sample, a three-dimensional view of the surface topology can be obtained. The versatility of this technique allows for the measurement of several different forces, often simultaneously, for a variety of images. All analyses can be conducted in air without special sample preparation. Even soft, easily damaged materials such as polymers or biological specimens can be imaged.

3.7.2. Principle of AFM

Atomic Force Microscopy is now becoming a standard instrument in surface science laboratories for obtaining images with atomic resolutions. AFM utilizes a sharp probe moving over the surface of a sample in a raster scan. In the case of the AFM (Figure 3-5), the probe is a tip on the end of a cantilever that bends in response to the force between the tip and the sample. When a tip, integrated to the end of a spring cantilever, is brought within the interatomic separations of a surface, interatomic potentials will be developed between the atoms of the tip and the atoms of the surface. As the tip travels across the surface, the interatomic potentials will then force the cantilever to bounce up and down

with the contours of the surface (Figure 3-6). Therefore, by measuring the deflection of the cantilever, the topographic features of the surface can be mapped.
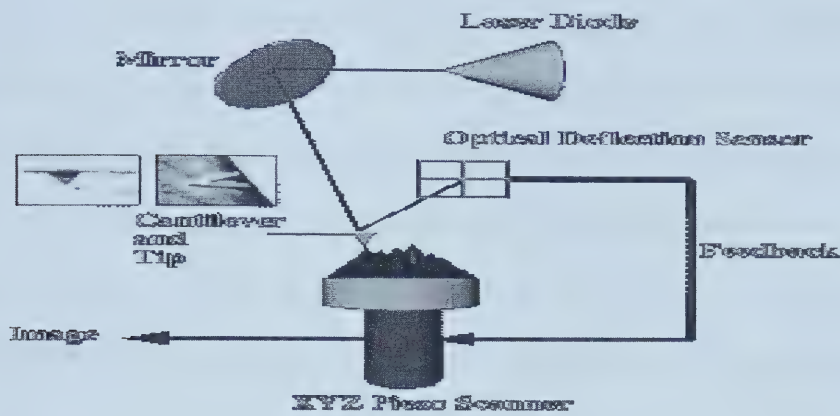
Figure 3-5 Atomic Force Microscopy
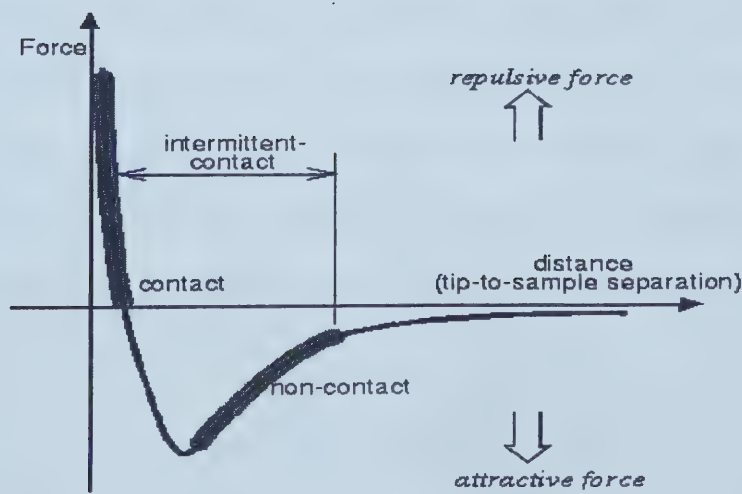
Figure 3-6 Inter-atomic Force vs. Distance Curve

Tapping mode (Figure 3-7) is a mode commonly used in AFM. When operated in air or other gases, the cantilever is oscillated at its resonant frequency (often hundreds of kHz) and positioned above the surface so that it only taps the surface for a very small fraction of its oscillation period. This is still contact with the sample in the sense defined earlier, but the very short time over which this contact occurs means that lateral forces are dramatically reduced as the tip scans over the surface. When imaging poorly immobilized or soft samples, tapping mode may be far better choice than contact mode for imaging.

Other (more interesting) methods of obtaining image contrast are also possible with tapping mode. In constant force mode, the feedback loop adjusts so that the amplitude of the cantilever oscillation remains (nearly) constant. An image can be formed from this amplitude signal, as there will be small variations in this oscillation amplitude due to the control electronics not responding instantaneously to changes on the specimen surface. Contact mode is the most common method of operation of the AFM. As the name suggests, the tip and sample remain in close contact as the scanning proceeds. By "contact" we mean in the repulsive regime of the inter-molecular force curve (see Figure 3-6).

Contact Mode   Non -Contact Mode   Tapping Mode
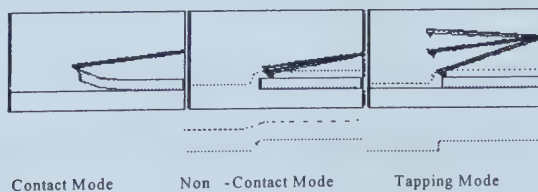
Figure 3-7 AFM Modes

The repulsive region of the curve lies above the x-axis. One of the drawbacks of remaining in contact with the sample is that there exist large lateral forces on the sample as the tip is "dragged" over the specimen.

Non-contact operation is another method, which may be employed when imaging by AFM. The cantilever must be oscillated above the surface of the sample at such a distance that we are no longer in the repulsive regime of the inter-molecular force curve. This is a very difficult mode to operate in ambient conditions with the AFM. A thin layer of water contamination, which exists on the surface on the sample will invariably form a small capillary bridge between the tip and the sample and cause the tip to "jump-to-contact". Even under liquids and in vacuum, jump-to-contact is extremely likely, and imaging is most probably occurring using tapping mode.

3.7.2.2 Sample Preparation

$A\beta_{1-40}$ was prepared in DMSO at 8mM. Then the stock solution was diluted into PBS at different concentrations 50µM, 115µM and 250µM and vortex mixing for 30 sec. Each concentration of $A\beta_{1-40}$ PBS solution was incubated at 4°C, room temperature and 37°C for 10min, 1day, 3 days or 1 week. After incubation, dry samples for *ex situ* imaging were prepared by pipetting 1µL of a mixed solution onto freshly cleaved mica and distributing it evenly, then washing it with DD H_2O, and drying in the air.

3.7.2.3 AFM Analysis

Topographic and phase data were generated on a Nanoscope IIIa MultiMode scanning probe workstation. Tapping Mode imaging was performed in air using etched (silicon nanoprobes) with cantilever length 125μm and resonant frequency (307-375kHz). Scan rates on all images were 2Hz. The drive vibration amplitude was 15 to 45mV generating a free cantilever vibration amplitude of 1V.

3.7.3. Inhibition of Aβ Aggregation by BL01.94 mAb and BL03.21 mAb

3.7.3.1. Atomic Force Microscopy

Sample preparation: All samples described in Table 3-8 were incubated at 37°C for 1 week. After incubation, dry samples for *ex situ* imaging were prepared by pipetting 1μL of a mixed solution onto freshly cleaved mica and distributing it evenly, then washing it with DD H_2O, and drying in the air.

3.7.3.2. Confocal Microscopy

Confocal laser scanning microscopy (CLSM) is a light microscopy imaging technique (introduced around 1980 by M. Petran and A. Boyde) which has found wide application in the biological sciences [c.f. Pawley,1990; Boyde, 1994]. It is now established as a

valuable tool for obtaining high-resolution images and 3-D reconstructions of a variety of biological specimens.

3.7.4 Principle of Confocal Microscopy

In Figure 3-8, the confocal principle is illustrated schematically for the epi-fluorescence imaging mode [c.f. Wilson & Sheppard, 1984; Lichtman, 1994]. To image the specimen point-by-point, a laser beam is deflected stepwise in the x- and y-directions by a scanning unit (not shown) before it is reflected by a dichroic mirror (beam splitter) so as to pass through the objective lens of the microscope, and focus onto the specimen. The emitted, longer-wavelength fluorescent light collected by the objective lens passes through the dichroic mirror (transparent for the longer wavelength) and traverses a small pinhole (i.e., the confocal aperture) to eliminate all the out-of-focus light, i.e., all light coming from regions of the specimen above or below the plane of focus. Therefore, the CLSM not only provides excellent resolution within the plane of the section (0.25 nm in x- and y-directions), but also yields similarly good resolution between Section planes (0.3 nm in z-direction). The in-focus information of each specimen point is recorded by a light-sensitive detector (i.e., a photo-multiplier) positioned behind the confocal aperture, and the analog output signal is digitized and fed into a computer. At the same time, the analog photo-multiplier signal can be used to generate a video image. The obvious advantage of having a stack of serial optical sections through the specimen pixel by pixel in digital form is that either a composite projection image can be computed (Figure 3-8), or a

volume-rendered 3-D representation of the specimen can be generated on a graphics computer.

Detector

Pinhole

Beam Splitter

Laser source

Objective lens

Specimen

Note: arrow heads denote light path direction
······ Out of focus light
———— In focus light
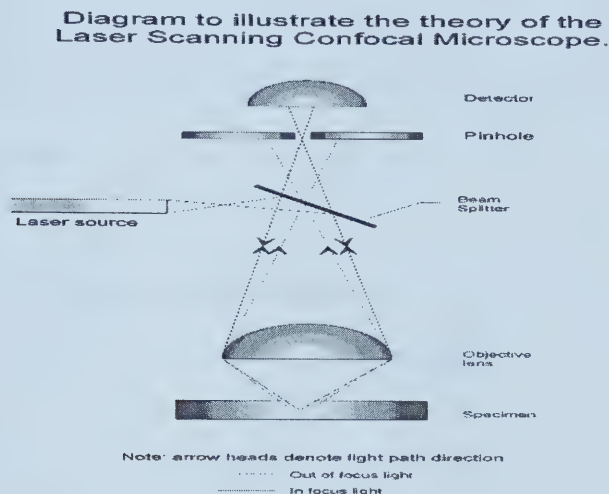
Figure 3-8 The Principle of Confocal Laser Scanning Microscope

Cell culture: One day before experiment, dendritic cells or macrophages were cultured in 8 chamber glass slides with RPMI-1640 supplemented with 2mM L-glutamine, 50U/mL penicillin and 50U/mL streptomycin, 10% v/v FB and GM-CSF. The cells were seeded at 5,000 cells/well. Cells were incubated at 37°C in a humidified atmosphere of 95% air, 5% CO_2.

Sample Preparation: 3 different samples were prepared. First, 16μg of biotin-Aβ_{1-40} was mixed in 200μL PBS alone and its concentration was 20μM. 16μg of biotin-Aβ_{1-40} was mixed with BL01.94 mAb at peptide to antibody molar ratio of 1:10 in 200μL PBS. 16μg of biotin-Aβ_{1-40} was also mixed with mouse IgM at peptide to antibody molar ratio of 1:10 in 200μL PBS (Table3-7). All samples were incubated with macrophages at 37°C for 2 hr

or overnight. After the cells were washed 3 times with PBS, the cells were fixed by using 3.7% formalin about 10 min. After 3 times washing with PBS, the cells were incubated with streptavidin-phycoerythrin for 30 min. Finally the cells were washed 3 times with PBS. A mixture of 70% glycerol in PBS was used as mounting medium prior to cover-slipping the specimens.

Table 3-7 Descriptions of Samples for Confocal Microscopy

No.	Description of samples
1	$A\beta_{1-40}$-biotin in PBS
2	$A\beta_{1-40}$-biotin with BL01.94 in PBS
3	$A\beta_{1-40}$-biotin with control IgM in PBS

*Aβ1-40-biotin : antibodies =10:1 molar ratio

Confocal analysis: The confocal images were taken with a Leitz Fluorescence Microscope with excitation at 458nm and emission at 514nm for scanning. Each sample was duplicated and a 1024 × 1024 pixel image of each was saved on the disk. Other parameters were used in this study as below: 40× 1.25 oil objective lens; pinhole, 90; off-set, 0; scan speed, 400Hz; image dimension, 750μM × 750μM × 0.00; beam expender, 6.

3.7.3. Inhibition of Aβ Neurotoxicity by BL01.94 mAb and BL03.21 mAb

Cell culture: SK-NSH cells were cultured routinely in RPMI-1640 + 2% FBS +1% streptomycin-penicillin-glutamine medium. Then growing cells were plated at approximately 3,600 cells/well with 100μL fresh culture medium in 96-well tissue culture plates.

Sample preparation: All samples described in Table 3-8 were incubated at 37°C for 1 week. The concentration of Aβ was at 50μM. The molar ratio of $Aβ_{1-40}$ to BL01.94 was 3.3:1/50:1 and non-specific IgM as negative control. The molar ratio of $Aβ_{1-42}$ to BL03.21 was 5:1/50:1 and 47.47 mAb as negative control. All samples were also used for testing the inhibition of Aβ aggregation by mAbs by using AFM.

MTT Reduction: Stock solution of MTT was prepared in RPMI at 5mg/mL. The solution was filter-sterilized (0.2μm), aliquoted, and stored at –20°C. After the cells were incubated with samples about 3 days, MTT (10μL) was added to a final concentration of 0.42mg/mL. The incubation was continued for a further 4-6hr. Cell lysis buffer (100μL/well; 20% (v/v) sodium dodecyl sulfate (SDS), 50% (v/v) N,N,-dimethylformamide, pH 4.7) was then added. The plate was kept at 37°C overnight. Next day, following mixing, colorimetric determination of MTT formazan product formation was made at 590nm.

Table 3-8 Descriptions of Samples for AFM and MTT Assay

No.	Description of Samples for AFM and MTT S Assay
1	$Aβ_{1-40}$ & BL01.94 mAb
2	$Aβ_{1-40}$ & control IgM
3	$Aβ_{1-40}$ alone
4	BL01.94 mAb
5	control IgM
6	$Aβ_{1-42}$ to BL03.21 mAb
7	$Aβ_{1-42}$ to 47.47 mAb
8	$Aβ_{1-42}$ alone
9	BL03.21 mAb
10	47.47 mAb

*Aβ peptides: antibodies in molar ratio

CHAPTER 4 RESULTS AND DISCUSSION

4.1 Generation of a Monoclonal Antibody Directed Against $A\beta_{1-40}$ (BL01.94)

4.1.1. Immunization and Measurement of the Immune Response in Mice

Two Balb/c mice were immunized with $A\beta_{1-40}$ or $A\beta_{1-40}$ conjugated to KLH. The induction of a specific $A\beta_{1-40}$ immune response in mice was measured by ELISA using biotinylated $A\beta_{1-40}$ immobilized on a streptavidin-coated plate. The results revealed that although $A\beta_{1-40}$ is of low molecular weight, the mouse immunized with non-conjugated peptide gave a better immune response toward $A\beta_{1-40}$ (as shown in Figure 4-1). The Aß peptide is known to self-aggregate *in vitro*, this phenomenon may explain the strong immune reaction induced in mice immunized with non-conjugated peptide. The mouse immunized with Aß$_{1-40}$ was chosen for hybridoma fusion. The serum was collected and the extent of immune response directed against $A\beta_{1-40}$ was analyzed using various serum dilutions. As shown in Figure 4-2, a very strong immune response could be observed at a serum dilution of 1/10,000 the day the fusion was performed. ELISA for measuring serum antibody titer was used to detect and quantify the antibodies in serum that we generated (Figure 4-3). The titer of the antibody in mouse serum raised against $A\beta_{1-40}$ was determined at 1:4,600 serum dilution. A positive signal could still be detected at a serum dilution as low as 1:10,000.
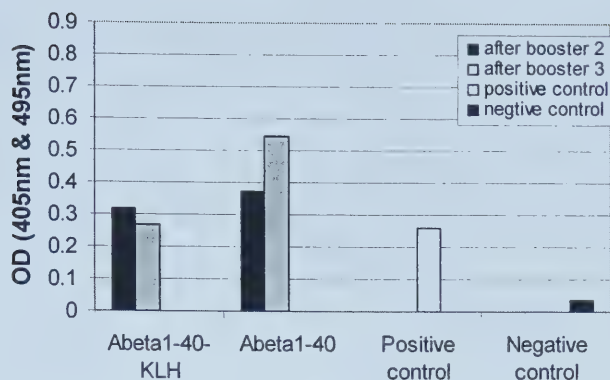
Figure 4-1: Measurement of the Immune Response in Mice Immunized with $A\beta_{1-40}$ and $A\beta_{1-40}$-KLH

The sera of mice collected after the second boost and third boost of immunization were tested for the presence of antibodies directed against $A\beta_{1-40}$. This experiment was performed by using biotinylated $A\beta_{1-40}$ immobilized on streptavidin ELISA coated plate, and mouse sera diluted at 1/100 (see MM section 3.4.3). The monoclonal antibody of murine anti-$A\beta_{1-16}$ (dilution 1/500, Chemicon international Inc.) was used as positive control. Mouse serum collected before immunization was used as negative control. (*$A\beta_{1-40}$ aggregate)
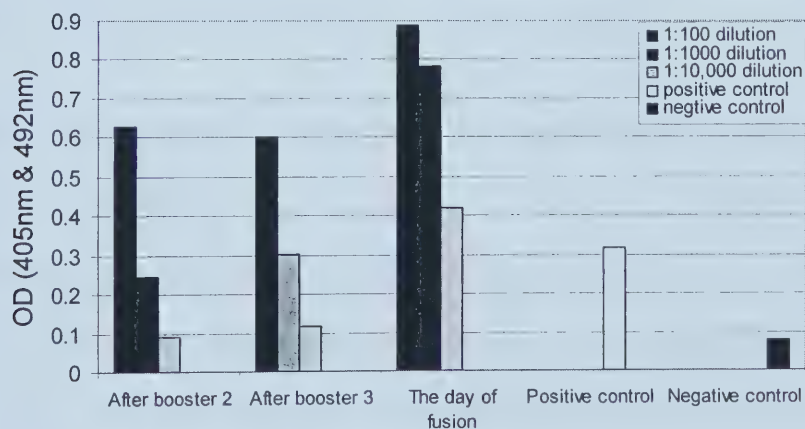
Figure 4-2 Detection of $A\beta_{1-40}$ Immunoreactivity in the Serum of the Mouse Immunized with $A\beta_{1-40}$

Mouse serum samples collected at different days were tested for the presence of antibodies directed against $A\beta_{1-40}$. The experiment was performed by using an ELISA plate coated with streptavidin, biotinylated $A\beta_{1-40}$, and diluted mouse serum (see MM section 3.4.3). The monoclonal antibody of murine anti-$A\beta_{1-16}$ (dilution 1/500, Chemicon International Inc.) was used as positive control. Mouse serum collected before immunization was used as negative control.

Titer of the antibody in mouse serum against A-beta1-40
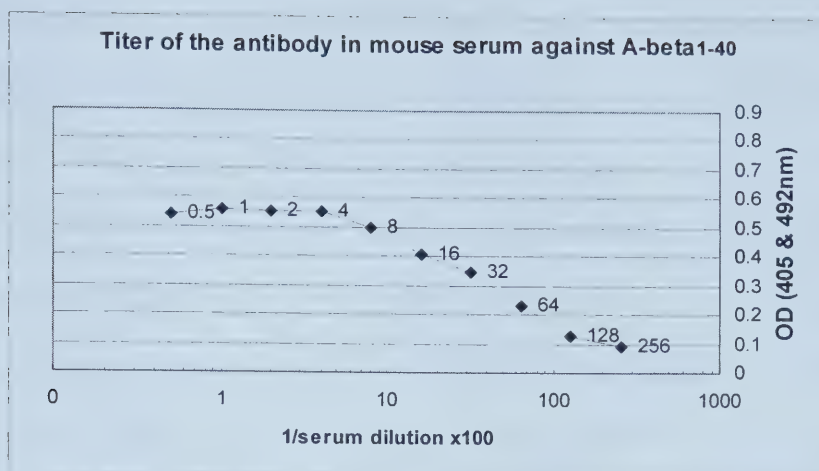
Figure 4-3 Detection of $A\beta_{1-40}$ Immunoreactivity in the Serum the Mouse Immunized with $A\beta_{1-40}$

Mouse serum samples collected at the day of fusion were tested for the presence of anti-$A\beta_{1-40}$ antibodies. This experiment was performed by using an ELISA plate coated with streptavidin, biotinylated $A\beta_{1-40}$, and diluted mouse sera (see MM section 3.4.3).

4.1.2 Screening of the Hybridoma Clones

The screening of the arising hybridoma clones was performed using 3 different ELISAs (See Materials & Methods 3.4.2. 3.4.3. 3.4.4.). First $A\beta_{1-40}$ was immobilized directly to the ELISA plate. Although a positive immunoreaction was observed with this assay when the serum of $A\beta$-immunized mice or when the anti-$A\beta_{1-16}$ mAb was used (data not shown or figure), only weak positive immunoreactions could be detected with the supernatant of arising clones. Because $A\beta_{1-40}$ is of low molecular weight, the immobilization of the peptide onto the plate may not be very efficient and this assay may therefore not be very sensitive. A second ELISA method was therefore tested that uses biotinylated $A\beta_{1-40}$ immobilized on a streptavidin coated plate. Only very few clones were detected as positive. It was questioned whether agents present in HT medium could compete and/or

73

inhibit the binding of antibodies to $A\beta_{1-40}$. For this reason, we developed a third screening assay that employs anti-murine antibodies as capturing agent. Only the immunoglobulins produced by the hybridoma clones were retained on the goat anti-murine polyvalent Ig coated plate and other proteins were washed away before biotinylated $A\beta_{1-40}$ was added. Using this method, a total of 78 clones were considered positive (OD of positive clones > $2 \times$ OD of negative control) and six of the most promising hybridoma clones (BL01.56, BL01.32, BL01.55, BL01.94, BL01.23, BL01.87) were chosen for recloning.

4.1.3. Recloning

As soon as positive wells are identified during the screening, the hybrid cells should be cloned. Cloning is important to reduce the risk of overgrowth by non-producing cells, and to ensure that the antibodies are truly monoclonal. The following criteria were measured to evaluate whether a hybridoma clone specific for $A\beta$ was isolated.

$$\text{The recloning efficiency: } \frac{\text{\# of wells with growing hybridoma cells}}{\text{Total \# of wells seeded}} \times 100 \qquad (4\text{-}1)$$

$$\text{\% of } A\beta_{1-40} \text{ immunoreactive clones: } \frac{\text{\# of } A\beta_{1-40} \text{ positive clones}}{\text{Total \# of clones}} \times 100 \qquad (4\text{-}2)$$

Poisson statistics indicate that if <22% of the wells have growing cells, it is considered to be a good recloning efficiency and 100% of $A\beta_{1-40}$ immunoreactive clones is expected for % of $A\beta$ clones to assure that we reached true monoclonality.

Of the 6 selected clones, 5 clones were frozen after first recloning step. BL01.94 was selected as the best clone and further recloned to ensure true monoclonality (Figure 4-4).

```
                        ┌─────────────────┐
                        │   Recloning     │
                        │ 6 selected clones│
                        └─────────────────┘
 1 ST recloning

┌──────────┐ ┌──────────────┐ ┌──────────┐ ┌──────────────┐ ┌──────────────┐ ┌──────────────┐
│ BL01.56  │ │  BL01.32     │ │ BL01.55  │ │  BL01.94     │ │  BL01.23     │ │  BL01.87     │
│ Re : 80% │ │ Re : 99% & 93%│ │ Re : 60% │ │ Re : 64% & 69%│ │ Re : 66% & 66%│ │ Re : 59% & 54%│
│ Aβ : 69% │ │ Aβ : 22% & 48%│ │ Aβ : 78% │ │ Aβ : 54% & 42%│ │ Aβ : 40% & 16%│ │ Aβ : 60% & 60%│
└──────────┘ └──────────────┘ └──────────┘ └──────────────┘ └──────────────┘ └──────────────┘

 2 nd recloning

                    ┌──────────────┐ ┌──────────────┐
                    │ BL01.94.R2   │ │ BL01.94.R4   │
                    │ Re : 38% & 78%│ │ Re : 56% & 57%│
                    │ Aβ : 78% & 84%│ │ Aβ : 92% & 100%│
                    └──────────────┘ └──────────────┘

      3        rd recloning

                              ┌────────────────────┐
                              │  BL01.94.R4.R1     │
                              │ Re : 82%, 50% & 37.5%│
                              │ Aβ : 100%, 100% & 97%│
                              └────────────────────┘

                              ┌────────────────────┐
                              │      IgM           │
                              │ BL01.94.R4.R1.R1   │
                              └────────────────────┘
```
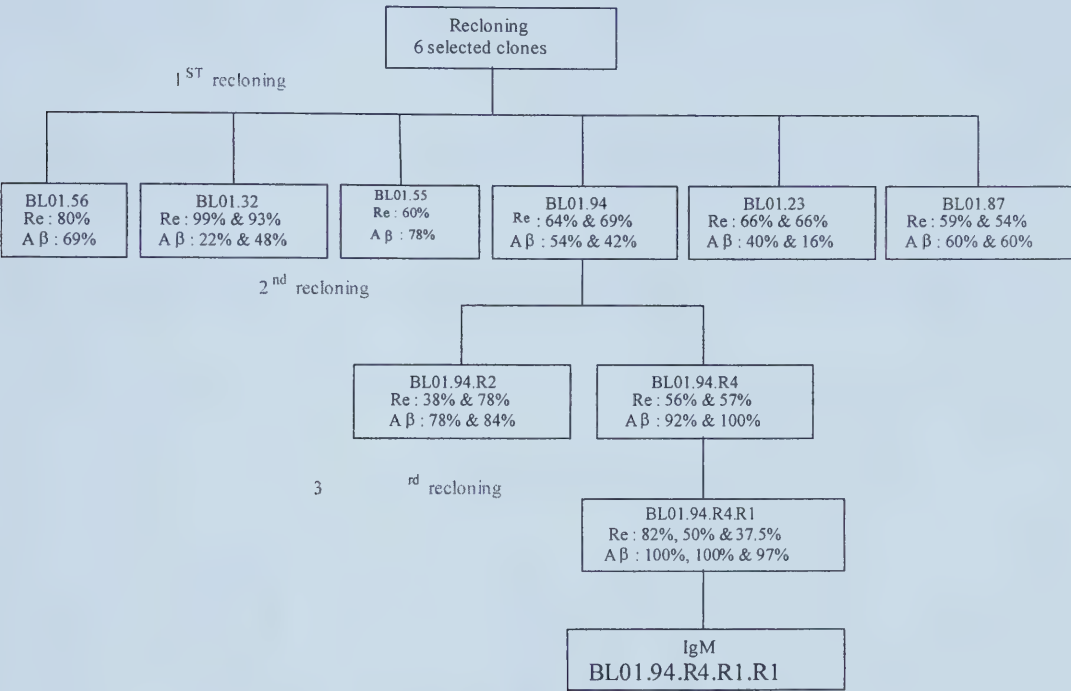
Figure 4-4 Sequence of Events Leading to the Production of BL01.94.R4.R1.R1 Hybridoma Clone

Re: Recloning efficiency; Aβ : $A\beta_{1-40}$ immunoreactivity

4.1.4. Characteristics of BL01.94 Hybridoma Clone

Growth characteristics of BL01.94 hybridoma cell line seeded at 2×10^5 cells/mL and maintained in SM for 7 days were determined. Every day, the number of cells was counted and the viability of the cells was determined using a hemacytometer and trypan blue exclusion assay. mAb production was tested by ELISA with biotinylated $A\beta_{1-40}$

75

immobilized on a streptavidin-coated plate (Figure 4-5). The cell number reached a maximum at day 4 of the experiment whereas the viability of the cells declined rapidly immediately after seeding. The concentration of antibody in the culture medium increased rapidly from day 1 to day 3.

Ascites production in mice: Ascites can be produced in mice pretreated with pristane (0.7 mL/mouse) and injected with 4×10^6 cells. An average of 5 mL of ascites/mouse could be collected (2 taps total). The concentration of BL01.94 mAb in ascites was calculated to be 7.8 mg/mL.

Growth Characteristics

(a)

Viability of BL01.94

(b)

Secretion of BL01.94 mAb by hybridomas

(c)
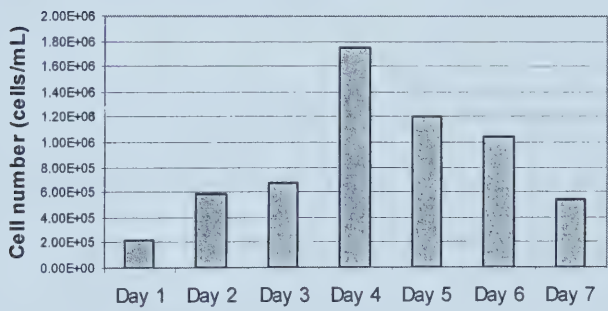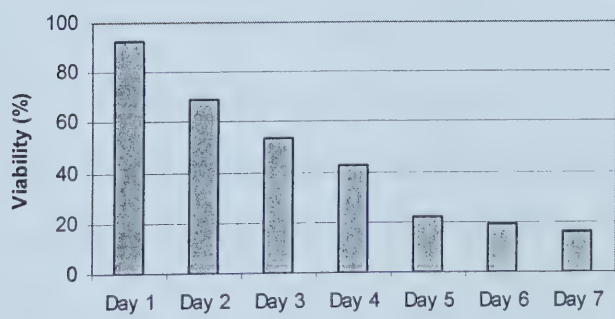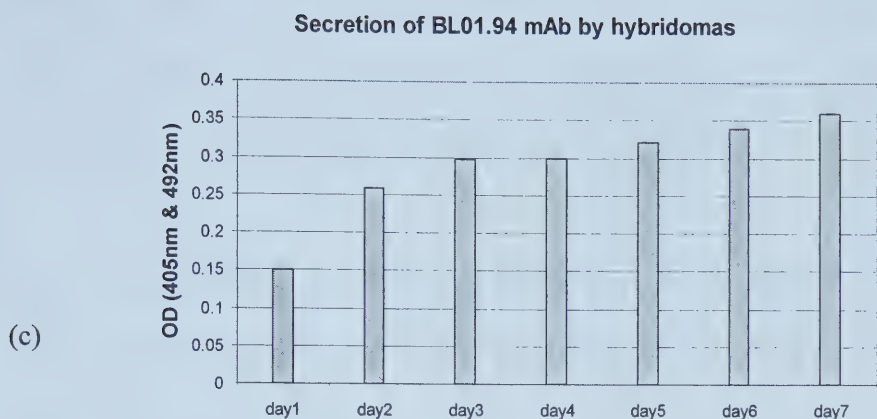
Figure 4-5 Growth Characteristics of BL01.94 Hybridoma Clone

Hybridoma cells were grown for 7 days in standard medium. Every day the cell number and viability were measured. The culture medium was collected and the amount of secreted anti-Aß antibodies was evaluated by using biotinylated $Aß_{1-40}$ immobilized on streptavidin ELISA coated plate.

4.1.5. Characteristics of BL01.94 Antibody

Isotype: Using the clonotyping system-HRP kit (Southern Biotechnology Associates Inc) we identified BL01.94 as an IgMk mAb. Using this same kit we also tested some other positive clones. Interestingly all the clones tested secreted IgM mAbs. This might be related to the third screening assay that employs anti-murine antibodies as capturing agent. Only the immunoglobulins produced by the hybridoma clones were retained on goat anti-murine polyvalent Ig coated plate and other proteins were washed away before biotinylated $Aß_{1-40\ was}$ added. IgM has more binding sites than IgG and give strong signal. It may be the mouse that did not develop strong immune response. If the present immune response against $Aß_{1-40}$ in immunized mouse serum can be detected, we will know the answer.

Binding specificity: Direct Binding ELISA assays and Competitive ELISA assays using various Aβ peptides and anti-Aβ mAbs of known specificities were carried out in order to identify the epitopes within Aβ peptide recognized by BL01.94.

Direct Binding ELISA assays: The first ELISA was performed on a BSA-Aβ$_{37-42}$ peptide coated plate. In Figure 4-6, with BL03.21 as positive control, it showed a weak binding between BL01.94 and BSA-Aβ$_{37-42}$ peptide.

The second ELISA was performed on an Aβ$_{25-35}$ peptide coated plate. BL01.94 binds weakly to Aβ$_{25-35}$ peptide (data not shown). Because there was no positive control, the binding specificity of BL01.94 to Aβ$_{25-35}$ peptide should be determined by Competitive ELISA assays
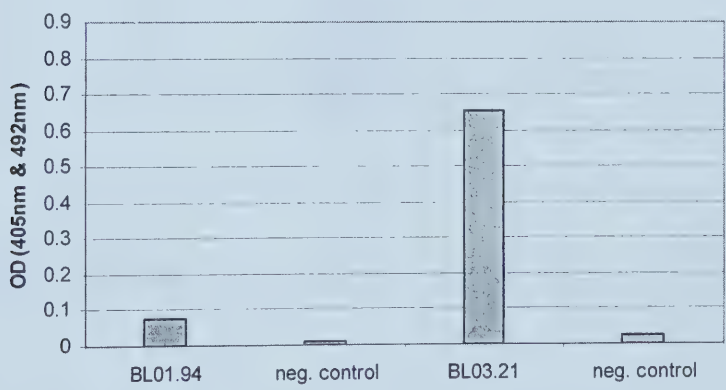
Figure 4-6 Comparison of Direct Binding Specificity of BL01.94/BL03.21mAbs to Aβ$_{37-42}$ Peptide.

Three Competitive ELISA assays: The first competitive ELISA assay is an ELISA plate coated with streptavidin, biotinylated Aβ$_{1-40}$, following an incubation with BL01.94 alone or with BL01.94 mixed with Aβ$_{1-16}$ (See MM section 3.4.9.). The monoclonal antibody of

murine anti-Aβ_{1-16} (dilution 1/500) was used as positive control. The concentration of anti-Aβ mAbs used in this assay was shown to be non-saturating. As shown in Figure 4-7, Aβ_{1-16} peptide did not inhibit the binding of BL01.94 to Aβ_{1-40} whereas a complete inhibition was observed with the anti-Aβ_{1-16} mAb was used as positive control mAb. It should be noted that in this assay, Aβ_{1-16} peptide inhibits the binding of anti-Aβ_{1-16} mAb to Aβ_{1-40} at a concentration as low as 0.156µg/mL (data not shown). Using the same ELISA format, we also show the absence of inhibition for BL01.94 mAb was observed for large excess of Aβ_{1-16} peptide at 10µg/mL.

■ BL01.94 □ BL01.94 + Abeta1-16 □ anti-Abeta1-16 IgG1 ■ anti-Abeta1-16 IgG1+Abeta1-16
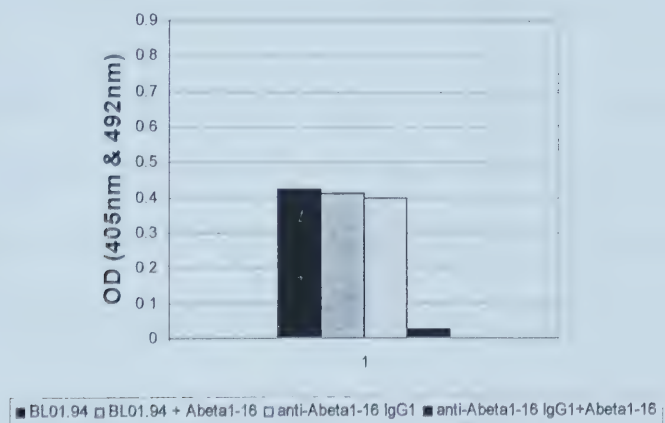
Figure 4-7 Inhibitory Effect of Aβ_{1-16} on the Binding of BL01.94 to Aβ_{1-40}

The second competitive ELISA assay is an ELISA plate coated with streptavidin, biotinylated Aβ_{1-40}, following an incubation with BL01.94 alone or with BL01.94 mixed with anti-Aβ_{1-16} IgG1. For concentrations of BL01.94 mAb used in this assay was shown to be non-saturating. The absence of inhibition with mouse anti Aβ_{1-16} IgG1 is shown in

Figure 4-8. The absorbance of BL01.94 mixed with anti-Aβ_{1-16} IgG1 was equal to the total absorbance from anti-Aβ_{1-16} IgG1 and BL01.94 alone.

IgG1: mouse anti-Aβ_{1-16}
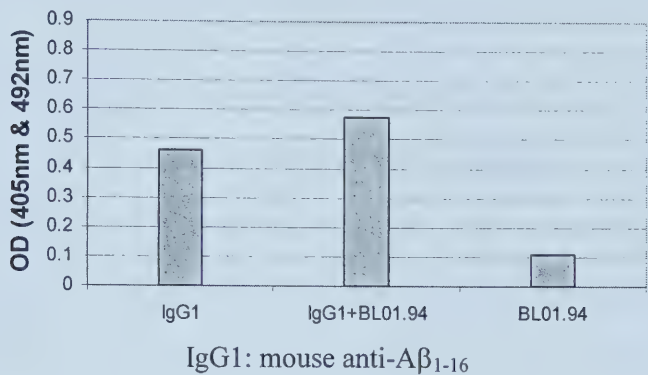
Figure 4-8 Inhibitory Effect of Anti-Aβ_{1-16} mAb on the Binding of BL01.94 to Aβ_{1-40}

The third competitive ELISA is an ELISA plate coated with streptavidin, biotinylated Aβ_{1-40}, following an incubation with BL01.94 alone or with BL01.94 mixed with Aβ_{25-35} peptide. The results showed in Figure 4-9. Large excess of Aβ_{25-35} peptide was added, and there was only a weak binding between Aβ_{25-35} peptide and BL01.94 mAb.
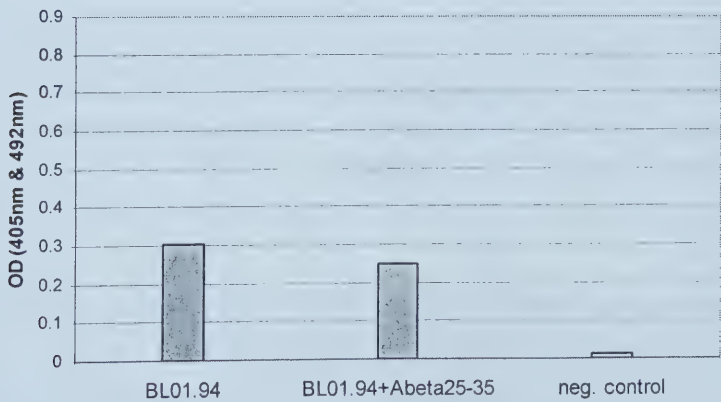
Figure 4-9 Inhibitory Effect of Aβ_{25-35} on the Binding of BL01.94 to Aβ_{1-40}

These results therefore demonstrate that the epitope recognized by BL01.94 is not included within the first 16 amino acids of the amyloid peptide, the 25 to 35 amino acid domain of amyloid peptide or the 37 to 42 amino acid domain of amyloid peptide.

Purification: BL01.94 mAb (IgM) was purified from ascites fluid by using either Mannan Binding Protein affinity chromatography or Euglobulin precipitation. The chromatography profile of the Mannan binding protein affinity chromatography is shown in Figure 4-10. Using this method, a total of 42mg of antibody was purified from 10 mL of ascites (yield 55%). Compared to affinity chromatography, the purification of BL01.94 by Euglobulin precipitation resulted in a much lower yield of BL01.94 from 10 mL of ascites. The purity of BL01.94 mAb (IgM) was checked by using SDS-PAGE was 93%.
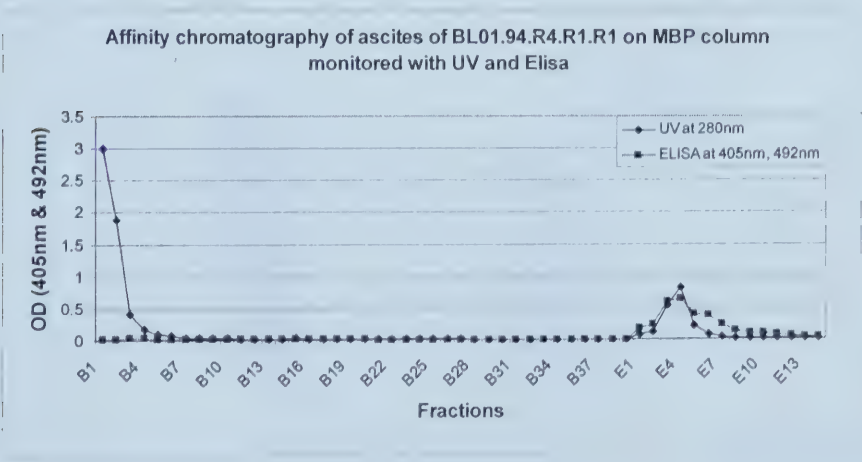
Figure 4-10 Purification of BL01.94 by Affinity Chromatography on Mannan Binding Protein Column

BL01.94 mAb (IgM) was purified from ascites by Affinity Chromatography on an MBP column as described in MM (section 3.2.6.2.). Elution of the proteins was monitored by measuring the absorbance at 280 nm. The elution of BL01.94 was monitored by ELISA using a streptavidin-coated plate.

4.2 Generation of Monoclonal and Polyclonal Antibodies Directed against $A\beta_{37-42}$

4.2.1 Generation of a Monoclonal Antibody Directed against $A\beta_{37-42}$ (BL03.21)

4.2.1.1 Immunization and Measurement of the Immune Response in Mice

Two mice were immunized with $A\beta_{37-42}$ conjugated to KLH. The induction of a specific $A\beta_{37-42}$ immune response in mice was measured by ELISA using plates coated with $A\beta_{37-42}$-BSA. As shown in Figure 4-11, mouse # 1 gave a slightly higher immune response than mouse # 2 and was therefore chosen for hybridoma fusion. The immune response of mouse #2 was monitored until the day of fusion (Figure 4-12).
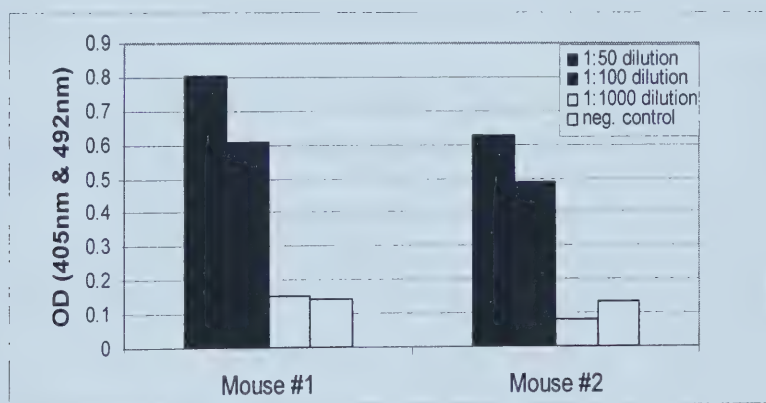
Figure 4-11 Measurement of the Immune Response in Mice Immunized with $A\beta_{37-42}$-KLH

The sera of mice collected after the second boost of immunization were tested for the presence of the antibody against $A\beta_{37-42}$ by ELISA assay. This experiment was performed by using $A\beta_{37-42}$-BSA immobilized on ELISA plate, and mouse sera diluted at 1/50, 1/100, 1/1000 (see MM section 3.4.5.). Mouse serum collected before immunization was used as negative control.
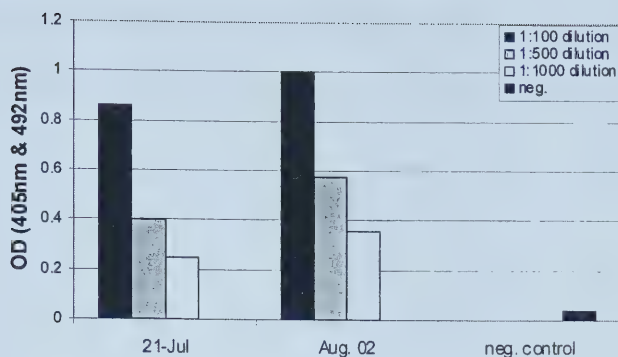
Figure 4-12 Detection of Aß$_{37-42}$ Immunoreactivity with BSA-conjugate in the Serum of the Mouse Immunized with Aß$_{37-42}$-KLH

Mouse serum samples collected on different days were tested for the presence of antibodies directed against Aß$_{37-42}$. This experiment was performed by using ELISA plate coated with Aß$_{37-42}$-BSA and diluted mouse sera (see MM section 3.4.5.). Mouse serum collected before immunization was used as negative control.

4.2.1.2. Screening of the Hybridoma Clones

The arising clones were first tested for their ability to secrete antibodies directed against Aβ$_{37-42}$ using ELISA plates coated with BSA-Aβ$_{37-42}$. Using this method, a total of 50 positive clones were identified. Positive clones were transferred to 24 well plates and further tested for their immunoreactivity towards full length Aβ$_{1-40}$ and Aβ$_{1-42}$ (peptide coated to the plate directly). Clones presenting a strong immunoreactivity for Aß$_{1-42}$ were also positive for Aß$_{1-40}$. Two outstanding clones BL03.01 and BL03.21 were chosen for recloning.

4.2.1.3 Recloning

BL03.01 and BL03.21 were recloned by limiting dilution as described in MM. After the first recloning BL03.01 was kept frozen and BL03.21 was subjected to an additional

recloning (Figure 4-13). The same criteria, recloning efficiency and % of positive clones, were used to determine whether the selected clones were efficiently recloned.


```
                        ┌─────────────────────┐
                        │   FUSION BL03       │
                        └─────────────────────┘
                          ┌───────────────────┐
                          │   Screening       │
                          │   50 positive clones │
                          └───────────────────┘
                          ┌───────────────────┐
                          │   Recloning       │
                          │   2 selected clones │
                          └───────────────────┘
```

1ST recloning

BL03.01	BL03.21
Re : 62%, 69%, 33% & 53%	Re : 52%, 34% & 26%
Aβ_{37-42}: 100%, 100%, 100% & 100%	A β_{37-42} : 100%, 97% & 100%

2nd recloning

BL03.21.R1
Re : 22% & 22%
Aβ_{37-42} 100% & 100%

IgG1

BL03.21.R1.R1

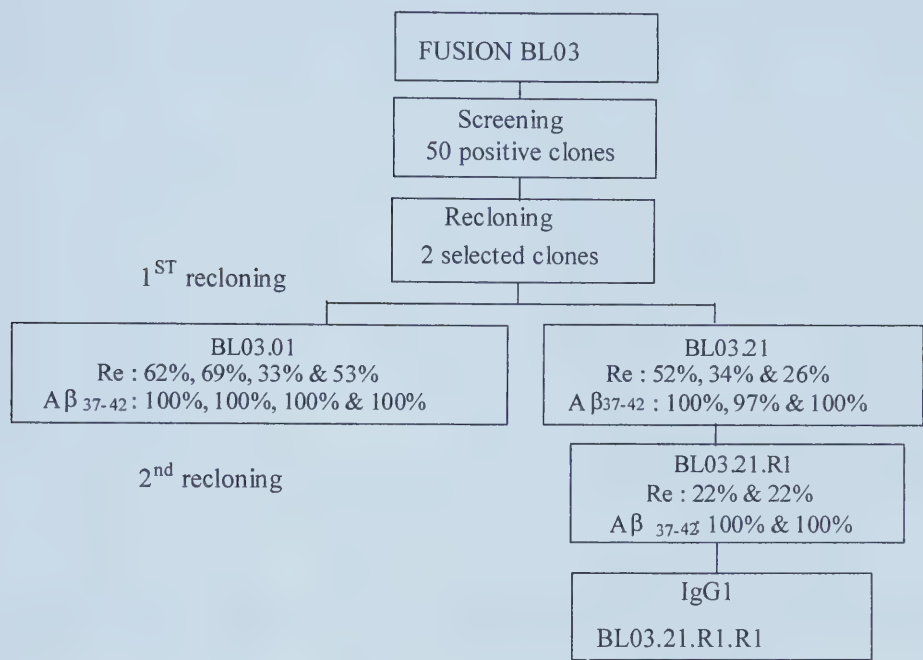**Figure 4-13 The Sequence of Events Leading to the Production of BL03.21 Hybridoma Clone**

*Re: Recloning efficiency; Aβ_{37-42}: Aβ_{37-42} immunoreactivity

4.2.1.4 Characteristics of BL03.21 Antibody

Isotype: The isotype of BL03.21 mAb was determined by ELISA with clonotyping system-HRP kit (Southern Biotechnology Associates Inc). BL03.21 mAb was identified as IgG1k.

Binding specificity: The specificity of BL03.21 mAb toward the $A\beta_{1-40}$ or $A\beta_{1-42}$ peptide was tested by ELISA assay (see MM section 3.4.10.). 5μg/mL of $A\beta_{1-40}$ and $A\beta_{1-42}$ coated ELISA plates were incubated with different dilutions of BL03.21 mAb (Figure 4-14). This figure shows BL03.21 bind to $A\beta_{1-42}$ specifically but not to $A\beta_{1-40}$.
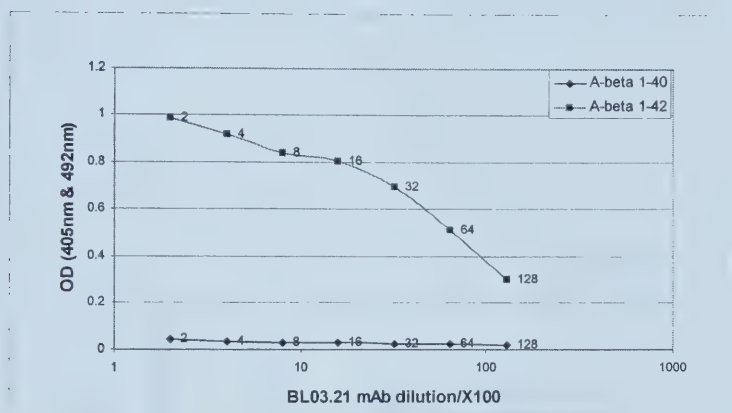
Figure 4-14 The Specificity of BL03.21 mAb Toward the $A\beta_{1-40}$ or $A\beta_{1-42}$ Peptide

Ascites production in mice: Ascites can be produced in mice pretreated with pristane (0.7 mL/mouse) and injected with 4×10^6 cells. An average of 5 mL of ascites / mouse could be collected (2 taps total).

Purification: BL03.21 mAb (IgG1) was purified from ascites fluid by affinity chromatography on Protein G column. The purity of BL03.21 mAb (IgG1) checked by using SDS-PAGE, was up to 98%.

4.2.2 Generation of Polyclonal Antibodies Directed against $A\beta_{37-42}$

Polyclonal antibodies directed against $A\beta_{37-42}$ were generated from the NZW rabbit. The binding of polyclonal antibodies directed against $A\beta_{37-42}$ was determined by ELISA assay as described in MM. The immune response in rabbit sera was monitored (Figure 4-15). The immunoreactivity of polyclonal antibodies directed against $A\beta_{37-42}$ in rabbit sera was determined at different serum dilutions. Maximum immunoreactivity for $A\beta_{37-42}$ was observed after Booster 2. Subsequent boosts did not enhance the immune response and a decrease of immunoreactive signal was even observed. For this reason the rabbit was sacrificed. A total of 110 mL of rabbit serum was collected.
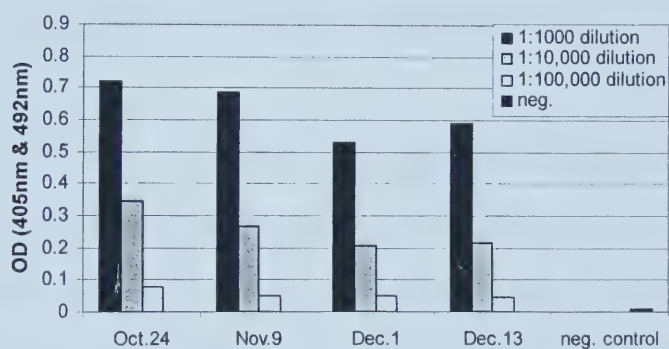
Figure 4-15 Detection of Aß$_{37-42}$ Immunoreactivity with BSA-conjugate in the Serum of the Rabbit Immunized with $A\beta_{37-42}$-KLH

Binding sepcifity: The binding of polyclonal antibodies on $A\beta_{1-40}$ and $A\beta_{1-42}$ coated ELISA plates is shown in Figure 4-16. This figure shows that the polyclonal antibodies bound to $A\beta_{1-42}$ peptide specifically, and weak binding to $A\beta_{1-40}$ peptide.

.

Purification: Polyclonal antibodies directed against $A\beta_{37-42}$ were purified from rabbit sera by affinity chromatography on a Protein G column. The purity of polyclonal antibodies directed against $A\beta_{37-42}$ was about 90% by SDS-PAGE.

Figure 4-16 The Specificity of Rabbit Sera towards the $A\beta_{1-40}$ or $A\beta_{1-42}$ Peptide

4.3 Generation of Polyclonal Antibodies Directed against APPβ

Polyclonal antibodies directed against APPβ were generated from the NZW rabbit. The binding of polyclonal antibodies directed against APPβ was determined by ELISA assay using a biotinylated APPβ-coated plate (described in MM). The immune response in rabbit sera was monitored (Figure 4-17). Maximum immunoreactivity for APPβ was observed after Booster 2. Subsequent boosts did not enhance the immune response and a decrease of immunoreactive signal was even observed. For this reason the rabbit was sacrificed. A total of 95 mL of rabbit serum was collected. The titers of polyclonal antibodies directed against APPβ in rabbit sera were determined to be 1:58,000 serum dilution. The maximum dilution of the rabbit sera was up to 1:200,000 for the immunoreactivity against APPβ.
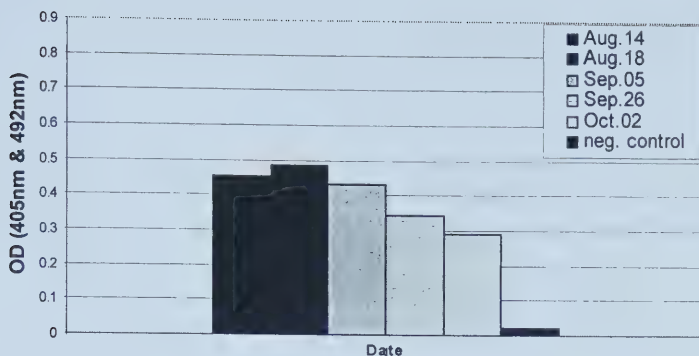
Figure 4-17 Detection of APPβ Immunoreactivity in the Serum of the Rabbit Immunized with APPß-KLH

Rabbit serum samples collected on different days were tested for the presence of antibodies directed against APPβ. This experiment was performed by using an ELISA plate coated with APPβ-biotin and diluted rabbit sera (see MM section 3.4.8.). Rabbit serum collected before immunization was used as a negative control. The titer of polyclonal antibodies against APPβ in rabbit sera declined gradually.

Binding specificity: APPβ+2 peptide has two more amino acid than the APPβ peptide. Both peptides are small fragments of APP. The C-terminus of APPβ peptide is the β-secretase cleavage site. Binding specificity of polyclonal antibodies toward APPβ & APPβ+2 peptide is shown in Figure 4-18. At lower serum dilutions, polyclonal antibodies show a strong immunoreactivity for APPβ peptide and a lower extant APPβ+2 peptide. However, as the serum dilution reached as high as 1:10,000, polyclonal antibodies directed against APPβ were more specific for APPβ peptide. We also need to test the binding specificity of our polyclonal antibodies toward full-length APP.

Purification: Polyclonal antibodies directed against APPβ were purified from rabbit sera by affinity chromatography on a Protein G column. The purity of polyclonal antibodies directed against APPβ was about 90% by SDS-PAGE.

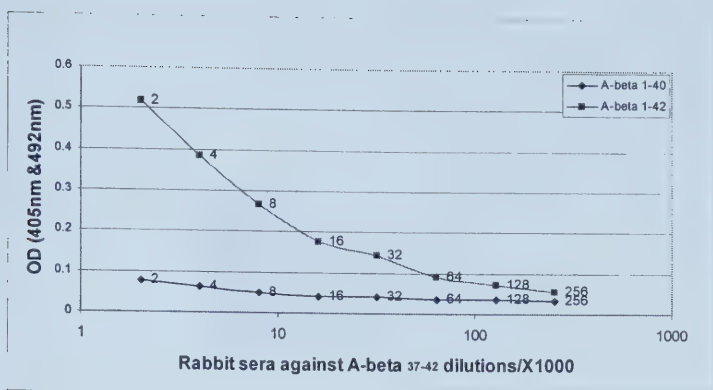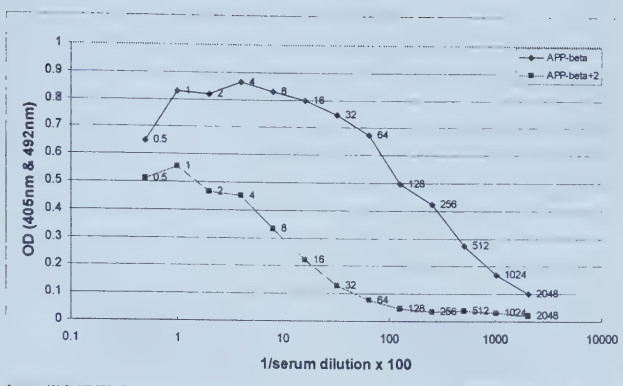**Figure 4-18 The Specificity of Rabbit Sera Toward the APPβ or APPβ+2 Peptide**

The specificity of rabbit sera toward the APPβ or APPβ+2 peptide was tested by ELISA assay (see MM section 3.4.7.). This figure shows rabbit sera against APPβ bound to the APPβ specifically at higher dilutions, and at lower dilutions rabbit sera bound to both of them. However, rabbit sera bound to APPβ peptide much stronger than to APPβ+2 peptide.

4.4 Evaluation of the Potential Utility of the Antibodies for the Study of AD

4.4.1 Preliminary Study for the Development of a Sandwich ELISA Specific for Aβ₁₋₄₂

The brain and cerebrospinal fluid of AD patients contain altered levels of Aβ peptide, mainly $A\beta_{1-40}$ and $A\beta_{1-42}$. Measurement of the Aβ level in human CSF or serum is of importance for understanding the disease mechanisms. Reliable methods will be needed. Three different ELISA assays were designed for this purpose. Two assays in total could be used to detect synthetic Aβ peptide. Capture antibody--anti-$A\beta_{37-42}$ BL03.21 mAb, detecting antibody-anti-$A\beta_{1-40}$ BL01.94 mAb; purified rabbit anti-$A\beta_{37-42}$ antibodies as capture antibodies, anti-$A\beta_{1-40}$ mAb as detecting antibody (Figure 4-19). Whether these two assays can detect Aβ peptide from human body fluid and the specificity of them toward $A\beta_{1-42}$ needs to be further tested.
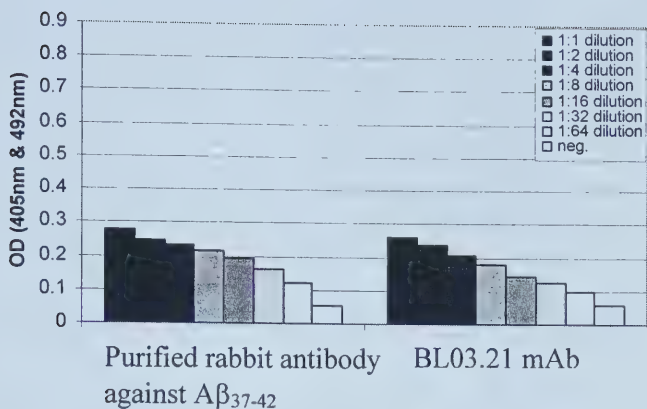
Figure 4-19 Sandwich ELISA Assay for Specifically Detecting Aβ$_{1-42}$ Peptide

Aβ$_{1-42}$ (1μg/mL) was incubated on the BL03.21 mAb/purified rabbit antibody (5μg/mL) coated ELISA plate, followed by incubation with different concentrations of BL01.94 mAb. Bound antibodies were detected with corresponding HRP-labeled secondary antibody.

4. 5 Evaluation of the Potential Utility of the Antibodies for AD Therapy

4.5.1 Inhibition of Aβ Aggregation

4.5.1.1 Detection of Aβ Aggregation by SDS-PAGE

125μM of Aβ$_{1-40}$ peptide was aged for 1 week at 37 °C. On the tricine gel, only dimeric Aβ was observed and different sizes of Aβ aggregates were not observed. 15% native gel was also tried; even dimeric Aβ could not observed. We expected dimer, tetramer, hexamer and oligomers Aβ may show on the gel. There is one possibility, which can explain what we observed in this experiment. One is 125μM of Aβ$_{1-40}$ that formed large aggregates. Those aggregates were too large to enter into the gel. 115μM of Aβ$_{1-40}$ was

90

studied by AFM, and large aggregates were observed. Also maybe SDS has some effect on Aβ aggregates, it needs to be clarified in the future.

4.5.1.2 Investigating the Process of Aβ Aggregation by AFM

AFM could reveal more detailed information about the process of Aβ peptide aggregation. It was thought that fibril formation proceeds via a nucleation dependent mechanism. In order to investigate what factors could effect on the aggregation of Aβ, different concentrations of Aβ in PBS were prepared and incubated in 4°C, RT or 37°C with different time intervals (See Materials & Methods). All results in Figure 4-20, Figure 4-21 & Figure 4-22 showed that the aggregation of Aβ is temperature-, concentration- and time dependent.
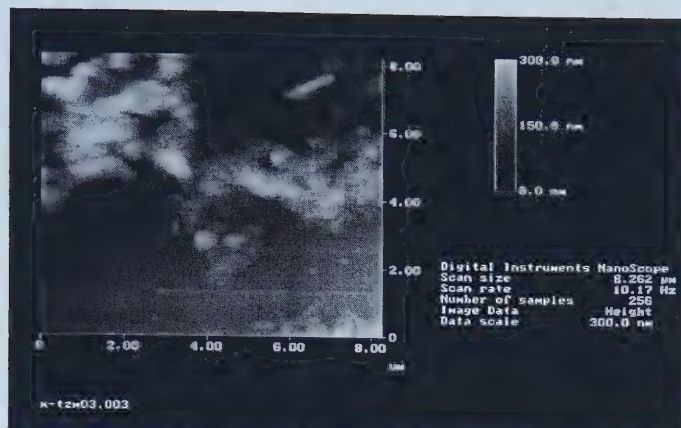
a. 4°C
amorphous aggregates, with no order and no orientation.
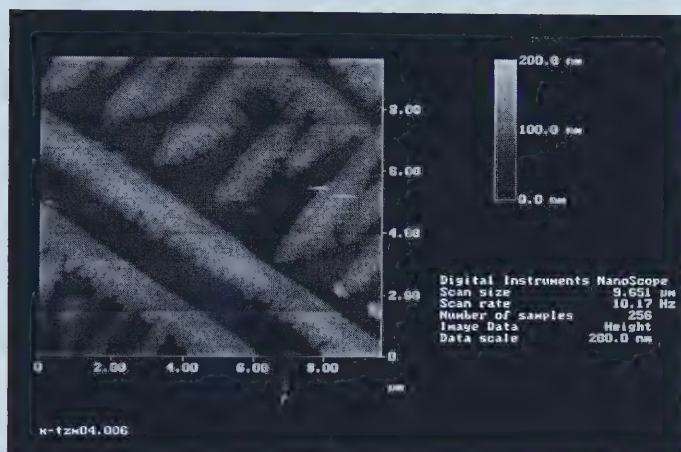
b. room temperature
elongated, narrow sheets with order and characteristic orientation. The height of sheets was up to 200nm.
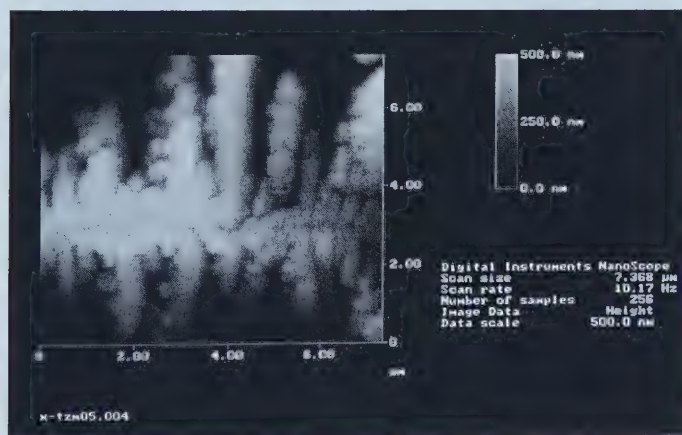
c. 37°C
elongated sheets with order and characteristic orientation. The growth of sheets was much more significant in Y direction and Z direction. The height of sheets was up to 500nm.

Figure 4-20 The Temperature Course of Aβ Aggregation
115μM of Aβ$_{1-40}$ peptide solution was incubated at 4°C (a), room temperature (b) or 37°C (c) for 1 week.
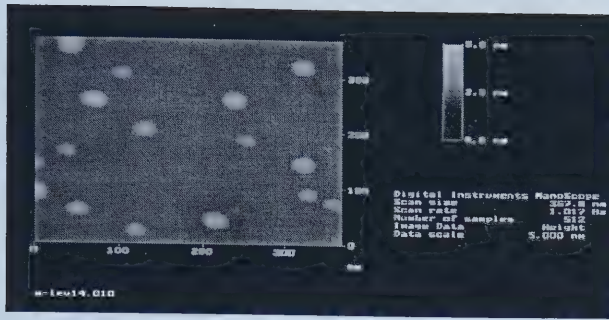
a. 10μM

At such lower concentration, globular aggregates of Aβ did not extend into sheets after one-week incubation at 37°C.

b. 50μM
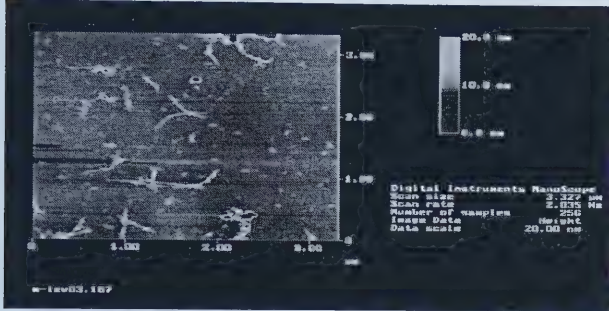
At 50μM, globular aggregates of Aβ did extend into protofibrils after one-week incubation at 37°C

c. 115μM

With the increasing concentration of Aβ peptide, oriented growth of Aβ sheets was significant.
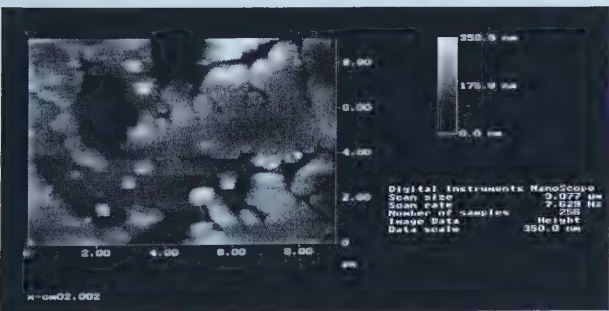
d. 250μM

At the highest concentration of Aβ peptide, the extension of Aβ sheets was more rapid. In this image, some small globular aggregates were sticking onto the larger sheets.

Figure 4-21 The Concentration Dependency of Aβ Aggregation

10, 50, 115, 250μM of Aβ$_{1-40}$ peptide solutions were incubated at 37°C for 1 week.

93

a. 10 minutes
Globular aggregates of Aβ appear on the surface of mica immediately after dissolution in PBS.

b. 1 day
After one-day incubation, globular aggregates of Aβ tend to gather together.

c. 3 days
Three days later, Aβ peptide aggregated into elongated, narrow sheets with characteristic orientation. The height of sheets was up to 400nm.

d. 7 days
At one week, those narrow sheets extended randomly into amorphous sheets. The height of the sheets reached to 800nm.

Figure 4-22 The Time Course of Aβ Aggregation

115μM of Aβ$_{1-40}$ peptide solutions were incubated at 4°C for 10 minute, 1 day, 3 days or 7 days.

4.5.1.3 Discussion of the Course of Aβ Aggregation

Recent studies of AD focused more and more on the structural properties of Aβ peptide and its fibrils, particularly, in the *in vitro* study of Aβ aggregation by AFM. Stine et al (1996) studied the 3-dimensional structure of the Aβ fibrils. They used Aβ in PBS in concentrations ranging from 10 to 500μM at room temperature for periods from a few minutes to 120 hours. Their study demonstrated that AFM imaging of Aβ fibrils could provide information on z-axis, the thickness of fibril features with nanometer resolution. They confirmed that AFM could be used to follow the course of Aβ aggregation and help define the mechanisms of Aβ aggregation. Under similar conditions, Kowalewski and Holtzman (1999) studied Aβ aggregation on two solid surfaces: hydrophilic mica and hydrophobic graphite. Their study suggested that the formation of Aβ aggregation might be driven by interactions at the interface of aqueous solutions and hydrophobic substrates. Harper *et al* (1997) studied the differences between $A\beta_{1-40}$ (45μM) and $A\beta_{1-42}$ (20μM) at several time points at room temperature and found $A\beta_{1-42}$ might play a role in the early steps of the process of Aβ aggregation.

In order to study the course of Aβ aggregation, our laboratory focused on the factors such as: time, temperature, and concentration, which may contribute to Aβ peptide aggregation. To study the interaction of those factors, several parameters for each factor were examined. Sampling times were chosen at 10 minutes, 1 days, 3 days and 7 days during the test. The concentrations of the Aβ in PBS in the tests were set at 10, 50, 115 and

250μM. Each concentration of Aβ was incubated either at 4°C, room temperature or 37°C for periods from 10 minutes to 7 days. Then, all dry samples were prepared as mentioned in the Materials & Methods section. The AFM imaging of this study is discussed below.

In the study, it was found that incubation temperature has significant impact on the structure of Aβ aggregation. 115μM of Aβ in PBS with 1 week incubation at 4 °C showed amorphous aggregates, with no order and no orientation (Figure 4-20a). At room temperature, those amorphous aggregates became elongated, narrow sheets with order and characteristic orientation. The height of the sheets was up to 200nm (Figure 4-20b). When temperature reached up to 37 °C, the growth of sheets was much more significant in the Y and Z directions. The height of sheets was up to 500nm. In a certain incubation time and a certain concentration, increasing temperature can promote the Aβ aggregation (Figure 4-20c).

The concentration of the Aβ solution also has an important impact on the structure of Aβ aggregation. With one-week incubation at 37°C, Aβ at a concentration of 10μM in PBS only formed globular aggregates and did not extend into sheets (Figure 4-21a). In Figure 4-21b, protofibrils were formed at Aβ 50μM. With the increased concentration of Aβ peptide (115μM), oriented growth of Aβ sheets was significant (Figure 4-21c). At the highest concentration of Aβ peptide (250μM), the extension of Aβ sheets was more rapid. In Figure 4-21d, some small globular aggregates were sticking onto the bigger sheets at that moment. Thus, we concluded that higher concentration can accelerate Aβ aggregation.

Similarly, time is also a key factor in forming Aβ aggregation. Aβ in PBS (115μM) was incubated at four different time points at 4°C. Globular aggregates of Aβ appeared on the surface of mica immediately after dissolution in PBS for only 10min (Figure 4-22a). After one-day incubation, more globular aggregates of Aβ gathered (Figure 4-22b). Three days later, Aβ peptide aggregated into elongated, narrow sheets with characteristic orientation. The height of sheets was up to 400nm (Figure 4-22c). At one week, those narrow sheets extended randomly into amorphous sheets. The height of the sheets reached to 800nm (Figure 4-22d). Thus, time can also have major impact on the acceleration of Aβ aggregation.

The understanding of which factors are significant to the formation of Aβ aggregation and to what degree these factors can impact the formation of Aβ aggregation can be a very useful guide to different approaches of the treatment of AD. We also found that 50μM is really good working concentration. At higher concentrations (such as 115, 250μM), Aβ peptide could form large aggregates, which are difficult to work with. Therefore, the most important thing is to check how long has Aβ stock solution been made, what the concentration of this solution is and how often this solution has been used in the past before starting an experiment.

4.5.1.4 Investigating the inhibition of Aβ aggregation by mAbs

The samples used for AFM were the same as those used in MTT assay. The images were shown below (Figure 4-23).
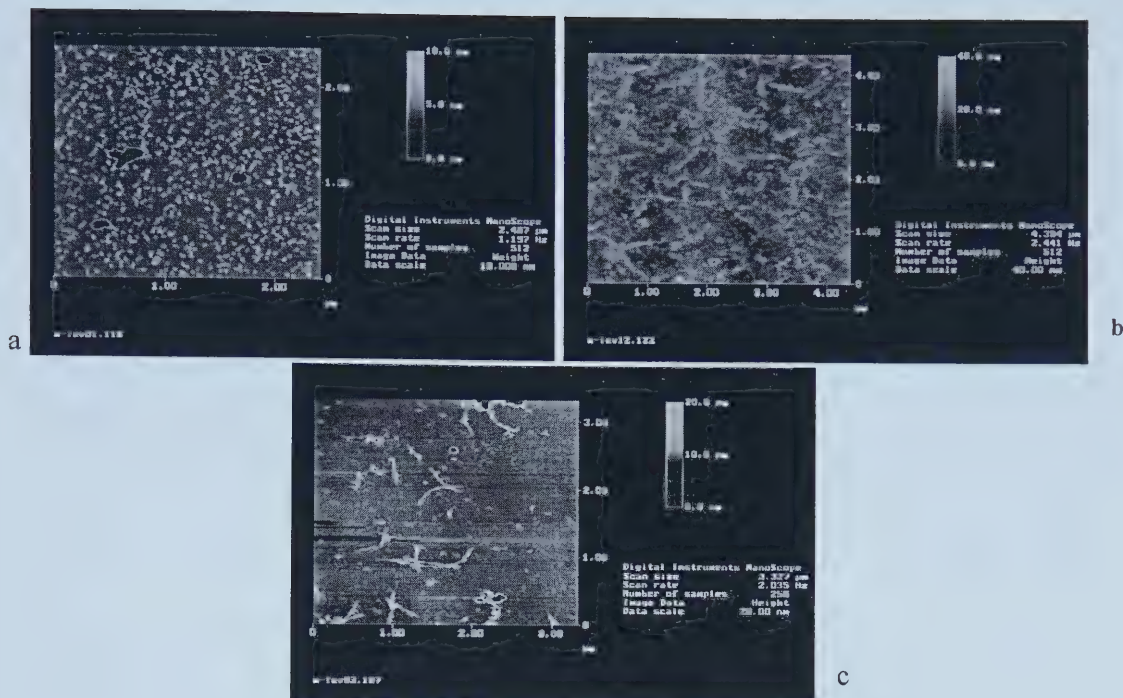
Figure 4-23 AFM images: the Inhibition of Aβ Aggregation

a. The mixture of Aβ (50μM) and BL01.94 mAb. b. The mixture of Aβ (50μM) and control antibody. C. Aβ alone (control group concentration: 50μM)

BL01.94 and BL03.21 mAbs were tested for the inhibitory effect on Aβ aggregation by using AFM. Aβ peptide at 10μM tends to form globular aggregates (dimer-hexamer) (Figure 4-21a). If the concentration of Aβ was increased up to 50μM, the protofibrils could be formed easily (Figure 4-23c the same as Figure 4-21b). Figure 4-23a showed that under the same concentration as Figure 4-23b, BL01.94 mAb bound to Aβ peptide and did inhibit the formation of protofibrils. However, the protofibrils and amorphous aggregates can be observed in Figure 4-23b. Therefore, the inhibitory effect on Aβ aggregation by mAb was also confirmed by using AFM .

4.5.2 Promotion of Aβ Phagocytosis by Macrophages

Biotin-Aβ_{1-40} alone, biotin-Aβ_{1-40} with BL01.94 mAb (1:10 molar ratio) and biotin-Aβ_{1-40} with non-specific mouse IgM (1:10 Molar ratio) were incubated with mouse macrophages at 37°C overnight. The concentration of Aβ was 20μM. Streptavidin-PE was the detective agent, as described in the Materials and Methods section.

When biotin-Aβ_{1-40} alone incubated with macrophages, there were many Aβ aggregates in Figure 4-24a. Phagocytosis was not observed. In Figure 4-24b, when biotin-Aβ_{1-40} and BL01.94 mAb were incubated together with macrophages, there were fewer Aβ aggregates in this image. The macrophages gave off bright fluorescent light and the phagocytosis by macrophages was significant. Because Aβ and BL01.94 mAb formed an immunocomplex, the immunocomplex triggered the phagocytosis by macrophages. The negative control group was biotin-Aβ_{1-40} and non-specific IgM incubated with macrophages (Figure 4-24c). The non-specific IgM used in this experiment was clarified from ascitic fluid and contained some other proteins, which Aβ peptide might bind to. Slight phagocytosis by macrophages can be observed in negative control imaging. However, compared to the intensity of fluorescence in the images (Figure 4-30b) by imaging analysis software, slight phagocytosis by macrophages was insignificant.

a.   b.   c.
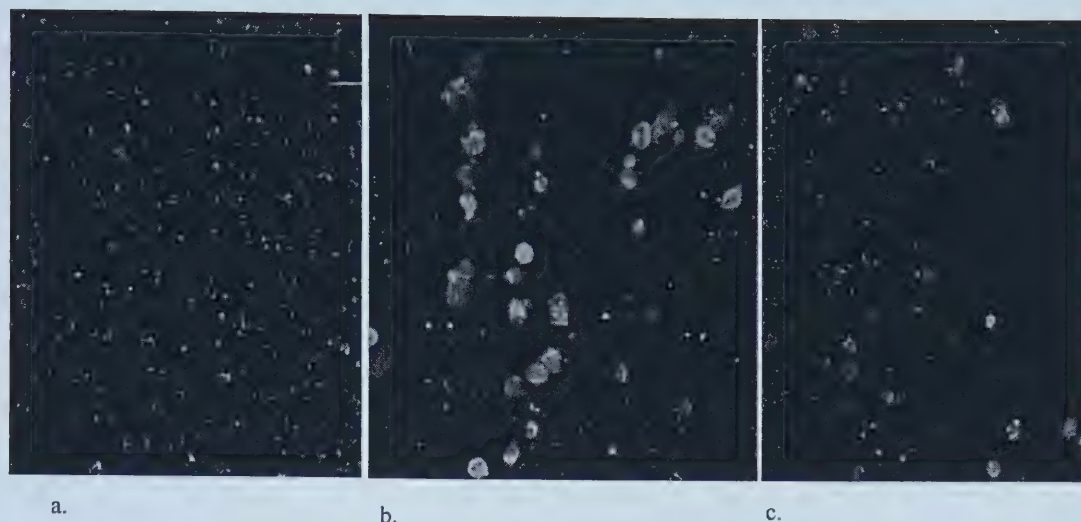
Figure 4-24 Confocal Images: the Phagocytosis of Aβ Peptide by Macrophages

a.   *Positive control:* only Aβ peptide was incubated with macrophages.
b.   Aβ peptide and BL01.94 mAb were incubated with macrophages.
c.   Negative control: Aβ peptide and clarified non-specific mouse IgM were incubated with macrophages. (overnight incubation at 37°C)

4.5.3. Inhibition of Aβ Neurotoxicity by BL01.94 mAb and BL03.21 mAb

Aβ neurotoxicity has been shown by other researchers using the PC 12 cell line. However because we did not have the PC 12 cell line, the SK-N-SH human neuroblastoma cell line was chosen for this study. This cell line secretes APP (Leveugle *et al.*, 1998). The aim of this study is to see whether Aβ is toxic to SK-N-SH cell line. Also the inhibition of Aβ neurotoxicity by BL01.94 mAb/BL03.21 mAb was investigated. The molar ratios of $A\beta_{1-40}$ peptide to BL01.94 mAb were 3.3:1, 50:1, and the molar ratios of $A\beta_{1-40}$ peptide to BL03.21 mAb were 5:1, 50:1. $A\beta_{1-40}$ peptide alone was as positive control. Non-specific antibodies and 47.47 mAb were as negative control. The concentration of $A\beta_{1-40}$ peptide was 50μM. All the samples were aged at 37°C for 1 week. However, after adding all the

100

samples to SK-N-SH, SK-N-SH cells were growing well compared to the control group (without adding $A\beta_{1-40}$ peptide). Because SK-N-SH cells were cultured in RPMI medium containing 2% FBS, some protein in FBS may have some effect on $A\beta$ neurotoxicity. Thus serum-free medium was chosen to replace RPMI medium. But the SK-N-SH cells did not grow well in serum free medium. Maybe SK-N-SH cells are resistant to $A\beta$ neurotoxicity. Further investigations on SK-N-SH cells or PC 12 cells might give some clues on that.

CHAPTER 5 CONCLUSION AND FUTURE WORK

5.1 Conclusion

Although the etiology and pathogenesis of AD is not yet clear, the mechanism of the formation of Aβ aggregation has proven critical to our understanding of the role Aβ plays in AD. Thus reconstructing the formation of Aβ aggregation *in vitro* may provide valuable information. The time-, concentration-, and temperature course of Aβ aggregation were studied by continuous imaging of surfaces carrying 50-250μM solutions of Aβ in PBS (pH 7.4). Nanoscale aggregates of Aβ could be visualized by the application of a tapping mode of imaging. Particulate aggregates formed on hydrophilic mica Aβ, which then form protofibrils (linear assemblies), fibrils and large sheets as the concentration, time and/or temperature increase. This emphasizes the importance of rapid clearance of Aβ peptide once formed in order to avoid the formation of neurotoxic aggregates *in vivo*. In the future, if the level of Aβ peptide in body fluids can be lowered to a non-aggregating concentration, it might prevent people from developing AD.

These results also point out the importance of experimental conditions for the experiment performed in the research lab. Indeed, regarding the temperature, most experiments are performed at room temperature. Since Aβ aggregation occurs much faster at 37°C, experiments should be performed at this temperature instead of room temperature to reflect more closely *in vivo* conditions. Aβ aging is also strongly affected by time. Thus, it is important to work with fresh Aβ preparations. If one wants to study protofibrils'

effect on Aβ neurotoxicity, Aβ stock solution should be always checked by AFM. Also the Aβ concentration should be chosen carefully according to the goal of the experiments. In conclusion, manipulation of Aβ is of great importance for the experiment.

We have produced several monoclonal and polyclonal antibodies directed against $Aβ_{1-40}$, $Aβ_{1-42}$ and APPβ peptides. In the research lab, the detection of $Aβ_{1-40}$, $Aβ_{1-42}$ and APPβ peptides is useful for the study of the APP metabolism and identification of factors that can influence the processing of APP towards amyloidogenic or non-amyloidogenic pathway. Such studies may lead to the identification of potential therapeutic agents for AD. The antibodies produced may also be useful as serodiagnostics agents for AD. Tremendous progress has been made recently in the field of Alzheimer's diagnostics with the discovery of FDDNP, a new agent that can be used in AD patients to visualize by Positron Emission Tomography, amyloid and neurofibrillary tangles . [Shoghi-Jadid et al 2002]. However, PET imaging compare to serodiagnostic is more expensive and requires specialized personnel and equipment.

There is a rationale for a therapeutic strategy based on developing antibodies against Aβ protein to lower Aβ concentration, disrupt the aggregation of Aβ into fibrils, and/or promote the elimination of Aβ aggregates. It was found that BL01.94 interfered with the aggregation of Aβ and promoted the elimination of Aβ. These results are therefore in accordance with previous studies highlighting the potential of anti-Aβ antibodies for AD therapy. Elan Pharmaceuticals Inc. just announced that active immunization of Aβ peptide in clinical trials had been halted due to CNS inflammation in 4 out of 360 patients.

Although, it is not known whether the observed inflammation is induced by the given treatment, it is possible that the passage of anti-Aβ antibodies across the blood brain barrier and the decoration of the amyloid plaques by such antibodies exacerbate an inflammatory reaction due to the excessive activation of microglial cells. Several studies have demonstrated that single chain antibodies can inhibit Aβ aggregation and clear amyloid plaques in vivo. Thus passive immunization with anti-Aβ antibodies or its fragments lacking the Fc portion may be an alternative to Aβ vaccination.

5.2 Future Work

5.2.1 Binding Specificity of BL01.94 Antibody

The binding specificity of BL01.94 mAb was tested by ELISA assays and the results were shown in section 3.1.5. It was found that the epitope recognized by BL01.94 is not comprised within three zones of the Aβ: the first 16 amino acids of the amyloid peptide (Figure 4-7), the 25th to 35th amino acids of amyloid peptide (Figure 4-9), and the 37th to 42nd amino acids of amyloid peptide (Figure 4-6). However, the region of the16th-25th and the region of the 35th-37th amino acids of amyloid peptide were not tested for their binding specificities. Thus, it is possible that BL01.94 mAb may be directed against either the region of the16th-25th amino acids of amyloid peptide, or the region of the 35th-37th amino acids of amyloid peptide. The other possibility is that BL01.94 mAb may be directed against the epitope on the aggregated Aβ. The epitope on soluble Aβ may

undergo conformational change because of the aggregation of these soluble Aβ peptides. The binding specificity of BL01.94 needs to be further investigated.

5.2.2 Binding Specificity of Polyclonal Antibodies Against APPβ

The β-secretase cleavage site is very important for the formation of Aβ peptide (see Appendix-I peptide sequence). If polyclonal antibodies are specific against this binding site, the formation of Aβ could be prevented or slowed down. Also polyclonal antibodies against APPβ can be used to monitor the level of sAPPβ in body fluids and to track the production of Aβ. The binding specificity of polyclonal antibodies directed against APPβ towards APPβ and APPβ+2 (see Appendix-I peptide sequence) is shown in Figure 3-20. Our polyclonal antibodies bind preferentially to APPβ fragments compared to APPβ+2 fragments. The binding specificity of produced polyclonal antibodies in the presence of a large excess of the APPβ+2 fragment or with APP protein should be tested.

5.2.3 Evaluation of the Potential Use of the Antibodies for the Study and Therapy of AD

5.2.3.1 Serodiagnostics

Because no single test can determine whether a person has Alzheimer's disease, diagnosing someone in the early stages of the disease remains challenging. An early diagnosis of Alzheimer's may allow medications to have more of an effect on the disease's

symptoms. Increased understanding of Alzheimer's in recent years allows doctors to recognize some of the disease's earlier manifestations through a variety of tests and examinations.

Basic Medical Tests: Tests of blood and urine may be done to help the doctor eliminate other possible diseases. In addition, scientists are trying to develop a test to diagnose AD that will be easy and accurate. Researchers are looking for early biological markers-- changes in body fluids. The possibility that there are biological markers for Alzheimer's disease--tau protein or $A\beta_{1-42}$ in blood as well as CSF has been investigated currently (Boss MA, 2000). Matter et al 1995, found that $A\beta_{1-42}$ comprised about 5% of total soluble $A\beta$ and $A\beta_{1-42}$ levels were significantly lower in AD patients *vs*. age-related healthy controls or diseased controls. Some other independent groups studied and confirmed these findings. Then, the measurement of $A\beta_{1-42}$ levels in CSF could be a potential biological diagnostic marker of AD. The most commonly used technique to detect $A\beta$ is sandwich ELISA. Although ELISA could not differentiate nonspecific binding of antibodies, the influence of culture media, and the interferences of other secreted substances, it can detect those two peptides with monoclonal antibody (Jensen et al., 1999).

Jensen et al, 2000 have established a highly sensitive sandwich-ELISA assay for quantifying and differentiating $A\beta_{1-40}$ and $A\beta_{1-42}$ peptides. They reported that the detection range for ELISA assays was 20-250pM, and they provided valuable data about $A\beta$ stability in human CSF obtained from lumbar puncture. Skovronsky et al (Hooper,

2000) have established a standard sandwich-ELISA assay and studied the quantification of both $A\beta_{1-40}$ and $A\beta_{1-42}$ peptides in cell culture medium or in human CSF samples. The ELISA that they used could distinguish $A\beta_{1-40}$ and $A\beta_{1-42}$ at a sensitivity of 0.1-0.5 femtomoles. Our laboratory developed several antibodies: BL01.94 mAb, BL03.21mAb and rabbit antisera against $A\beta_{37-42}$. BL03.21mAb or rabbit antisera against $A\beta_{37-42}$ was used as a capturing antibody, whereas BL01.94 mAb was used as detecting antibody. The corresponding antibody conjugated with HRP was used as a reporter antibody. In the present study, a sandwich ELISA was developed and can be used to detect $A\beta_{1-42}$ (Figure 3-19). However, the sensitivity of this ELISA has not been tested and the detection range of this sandwich ELISA needs to be further investigated.

Synx Pharmaceutical Company has developed a new device to detect biomarkers in AD patients. This way is more economic than brain imaging. Although brain imaging is complicated, it may provide more accuracy.

5.2.4 Inhibition of Aβ Neurotoxicity

5.2.4.1 MTT Assay

Many researchers studied Aβ neurotoxicity with the PC 12 cell line or rat cortical neurons. Walsh *et al* (1999) found that aggregated Aβ produced highly significant decreases in levels of reduced MTT in cultures of rat cortical neurons. In order to observe the inhibition of Aβ neurotoxicity, the MTT assay was used. The samples used for MTT

assay were the same as those used for AFM. SK-N-SH cells were used in this assay. Compared to the control group, levels of reduced MTT in sample groups did not show a large difference. Although we have evidence from AFM, studies that Aβ peptide was aggregated, we could not see any neurotoxic effect. We hypothesized that either SK-N-SH cells were resistant to the Aβ neurotoxic effect or that a substance in the cell culture medium inhibits the neurotoxic effect. Therefore these experiments should be repeated with PC 12 cells for which the Aβ neurotoxic effect has been extensively tested.

5.2.5 Promotion of Aβ Clearance

Although the phagocytosis of Aβ by macrophages was promoted by BL01.94 mAb, further experiments should be undertaken with microglial cells *in vitro*. Also transgenic mice (APP) with circulating Aβ can be tested in *vivo* for the formation of plaques and/or the sign of neurodegeneration, after passive immunization with antibody or its fragments.

References

Auld DS, Karr S and Quirion R. β-amyloid peptides as direct cholinergic neuromodulators: a missing link? *Trends Neurosci* 1998; **21**: 43-9

Asami-Odaka A, Ishibashi Y, Kikuchi T, Kitada C, Suzuki N. Long amyloid β-protein secreted from wild-type human neuroblastoma IMR-32 cells. *Biochem.* 1995; **34**: 10272-8

Bachman DL, Wolf PA, Linn RT, et al.. Incidence of dementia and probable Alzheimer's disease in a general population: The Framingham study. *NEURA* 1993; **43**: 515-9

Bacskai BJ. Kajdasz ST. Christie RH. Carter C. Games D. Seubert P. Schenk D. Hyman BT. Imaging of amyloid-beta deposits in brains of living mice permits direct observation of clearance of plaques with immunotherapy. *Nat Med.* 2001; **7(3)**:369-72

Bai DL, Tang XC and He XC. Huperzine A, a potential therapeutic agent for treatment of Alzheimer's disease. *Curr Med Chem* 2000; **7**: 355-74

Bard F, Cannon C, Barbour R, Burke RL, Games D, Grajeda H, Guido T, Hu K, Huang J, Johnson-Wood K, *et al.* Peripherally administered antibodies against amyloid beta-peptide enter the central nervous system and reduce pathology in a mouse model of Alzheimer disease. *Nat Med. 2000*; **6(8)**: 916-9

Bauer J, Strauss S and Schreiter-Gasser U. Interleukin-6 and alpha-2-macroglobulin indicate an acute phase response in Alzheimer's disease cortices. *FFBS Lett* 1991; **285**: 111-4

Biere, A. L., Ostaszewski, B., Stimson, E. R., Hyman, B. T., Maggio, J. E., Selkoe, D. J. Amyloid beta-peptide is transported on lipoproteins and albumin in human plasma. *J. Biol. Chem.* 1996; **271**,32916-22

Blake CCF and Serpell L. Synchrotron X-ray studies suggest that the core of the transthyretin amyloid fibril is a continuous beta-sheet helix. *Structure* 1996; **4**: 989-98

Blanc EM, Toborek M, Mark RJ, Hennig B, Mattson MP. Amyloid β-peptide induces cell monolayer albumin permeability, impairs glucose transport, and induces apoptosis in vascular endothelial cells. *J. Neurochem.* 1997; **68**: 1870–81

Bradury J. New mechanism proposed for NSAID reduction of Alzheimer's disease incidence. *Lancet.* 2001; **358(9293):** 1616

Canadian Study of Health and Aging: study methods and prevalence of dementia. *Can Med Assoc J* 994; **150**: 899-913

Choo-Smith LP, Garzon-Rodriguez W, Glabe CG and Surewicz WK. Acceleration of amyloid fibril formation by specific binding of Abeta-(1-40) peptide to ganglioside-containing membrane vesicles. *J Biol Chem* 1997; **272**: 22987-90

Citron M, Teplow DB, Selkoe DJ. Generation of amyloid beta protein from its precursor is sequence specific. *Neuron* 1995; **14**: 661-70

Clippingdale AB, Wade JD and Barrow CJ. The Amyloid-β Peptide and its Role in Alzheimer's Disease. *J Pept Sci* 2001; **7**: 227-49

Cook DG, Forman MS, Sung JC et al.. Alzheimer's Aβ(1-42) is generated in the endoplasmic reticulum/intermidiate compartment of NT2N cells. *Nat Med.* 1997; **3**: 1021-3

Das P, Murphy MP, Younkin LH, Younkin SG, Golde TE. Reduced effectiveness of Abeta1-42 immunization in APP transgenic mice with significant amyloid deposition. *Neurobiol Aging* 2001; **22(5)**:721-7

Davis KL and Mohs RC. Enhancement of memory processes in Alzheimer's disease with multi-dose intravenous physostigmine. *Am J Psychiatry* 1982; **139**: 1421-4

DeMattos RB, Bales KR, Cummins DJ, Dodart JC, Paul SM & Holtzman DM. Peripheral anti-Aβ antibody alters CNS and plasma Aβ clearance and decreases brain Aβ burden in a mouse model of Alzheimer's disease. *Proc. Natl. Acad. Sci. USA* 2001; **98**: 8850-5

Diaz Brinton R and Yamazaki RS. Advances and challenges in the prevention and treatment of Alzheimer's disease. *Pharm Res* 1998; **15**: 386-98

Doody RS. Clinical profile of donepezil in the treatment of Alzheimer's disease. *GERNDJ* 1999; **45** Suppl 1:23-32

Du Y. Dodel R. Hampel H. Buerger K. Lin S. Eastwood B. Bales K. Gao F. Moeller HJ. Oertel W. Farlow M and Paul S. Reduced levels of amyloid beta-peptide antibody in Alzheimer disease. *NEURA* 2001; **57(5):**801-5

Eikelenboom P, Hack CE, Kamphorst W and Rozemuller JM. Distribution pattern and functional state of complement proteins and α₁-antichymotrypsin in cerebral β/A4 deposits in Alzheimer's disease. *Res Immunol* 1992; **143**: 617-20

Engelborghs S and De Deyn PP. Biological and genetic markers of sporadic Alzheimer's disease. *ACTA Medica Okayama* 2001; **55 (2):**55-63

Ernst RL and Hay JW The U.S. economic and social costs of Alzheimer's disease revisited. *Am J Pub Health* 1994; **84**: 1261-4

Esch FS, Keim PS, Beattie EC *et al.*. Cleavage of amyloid β peptide during constitutive processing of its precursor. *SCI* 1990; **248**:1122-4

Estus S, Golde TE, Kunishita T *et al.*. Potentially amyloidogenic, carboxyl-terminal derivatives of the amyloid protein precursor. *SCI* 1992; **255**: 726-8

Evans KC, Berger EP, Cho CG, Weisgraber KH and Lansbury PT, Jr. Apolipoprotein E is a kinetic but not a thermodynamic inhibitor of amyloid formation: implications for the pathogenesis and treatment of Alzheimer disease. *Proc Natl Acad Sci USA* 1995; **92**: 763-7

Farlow M.R. and Evans R.M. Pharmacological treatment of cognition in Alzheimer's dementia. *NEURA* 1998; **51(Suppl 1):** S36-44

Fassbender K, Masters C and Beyreuther K. Alzheimer's disease: molecular concepts and therapeutic targets. *Naturwissen* 2001; **88**: 261-7

Frenkel D, Balass M, Solomon B. N-terminal EFRH sequence of Alzheimer's beta-amyloid peptide represents the epitope of its anti-aggregating antibodies. *J Neuroimmunol.* 1998; **88(1-2)**:85-90

Frenkel D, Balass M, Katchalski-Katzir E, Solomon B. High affinity binding of monoclonal antibodies to the sequential epitope EFRH of beta-amyloid peptide is essential for modulation of fibrillar aggregation. *J Neuroimmunol.* 1999; 95(1-2):136-42

Frenkel D. Solomon B. Benhar I. Modulation of Alzheimer's beta-amyloid neurotoxicity by site-directed single-chain antibody. *J Neuroimmunol.* 2000; **106(1-2)**: 23-31

Frenkel D, Katz O, Solomon B. Immunization against Alzheimer's beta -amyloid plaques via EFRH phage administration. *Proc Natl Acad Sci* U S A. 2000 **97(21)**:11455-9

Fuller SJ, Storey E, Li Q-X, Smith AI, Beyreuther K, Masters CL. Intracellular production of βA4 amyloid of Alzheimer's disease modulation by phosphoramidon and lack of coupling to the secretion of the amyloid precursor protein. *Biochem.* 1995; **34**: 8091-8

Garzon-Rodriguez W, Yatsimirsky AK, Glabe CG. Binding of Zn(II), Cu(II), and Fe(II) ions to Alzheimer's A beta peptide studied by fluorescence. *Bioorg Med Chem Lett.* 1999; **9(15)**: 2243-8

Ghersi-Egea, J. F., Gorevic, P. D., Ghiso, J., Frangione, B., Patlak, C. S., Fenstermacher, J. D. Fate of cerebrospinal fluid-borne amyloid beta-peptide: rapid clearance into blood and appreciable accumulation by cerebral arteries. *J. Neurochem.* 1996; **67**:880-3

Ghiso, J., Matsubara, E., Koudinov, A., Choi-Miura, N. H., Tomita, M., Wisniewski, T., Frangione, B. The cerebrospinal-fluid soluble form of Alzheimer's amyloid beta is complexed to SP-40,40 (apolipoprotein J), an inhibitor of the complement membrane-attack complex. *Biochem. J.* 1993; **293**:27-30

Golde TE, Estus S, Younkin LH, Selkoe DJ and Younkin SG. Processing of the amyloid protein precursor to potentially amyloidogenic derivatives. *SCI* 1992; **255:** 728-30

Haass C, Koo EH, Mellon A, Hung AY, Selkoe DJ. Targeting of cell-surface β-amyloid precursor protein to lysosomes: alternitive processing into amyloid-bearing fragments. *Nat* 1992; **357:** 500-3

Haass C. Presenilins: genes for life and death. *Neuron* 1997; **18:** 687-90

Hardy J. Amyloid, the presenilins and Alzheimer's disease. *Trends Neurosci* 1997; **20:** 154-9

Harper JD, Wong SS, Lieber CM and Lansbury, Jr PT. Observation of metastable Aβ amyloid protofibrils by atomic force microscopy. *Chem Biol* 1997; 4: 119-25

Helmuth L. Neuroscience. An antibiotic to treat Alzheimer's? *SCI* 2000; **290(5495):** 1273-4

Henderson VW. Estrogen, cognition, and a woman's risk of Alzheimer's disease. *Am J Med.* 1997; 103(3A):11S-18S

Henderson VW, Paganini-Hill A, Miller BL, Elble RJ, Reyes PF, Shoupe D, McCleary CA, Klein RA, Hake AM, Farlow MR. Estrogen for Alzheimer's disease in women: randomized, double-blind, placebo-controlled trial. *NEURA.* 2000; **54(2)**: 295-301

Hux M.J, O'Brien BJ, Iskedjian M, Goeree R, Gagnon M and Gauthier S. Relation between severity of Alzheimer's disease and costs of caring. *CMAJ* 1998; **159:** 457-65.

Hyman BT, Smith C, Buldyrev I, Whelan C, Brown H, Tang MX, Mayeux R. Autoantibodies to amyloid-beta and Alzheimer's disease. *Ann Neurol.* 2001; 49(6):808-10

in 't Veld BA, Ruitenberg A, Hofman A, Launer LJ, van Duijn CM, Stijnen T, Breteler MMB and Stricker BHC. Nonsteroidal Antiinflammatory Drugs and the Risk of Alzheimer's Disease. *N Eng J Med* 2001; **345**: 1515-21

Jann MW. Rivastigmine, a new-generation cholinesterase inhibitor for the treatment of Alzheimer's disease. *Pharmacotherapy* 2000; **20**: 1-12

Janus C, Pearson J, Mclaurin J, Mathews PM, Jiang Y, Schmidt SD et al. Aβ peptide immunization reduces behavioural impairment and plaques in a model of Alzheimer's disease. *Nat* 2000; **408**: 979-82

Jarrett JT, Berger EP and Lansbury PT, Jr. The carboxy terminus of the beta amyloid protein is critical for the seeding of amyloid formation: implications for the pathogenesis of Alzheimer's disease. *Biochem.* 1993; **32**: 4693-7

Jarrett JT and Lansbury PT Jr. Seeding "one-dimensional crystallization" of amyloid: a pathogenic mechanism in Alzheimer's disease and scrapie? *Cell* 1993; **73**: 1055-8

Kisilevsky R. Can deposition of amyloid be prevented in Alzheimer's disease? *Ann N Y Acad Sci.* 1997; **826**:117-27

Klein WL, Krafft GA, Finch CE. Targeting small Abeta oligomers: the solution to an Alzheimer's disease conundrum? *Trends Neurosci.* 2001; **24(4)**: 219-24

Koliatsos VE, Clatterbuck RE, Nauta HJW, *et al.* Human nerve growth factor prevents degeneration of basal forebrain cholinergic neurons in primates. *Ann Neurol* 1991; **30**: 831-40

Koo EH, Squazzo SL. Evidence that production and release of amyloid β-protein involves the endocytic pathway. *J Biol Chem* 1994; **269**: 17386-9

Kowalewski T and Holtzman DM. In situ atomic force microscopy study of Alzheimer's β-amyloid peptide on different substrates: New insights into mechanism of β-sheet formation. *Proc. Natl. Acad. Sci. USA* 1999; **96**: 3688-93

Kurochkin, I. V., Goto, S. Alzheimer's beta-amyloid peptide specifically interacts with and is degraded by insulin degrading enzyme. *FEBS Lett* 1994; **345**:33-7

Lambert, M. P., Barlow, A. K., Chromy, B. A., Edwards, C., Freed, R., Liosatos, M., Morgan, T. E., Rozovsky, I., Trommer, B., Viola, K. L., Wals, P., Zhang, C., Finch, C. E., Krafft, G. A., and Klein, W. L. 1998 *Proc. Natl. Acad. Sci. U. S. A.* **95**, 6448-6453

Leveugle B, Ding W, Laurence F, Dehouck MP, Scanameo A, Cecchelli R, Fillit H. Heparin oligosaccharides that pass the blood-brain barrier inhibit beta-amyloid precursor protein secretion and heparin binding to beta-amyloid peptide. *J Neurochem.* 1998; **70(2)**:736-44.

Lin H, Bhatia R, Lal R. Amyloid beta protein forms ion channels: implications for Alzheimer's disease pathophysiology. *FASEB J.* 2001; **15(13)**: 2433-44

Lin X, Koelsch G, Wu S, Downs D, Dashti A and Tang J. Human aspartic protease memapsin 2 cleaves the β-secretase site of β-amyloid precursor protein. *Proc. Natl. Acad. Sci. USA.* 2000; **97(4)**: 1456-60

Lomakin A, Teplow DB, Kirschner DA and Benedek GB. Kinetic theory of fibrillogenesis of amyloid beta-protein. *Proc Natl Acad Sci USA* 1997; **94**: 7942-7

Matsuzaki K, Horikiri C. Interactions of amyloid β-peptide (1-40) with ganglioside containing membranes. *Biochem.* 1999; **38**: 4137–42

Mattson MP, Cheng B, Davis D, Bryant K, Lieberburg I and Rydel RE. β-amyloid peptides destabilize calcium homeosatsis and render human cortical neurons vulnerable to excitotoxicity. *J Neurosci* 1992; **12**: 379-89

McGeer PL and McGeer EG. Complement proteins and complement inhibitors in Alzheimer's disease. *Res Immunol* 1992; **143**: 621-4

McKhann G, Drachman D, Folstein M, *et al.*. Clinical diagnosis of Alzheimer's disease: report of the NINCDS-ADRDA Work Group under the auspices of Department of Health and Human Services Task Force on Alzheimer's disease. *NEURA* 1984; **34**: 939-44

McLaurin J, Chakrabartty A. Membrane disruption by Alzheimer β-amyloid peptides mediated through specific binding to either phospholipids or gangliosides. *J. Biol. Chem.* 1996; **271**: 26482–9

Meziane H, Dodart JC, Mathis C, Little S, Clemens J, Paul SM and Ungerer A. Memory-enhancing effects of secreted forms of the b-amyloid precursor protein in normal and amnestic mice. *Proc. Natl. Acad. Sci. USA* 1998; **95:** 12683-8

Mills J and Reiner PB. Regulation of amyloid precursor protein cleavage. *J Neurochem* 1998; **72:** 443-60

Monk D, Brodaty H. Use of estrogens for the prevention and treatment of Alzheimer's disease. *Dementia Geriatr Cognit Disord.* 2000; **11:**1-10

Morgan D, Diamond DM, Gottschali PE, Ugen KE, Dickey C, Hardy J, Duff K, Jantzen P, DiCarlo G, Wilcock D, *et al.* Aβ peptide vaccination prevents memory loss in an animal model of Alzheimer's disease. *Nat* 2000; **408**: 982-5

Motter R, Vigo-Pelfrey C, Kholodenko D, Barbour R et al. Reduction of β-Amyloid42 in the cerebrospinal fluid of patients with Alzheimer's disease. *Ann Neurol* 1995; **38**: 643-8

Mulnard RA. Estrogen as a treatment for Alzheimer disease. *JAMA.* 2000; **284(3):**307-8

Paganetti PA, Lis M, Klafki HW, Staufenbiel M. Amyloid precursor protein truncated at any of the gamma-secretase sites is not cleaved to β-amyloid. *J Neurosci Res* 1996; **46**: 283-93

Paganini-Hill A, Henderson VW. Estrogen replacement therapy and risk of Alzheimer disease. *Arch Intern Med.* 1996; **156(19):** 2213-7

Pike CJ and Cotman CW. Cultured GABA-immunoreactive neurons are resistant to toxicity induced by β-amyloid. *Neuroscience* 1993; **56**: 269-74

Poduslo, J. F., Curran, G. L., Sanyal, B., Selkoe, D. J. Receptor-mediated transport of human amyloid beta-protein 1–40 and 1–42 at the blood–brain barrier. *Neurobiol. Dis.* 1999; **6**,190-9

Qizilbash N, Birks J, Lopez-Arrieta J, Lewington S, Szeto S. Tacrine for Alzheimer's disease. Cochrane Database of Systematic Reviews 2000;[computer file] (2):CD000202

Rapoport SI. Osmotic opening of the Blood-Brain Barrier: principles, mechanism, and therapeutic applications. *Cell Mol Neurobiol* 2000; **20**:217-30

Ringman JM, Cummings JL. Metrifonate: update on a new antidementia agent. *J Clin Psych* 1999; **60**: 776-82

Ritchie K. Dementia in the elderly. *NEURA* 1995; **11**: 2112-3

Rogaev EI, Sherrington R, Rogaeva EA, Levesque G, Ikeda M, Liang Y, Chi H, Lin C, Holman K, Tsuda T, et al. Familial Alzheimer's disease in kindreds with missense mutations in a gene on chromosome 1 related to the Alzheimer's disease type 3 gene. *Nat* 1995; **376(6543)**: 775-8

Rosenberg MB, Friedmann T, Robertson RC, *et al*. Grafting genetically modified cells to the damaged brain: restorative effects of NGF expression. *SCI* 1988; **242**: 1575-8

Rother M, Erkinjuntti T, Roessner M, Kittner B, Marcusson J and Karlsson I. Propentofylline in the treatment of Alzheimer's disease and vascular dementia: a review of phase III trials. *Dementia Geriatr Cognit Disord* 1998; **9** Suppl 1:36-43

Schenk D, Barbour R, Dunn W, Gordon G, Grajeda H, Guido T, Hu K, Huang J, Johnson-Wood K, Khan K, *et al*. Immunization with amyloid-β attenuates Alzheimerdisease-like pathology in the PDAPP mouse. *Nat* 1999; **400**: 173-7

Schmechel DE, Saunder AM, Strittmatter WJ, Crain BJ, Hulette CM, Joo SH, Pericak-Vance MA, Goldgaber D and Roses AD. Increased amyloid beta-peptide deposition in cerebral cortex as a consequence of apolipoprotein E genotype in late-onset Alzheimer disease. *Proc Natl Acad Sci USA* 1993; **90**: 9649-53

Selkoe DJ. The cell biology of β-amyloid precursor protein and presenilin in Alzheimer's disease. *Trends Cell Biol* 1998; **8:** 447-53

Selkoe DJ. Clearing the Brain's Amyloid Cobwebs. *Neuron.* 2001; **32(2):**177-80

Seubert P, Oltersdorf T, Lee MG *et al*. Secretion of β-amyloid precursor protein cleaved at amino terminus of the β-amyloid peptide. *Nat* 1993; **361**: 260-3

Shoji M, Golde TE, Ghiso J *et al*. Production of the Alzheimer amyloid β protein by normal proteolytic processing. *SCI* 1992; **258**: 126-9

Simons M, Keller P, Dichgans J and Schulz JB. Cholesterol and Alzheimer's disease Is there a link? *NEURA* 2001; **57**: 1089-93

Sisodia SS, Koo EH, Beyreuther K, Unterbeck A, Price DL. Evidence that β-amyloid protein in Alzheimer's disease is not derived by normal processing. *SCI* 1990; **248**: 492-5

Smith MA, Perry G, Richey PL, *et al*. Oxidative damage in Alzheimer's. *Nat* 1996; **382**: 120-1

Solomon B, Koppel R, Hanan E and Katzav T. Monoclonal antibodies inhibits in vitro fibrillar aggregation of the Alzheimer β-amyloid peptide. *Proc. Natl. Acad. Sci. USA* 1996; **93**: 452-5

Soto C, Castano EM, Prelli F, Kumar RA and Baumann M. Apolipoprotein E increases the fibrillogenic potential of synthetic peptides derived from Alzheimer's, gelsolin and AA amyloids. *FEBS Lett* 1995; **371**: 110-4

Soto C. Sigurdsson EM. Morelli L. Kumar RA. Castano EM. Frangione B. Beta-sheet breaker peptides inhibit fibrillogenesis in a rat brain model of amyloidosis: implications for Alzheimer's therapy. *Nat. Med.* 1998; **4(7)**:822-6

Sramek JJ. Cutler NR. Recent developments in the drug treatment of Alzheimer's disease. *Drugs Aging* 1999; **14**: 359-73

Strittmatter WJ. Apolipoprotein E and Alzheimer's disease. *An NY Acad SCI* 2000; **924**: 91-2

Subramaniam R, Roediger F, Jordan B, Mattson MP, Keller JN, Waeg G, Butterfield DA. The lipid peroxidation product, 4-Hydroxy-2-trans-nonenal, alters the conformation of cortical synaptosomal membrane proteins. *J. Neurochem.* 1997; **69**: 1161–9

Sunde M, Serpell LC, Bartlam M, Fraser PE, Pepys MB and Blake CCF. Common core structure of amyloid fibrils by synchrotron X-ray diffraction. *J Mol Biol* 1997; **273**: 729-39

Terry RD, Masliah E, Salmon DP, Butters N, De Teresa R, Hill R, Hansen LA and Katzman R. Physical basis of cognitive alterations in Alzheimer's disease: synapse loss is the major correlate of cognitive impairment. *Ann Neurol* 1991; **30**: 572-80

Thomas T. Monoamine oxidase-B inhibitors in the treatment of Alzheimer's disease.

Neurobiol Aging. 2000; **21**: 343-8

Tienari PJ, Ida N, Ikonen E *et al.* Intracellular and secreted Alzheimer beta-amyloid species are generated by distinct mechanisms in cultured hippocampal neurons. *Proc Natl Acad Sci USA* 1997; **94**: 4125-30

Tjernberg LO, Callaway D JE, Tjernberg A, Hahne S, Lilliehook C, Terenius L, Thyberg J and Nordstedt C. A molecular model of Alzheimer amyloid β-peptide fibril formation. *J Biol Chem* 1999, **274**: 12619-25

Tomita T, Maruyama K, Saido TC, Kume H, Shinozaki K, Tokuhiro S, Capell A, Walter J, Grünberg J, Haass C, Iwatsubo T, and Obata K. The presenilin 2 mutation (N141I) linked to familial Alzheimer disease (Volga German families) increases the secretion of amyloid β protein ending at the 42nd (or 43rd) residue. *Proc. Natl. Acad. Sci. USA.* 1997; **94(5)**: 2025-30

US Government Printing Office publication NIH No. 96-4136. Alzheimer's Disease and Related Dementias: Acute and Long-Term Care Services. Washington, DC: Advisory Panel on Alzheimer's Disease.

Vassar R, Bennett BD, Babu-Khan S, Kahn S, Mendiaz EA, Denis P, Teplow DB, Ross S, Amarante P, Loeloff R, Luo Y, Fisher S, Fuller J, Edenson S, Lile J, Jarosinski MA, Biere AL, Curran E, Burgess T, Louis JC, Collins F, Treanor J, Rogers G, Citron M. Beta-

secretase cleavage of Alzheimer's amyloid precursor protein by the transmembrane aspartic protease BACE. *SCI* 1999; **286(5440)**: 735-41

Varadarajan S, Yatin S, Aksenova M, Butterfield DA. Alzheimer's amyloid beta-peptide-associated free radical oxidative stress and neurotoxicity. *J Struct Biol.* 2000; **130(2-3)**: 184-208

Vatassery GT. Vitamin E and other endogenous antioxidants in the central nervous system. *GERIA* 1998; **53** Suppl 1:S25-7

Vekrellis K, Ye Z, Qiu WQ, Walsh D, Hartley D, Chesneau V, Rosner MR, Selkoe DJ. Neurons regulate extracellular levels of amyloid beta-protein via proteolysis by insulin-degrading enzyme. *J Neurosci.* 2000; **20(5)**: 1657-65

Vickers JC, Dickson TC, Adlard PA, Saunders HL, King CE, McCormack G. The cause of neuronal degeneration in Alzheimer's disease. *Prog Neurobiol.* 2000; **60(2):** 139-65

Walsh DM, Lomakin A, Benedek GB, Condron MM and Teplow DB. Amyloid beta-protein fibrillogenesis. Detection of a protofibrillar intermediate. *J Biol Chem* 1997; **272**: 22364-72

Walsh DM, Hartley DM, Kusumoto Y, Fezoui Y, Condron MM, Lomakin A, Benedek GB, Selkoe DJ and Teplow DB. Amyloid β-protein fibrillogenesis: Structure and biological activity of protofibrillar intermediates. *J Biol Chem* 1999; **274**: 25945-52

Webster SD, Galvan MD, Ferran E, Garzon-Rodriguez W, Glabe CG and Tenner AJ. Antibody-Mediated Phagocytosis of the Amyloid -Peptide in Microglia Is Differentially Modulated by C1q[1]. *J of Immunol* 2001; **166**: 7496-503

Weggen S, Eriksen JL, Das P, Sagi SA, Wang R, Pietrzik CU, Findlay KA, Smith TE, Murphy MP, Bulter T, Kang DE, Marquez-Sterling N, Golde TE and Koo EH. A subset of NSAIDs lower amyloidogenic A42 independently of cyclooxygenase activity. *Nat* 2001; **414**: 212-6

Wertkin AM, Turner RS, Pleasure SJ *et al.* Human neurons derived from a teratocarcinoma cell line express solely the 696-amino acid precursor protein and produce intracellular β-amyloid or A4 peptides. *Proc Natl Acad Sci USA* 1993; **90**: 9513-7

Whiston JS, Selkoe DJ and Cotman CW. Amyloid β protein enhances the survival of hippocampal neurons *in vitro*. *SCI* 1989; **243**: 1488-90

Wisniewski T, Castano EM, Golabek A, Vogel T and Frangione B. Acceleration of Alzheimer's fibril formation by apolipoprotein E *in vitro*. *Am J Pathol* 1994; **145**: 1030-5

Wolfe MS. Secretase targets for Alzheimer's disease: Identification and therapeutic potential. *J Med Chem* 2001; **44 (13)**: 2039-60

Wood SJ, Chan W and Wetzel R. An ApoE-Abeta inhibition complex in Abeta fibril extension. *Chem Biol* 1996; **3**: 949-56

Yankner BA, Caceres A and Duffy LK. Nerve growth factor potentiates the neurotoxicity of β-amyloid. *Proc Natl Acad Sci USA* 1990a; **87**: 9020-3

Zhong Z, Higaki J, Murakami K *et al.* Secretion of β-amyloid precursor protein involves multiple cleavage sites. *J Biol Chem* 1994; **269**: 627-32

Appendix I: Peptide Sequence

N-terminus   C-terminus

$A\beta_{25-35}$: GSNKGAIIGLM

$A\beta_{1-40}$: DAEFRHDSGYEVHHQKLVFFAEDVGSNKGAIIGLMVGGVV

$A\beta_{1-42}$: DAEFRHDSGYEVHHQKLVFFAEDVGSNKGAIIGLMVGGVVIA

Biotin-APPβ: Biotin-KTEEISEVKM

Biotin-APPβ+2: Biotin-KTEEISEVKMDA

APPβ-KLH: KLH-KTEEISEVKM

Biotin-$A\beta_{1-40}$:Biotin-KDAEFRHDSGYEVHHQKLVFFAEDVGSNKGAIIGLMVGGVV

$A\beta_{37-42}$-KLH: KLH-KGGVVIA

$A\beta_{37-42}$-BSA: KLH-KGGVVIA

Appendix II: Compositions of Tricine/Tris Separating and Stacking Gels

Stock solution	Separating gel (5 mL) 15% acrylamide	Stacking gel (2 mL)
Urea	2.4 g	---
Acrylamide/bis	2.5 mL	256 μL
3× Gel Buffer	1.67 mL	500 μL
10% SDS	50 μL	50 μL
H_2O	Up to 5 mL	1.24 μL
APS	25 μL	16 μL
TEMED	2.5 μL	1.6 μL